AD_____

GRANT NUMBER DAMD17-95-1-5012

TITLE: Cell-Cell Adhesion and Breast Cancer

PRINCIPAL INVESTIGATOR: Stephen W. Byers, Ph.D.

CONTRACTING ORGANIZATION: Georgetown University
Washington, DC 20057

REPORT DATE: January 1998

TYPE OF REPORT: Annual

PREPARED FOR: Commander
U.S. Army Medical Research and Materiel Command
Fort Detrick, Frederick, Maryland 21702-5012

REPORT DOCUMENTATION PAGE

Form Approved
OMB No. 0704-0188

1. AGENCY USE ONLY *(Leave blank)*	2. REPORT DATE	3. REPORT TYPE AND DATES COVERED
	January 1998	Annual (15 Dec 96 - 14 Dec 97)

4. TITLE AND SUBTITLE
Cell-Cell Adhesion and Breast Cancer

5. FUNDING NUMBERS
DAMD17-95-1-5012

6. AUTHOR(S)
Stephen W. Byers, Ph.D.

7. PERFORMING ORGANIZATION NAME(S) AND ADDRESS(ES)
Georgetown University
Washington, DC 20057

8. PERFORMING ORGANIZATION REPORT NUMBER

9. SPONSORING/MONITORING AGENCY NAME(S) AND ADDRESS(ES)
Commander
U.S. Army Medical Research and Materiel Command
Fort Detrick, Frederick, MD 21702-5012

10. SPONSORING/MONITORING AGENCY REPORT NUMBER

11. SUPPLEMENTARY NOTES

12a. DISTRIBUTION / AVAILABILITY STATEMENT
Approved for public release; distribution unlimited

12b. DISTRIBUTION CODE

13. ABSTRACT *(Maximum 200*

Our results show that a mesenchymal cadherin, cadherin 11, is expressed in invasive breast cancer cells. The general model that loss of E-cadherin expression or function leads to the invasive, metastatic phenotype may not be the whole picture. Cadherin 11 may be required for cells to acquire a migratory invasive phenotype and may also promote the metastasis of cancer cells to bone where cadherin 11-expressing osteoblasts are present. Other results show that levels of the signaling, oncogenic pool of β-catenin in the cytoplasm is regulated by ubiquitination and proteosomal degradation and that mutation of a particular serine (S37) inhibits this process. We also show that the tumor suppressor gene APC normally targets β-catenin for degradation. Our results also show that in addition to its epithelial-differentiation properties, retinoic acid can inhibit the signaling activity of cytoplasmic β-catenin/LEF. This single result has very important implications in the area of cancer therapeutics. If the anti-cancer effects of retinoic acid are mediated in part by inhibition of β-catenin/LEF signaling this could lead to the development of agents which specifically inhibit this pathway in cancers which are resistant to the effects of retinoids

14. SUBJECT TERMS	15. NUMBER OF PAGES
Cell Biology, Metastasis, Cadherin, Adhesion, Junctions, Humans, Anatomical Samples, E-Cadherin, Breast Cancer	69
	16. PRICE CODE

17. SECURITY CLASSIFICATION OF REPORT	18. SECURITY CLASSIFICATION OF THIS PAGE	19. SECURITY CLASSIFICATION OF ABSTRACT	20. LIMITATION OF ABSTRACT
Unclassified	Unclassified	Unclassified	Unlimited

FOREWORD

Opinions, interpretations, conclusions and recommendations are those of the author and are not necessarily endorsed by the U.S. Army.

____ Where copyrighted material is quoted, permission has been obtained to use such material.

____ Where material from documents designated for limited distribution is quoted, permission has been obtained to use the material.

____ Citations of commercial organizations and trade names in this report do not constitute an official Department of Army endorsement or approval of the products or services of these organizations.

__✓__ In conducting research using animals, the investigator(s) adhered to the "Guide for the Care and Use of Laboratory Animals," prepared by the Committee on Care and Use of Laboratory Animals of the Institute of Laboratory Resources, National Research Council (NIH Publication No. 86-23, Revised 1985).

____ For the protection of human subjects, the investigator(s) adhered to policies of applicable Federal Law 45 CFR 46.

__✓__ In conducting research utilizing recombinant DNA technology, the investigator(s) adhered to current guidelines promulgated by the National Institutes of Health.

__✓__ In the conduct of research utilizing recombinant DNA, the investigator(s) adhered to the NIH Guidelines for Research Involving Recombinant DNA Molecules.

____ In the conduct of research involving hazardous organisms, the investigator(s) adhered to the CDC-NIH Guide for Biosafety in Microbiological and Biomedical Laboratories.

S.W. Byers 1/14/98

PI - Signature Date

TABLE OF CONTENTS:

5. Introduction

Nature of the Problem

Defects in cell-cell adhesion are commonly associated with tumor progression. There is evidence that alterations in the expression of the calcium-dependent cell adhesion molecule E-cadherin occur in a subset of invasive breast cancers and breast cancer cell lines. However, many invasive breast cancers and metastases are E-cadherin positive. Preliminary results indicate that breast tumor progression may more often be accompanied by alterations in the expression and function of several cadherin-associated molecules that are essential for cadherin-mediated cell-cell adhesion. It is the aim of this proposal to test the hypothesis that, in addition to the occasional loss of E-cadherin expression, breast tumor progression is more realistically modeled by a defect in cell-cell adhesion resulting from an alteration in any one or more of the steps (molecules) required for E-cadherin function. We will take two fundamental approaches. Firstly, we will use two methods for "non-specifically" assessing E-cadherin function and cell-cell adhesive strength in breast tumor samples and cell lines. Secondly, we will specifically investigate the molecular mechanisms that lead to defects in cell-cell adhesion by examining (and manipulating) the expression and phosphorylation state of several E-cadherin associated molecules in breast tumors and cell lines.

Background and Previous Work

Cell Adhesion, Cell junctions and Cancer The concept that alterations in cell to cell adhesion and intercellular communication are involved in tumorigenesis and tumor progression is certainly not new (1). However, it is only recently that the molecular basis underlying these changes has begun to be addressed. Homotypic cell-cell adhesion molecules (CAMs) and cell-cell junction molecules have now been implicated as tumor and metastasis suppressor genes in several systems (2-8). A gene often deleted in colon carcinoma (DCC) and associated with colon tumor progression is likely to be a homotypic CAM of the immunoglobulin superfamily (9). Of most interest to the present proposal are the calcium-dependent class of CAMs, cadherins, characteristically expressed by cells of epithelial origin (10,11). Cadherin-mediated adhesion is fundamentally involved in the organization of epithelial tissues during development, and manipulations of cadherin function result in profound disturbances of tissue organization (10-13). Several drosophila tumor suppressor genes are either cadherins or junction associated molecules and reduction in cadherin expression has been associated with the malignant phenotype in many advanced human carcinomas (2-8). In order for cadherins to function in cell-cell adhesion and promote the formation of junctions several other associated molecules need to be expressed (11,14-16). These molecules known as catenins, link the cadherins to the underlying actin cytoskeleton and are probably involved in propogating adhesion-related signaling (16,17). Our preliminary results show that the expression of certain catenins is lost in malignant breast carcinoma cells (16). Other studies have indicated that the phosphorylation state of catenins can also influence the transformed phenotype (17). The mechanism whereby alterations in cadherin-mediated adhesion affects cell proliferation, morphological differentiation and invasion is unknown. All differentiated epithelial cell collectives are linked by gap junctions permeable to intracellular calcium. In this situation, changes in intracellular calcium can be propogated rapidly among communicating cells. It is therefore not surprizing that many tumor cells including breast tumor cells are deficient in gap junctional communication ((18) and references therein). Interestingly, transfection of E-cadherin into squamous cell carcinoma cells lacking gap junction

function results in the expression of the gap junction proteins connexins and the assembly of functional gap junctions (19).

E-cadherin in Breast Cancer The presence of lymph node and distant metastases predict poor prognosis for cancer patients. For example, in a large clinical trial, percent treatment failure at 5 years for patients with no lymph node involvement upon histological examination was 13%, for those with 1-3 positive nodes the failure rate was 39% and for those with >4 positive nodes the failure rate was 69% (reviewed in (20)). These results underscore the necessity for research designed to understand the process of metastasis and to discover molecular markers that will predict whether a given tumor is likely to metastasize. The study of E-cadherin and associated protein expression and function in breast cancer cells can potentially provide information pertinent to both of these aims.

Several studies have examined the expression of E-cadherin in human breast cancer tissues (21-23). Loss or reduction of E-cadherin immunostaining was observed in a proportion of samples in each study. Normal breast epithelial structures consistently stain at cell-cell borders for E-cadherin. In one study (22), 53% of 120 tumors had reduced E-cadherin expression (defined as >10% of cells being E-cadherin-negative). The majority of the samples examined in this study were invasive ductal carcinomas, the most common form of breast cancer diagnosed. Loss of E-cadherin expression correlated with poorer differentiation state and with higher stage (T, N and M). In particular, 86% of samples from patients with distant metastasis (M_1) had reduced E-cadherin staining whereas 47% of samples from patients with no known distant metastasis (M_0) had reduced E-cadherin expression (22). Similar results were reported in a smaller study by Gamallo et al. (21). A third study examined a larger number of invasive lobular carcinomas (23). Complete loss of E-cadherin expression was detected in 29 of 35 samples. The remaining 6 samples had a diffuse staining pattern for E-cadherin. The ductal carcinoma samples had variable intensities of staining for E-cadherin although the proportions of E-cadherin-negative cells in each sample was not quantitated. Taken together, these results indicate that E-cadherin expression is lost in a significant proportion of lobular carcinoma specimens and reduced E-cadherin expression correlated with higher stage (poorer prognosis) and poorer differentiation in invasive ductal carcinomas.

One difficulty in comparing the results of E-cadherin staining of tumor tissues is the inconsistency between observers regarding when to classify a tumor as "E-cadherin-positive" or "E-cadherin-negative". In the study by Oka et al. (22), tumors with >10% of cells displaying no E-cadherin immunostaining were classified as having "reduced expression". However, in many studies no such cutoff was used (e.g. (21)). Many studies also describe "diffuse" or "disorganized" or "reduced" staining patterns for E-cadherin (21,23,24). These descriptions may indicate a defect in connection of E-cadherin to the actin cytoskeleton in these samples which could lead to a loss of adhesive function even in the presence of immunoreactive E-cadherin.

Although a trend between increasing stage and reduced E-cadherin expression was observed in breast cancer (22), the ability to predict metastatic spread based on expression of E-cadherin in a primary breast tumor is uncertain. An analysis of E-cadherin expression in 19 lymph node metastases and in their primary tumors was performed (22). Of the primary tumors, six were E-cadherin-positive, five were E-cadherin-negative and eight had a mixed phenotype. Five of the six lymph node metastases from E-cadherin-positive primary tumors were E-cadherin-positive

and one was mixed. All five of the lymph node metastases from E-cadherin-negative primary tumors were E-cadherin-negative. Among the lymph node metastases from the eight mixed primary tumors, three were E-cadherin-positive, two were E-cadherin-negative and two were mixed. The fact that five of the eight lymph node metastases from mixed primary tumors contained E-cadherin-positive indicates that a selection for E-cadherin-negative cells in the metastatic process does not occur.

Rationale and Hypothesis to be Tested The discussion above together with our preliminary data has led us to conclude that E-cadherin expression alone is a poor predictor of breast tumor invasive potential and metastatic spread. Significant loss of heterozygosity (LOH) of chromosomal locus 16q occurs in several carcinomas including breast (25-27). The human E-cadherin gene is localized to 16q22.1 and it is possible that an apparent reduction in staining intensity in some tumors may be due to this LOH. In breast cancer 16q LOH is correlated with distant metastatic spread. Although loss of functional homotypic cell-cell adhesion and intercellular communication are clearly associated with the transformed malignant epithelial cell phenotype this is not necessarily due to loss of cadherin expression or LOH at the cadherin locus. A defect in any one of the molecules involved in cadherin function, or a change in any of the pathways involved in cadherin responsive intra- and inter-cellular signalling could also result in the same phenotype. Other cell-cell adhesion molecules not discussed here are also likely to be affected. In other words, the two important carcinoma cell adhesion related phenotypes of **1)** alterations in contact dependent growth and **2)** invasion and metastasis, can be achieved in many different ways. Based on our own preliminary results and those in the literature we have calculated that there are several hundred potential routes whereby functional cell-cell adhesion could be altered during carcinogenesis and result in these phenotypes. Bearing in mind that we are limited by current knowledge this number is likely to be conservative. Not surprisingly, more than a dozen lesions in the cadherin-related adhesion system alone have already been uncovered in various carcinomas and cell lines (see discussion above). Whilst it is clearly of great importance to continue cataloging these molecular changes, indeed we propose to do so in one of our specific aims, it is equally important to develop methods in which functional cell-cell adhesion can be assessed directly. Such methods should uncover any defect in cell-cell adhesive strength no matter what the underlying molecular basis.

6. Body

Experimental Design And Methods

Task 1. To test the hypothesis that cell-cell adhesive strength and E-cadherin triton solubility is correlated with functional E-cadherin-mediated cell-cell adhesion. Years 1-4
The first "non-specific" approach that we will use for assessing tumor cell-cell adhesion strength is based on our recently described laminar flow assay (28). Using this assay developed originally to investigate cell-substratum interactions, we hypothesized that we should be able to distinguish cell-cell adhesive strength among tumor cells which express functional and non-functional E-cadherin. We will extend these studies to many more cell lines and to tumors derived from these lines. We will refine our procedures using tumors derived from cells which we already know express functional and non-functional E-cadherin and which are of known adhesive strength *in vitro*. It is not the goal of this specific aim to use these direct assays of cell-cell adhesive strength as a routine sceening procedure for breast cancer. For each sample we will correlate cell-cell

adhesion strength with E-cadherin triton solubility. We will restrict our analyses to tumors in which E-cadherin is present (but perhaps non-functional). In this way we can be certain that the cell aggregates that we analyze are derived from the tumor itself rather than any stromal elements which may contaminate it, since these will be E-cadherin negative and will not exhibit calcium-dependent cell-cell adhesion. We are not so interested in E-cadherin negative tumors since these have an obviously demonstrable lesion in cell-cell adhesion.

Task 1. Methods and Results (refer to figures in appendix 1)

Most of the experiments which we proposed to carry out in aim 1 have been completed (see previous report). This work has now been published or is in press (see appendix 1). The remaining aspects of task 1 involve the application of these assay systems to cells which have been isolated from tumors growing in nude mice. These studies are underway but we do not have results yet.

We will first refine our procedures using tumors derived from cells which we already know express functional and non-functional E-cadherin and which are of known adhesive strength *in vitro*. It is not the goal of this specific aim to use these direct assays of cell-cell adhesive strength as a routine sceening procedure for breast cancer. For each sample we will correlate cell-cell adhesion strength with E-cadherin triton solubility (see below). We will restrict our analyses to tumors in which E-cadherin is present (but perhaps non-functional). In this way we can be certain that the cell aggregates that we analyze are derived from the tumor itself rather than any stromal elements which may contaminate it, since these will be E-cadherin negative and will not exhibit calcium-dependent cell-cell adhesion. We are not so interested in E-cadherin negative tumors since these have an obviously demonstrable lesion in cell-cell adhesion.

Nude mice tumors In previous studies we have generated tumors in nude mice from several breast carcinoma cells lines. Some of these have been transfected with E-cadherin. We will continue to do this in the present proposal. 5 million carcinoma cells of varying E-cadherin status will be injected into the right upper mammary fat pad of 4-6 week-old athymic female nude mice (BALB/c-nu/nu) and the injection sites observed once or twice a week for the appearance and size of primary tumors. For estrogen responsive cells, 17-beta estradiol pellets (0.72 mg, 60 day release, Innovative Research of America) will be implanted in the interscapular region. After 3-6 weeks mice are sacrificed and tumor tissue used for the preparation of cells and for frozen sections. Cells from the tumors will be analyzed using the laminar flow assay and cell-cell adheison strength calculated as we described for the cell lines (see previous report and (28))

Task 2. To measure the expression and phosphorylation state of cadherin-associated proteins in breast tumors and cell lines (Years 1-4). We will examine the expression and phosphorylation state of the cadherin-associated proteins alpha catenin, beta catenin and plakoglobin in breast tumors and cell lines.

Task 2. Methods and Results

The methods for immunoprecipitation and western blot analysis were described in the previous report and have largely been published. At that time we had shown that serine rather than tyrosine phoshorylation was the prominent post-translational modification of β-catenin in breast cancer cells (see previous report). During the second and third grant periods we extended this

work to demonstrate that serine phosphorylation of β-catenin has profound effects on its stability and cellular localization. We have found that β-catenin in breast cancer cells is targeted for ubiquitination and proteosomal degradation by phosphorylation of a specific serine residue at the N-terminal. The materials and methods for this work are presented in appendix 2. This serine lies within a consensus sequence which is present in another protein, IκBα, which is also targeted for ubiquitination by serine phosphorylation. This work is now published (29). More recent results indicate that the product of the tumor suppressor gene APC normally targets β-catenin for ubiquitination (see results in appendix 3). This regulation of β-catenin protein levels by serine phosphorylation may well have implications in breast cancer since β-catenin is a central element in the wnt-1 signaling pathway (30). As emphasized in the original proposal wnt-1 overexpression is known to cause breast cancer in mice (31).

Task 3. Statistical analyses (years 3-4). Results will be correlated with tumor stage, blood vessel count, lymph node status, the expression of prognostic markers and period of metastasis-free survival. We are presently accumulating data on phosphorylation status and detergent solubility of cadherins and catenins in breast tumor tissues. This will continue until year 4 when we should have enough material to carry out a statistical analysis

Task 4. To directly examine the role of phosphorylation and plakoglobin expression on breast cancer cell-cell adhesion strength (Years 1-4). We will examine the role of phosphorylation and plakoglobin expression on breast cancer cell-cell adhesion strength by directly examining the effects of kinase inhibitors and plakoblobin transfection on cell-cell adhesion strength using biophysical methods.

Task 4. Methods and Results

To directly examine the role of phosphorylation and plakoglobin expression on breast cancer cell-cell adhesion. In the previous two reports we presented results showing that in two invasive cell lines β-catenin is constitutively tyrosine phosphorylated. We went on to test the hypothesis that this hyperphosphorylation or a lack of plakoglobin is the cause of the failure of transfected E-cadherin to alter the phenotype of the cells. Although we were successful in generating cell lines which expressed plakoglobin we found that increased plakoglobin expression did not make the cells more adhesive even in the presence of E-cadherin. Similarly, simply inhibiting tyrosine phosphorylation did not make the cells more adhesive.

Expression of the mesenchymal cadherin, cadherin 11 in invasive E-cadherin negative breast cancer cells (see results in appendix 4)

Our failure to reverse the poorly adhesive phenotype of invasive breast cancer cells by exogenous expression of E-cadherin or plakoglobin or by inhibition of tyrosine kinase activity prompted us to re-examine the cadherin profile of these cells. In our earlier studies we had generated a model in which invasive breast cancer cells had resulted from an epithelial to mesenchymal transition (EMT (32,33)). In contrast to general opinion, recent data in developing systems has demonstrated that during EMTs the resulting mesenchymal cells do in fact express a cadherin, now characterized as cadherin 11(34). We had demonstrated previously that the invasive breast cancer cells did exhibit a weak form of calcium-dependent adhesion even though they did not express E-cadherin. Immunoprecipitation studies with antibodies to β-catenin also

showed that a band of the appropriate molecular weight for a cadherin (~120 kD) was co-precipitated. Western blots with a pan-cadherin antibody also demonstrated the presence of high levels of an unknown cadherin in these cells. We recently investigated the expression of cadherin 11 in breast cancer cells by RT-PCR and our results are summarized in table 1 (appendix 4). We have now confirmed these results by Northern analysis and western blotting (see appendix 4). Cadherin 11 is expressed in all the invasive breast cancer cells and is never expressed with E-cadherin. In addition, we detected the presence of an alternatively spliced form of cadherin 11. These findings support our argument that breast cancer progression may well be in part due to an EMT. In other experiments we found that N-cadherin was expressed in many breast cancer cell lines but was not restricted to those of a mesenchymal phenotype. These data indicate that it is possible that invasive breast cancer cells express cadherin 11 which is in fact essential for their invasive phenotype. Perhaps specific blockade of cadherin 11 could reverse invasion and tumorigenicity. Another aspect of cadherin 11 is of some interest. Although cad 11 is expressed in embryonic mesenchyme it is not normally expressed in adult mesenchymal cells. However, it is expressed in osteoblasts raising the possibility that cad 11 expression by carcinoma cells could increase the opportunity of these cells to metastasize to bone (35). These data raise the possibility that therapeutic strategies directed at cadherin 11 function or expression should be investigated in the context of preventing invasion and metastasis to bone. It is also possible that cadherin 11 expression could be a useful indicator of tumors which are more likely to give rise to invasive and metastatic tumors. In order for us to pursue these goals it is important that we generate good antibodies to cadherin 11. The antibody we use presently is a gift from ICOS Corporation and is barely adequate for immunocytochemistry. We have made three constructs with which to generate recombinant proteins to be used for antibody preparation. The first encompasses the extracellular domain and should produce function-blocking antibodies, the second and third constructs correspond to the cytoplasmic domain and should produce antibodies specific for the two variants. We have also created a cell line stably expressing a ribozyme directed at cadherin 11.

Retinoid Experiments During the last year we continued our work related to the effect of retinoids on the molecular and cellular aspects of cell-cell adhesion and have the following additional results.

1. Retinoic acid-induced cadherin. In the previous report we showed that retinoid treatment results in increased expression of a cadherin and its localization to a triton-insoluble pool at the cell membrane. The cadherin was detected using a pan-cadherin antibody. We proposed to identify this cadherin, a task that has proved more difficult than we expected. We have tried a degenerate PCR strategy without success and have tried screening a library with the pan-cadherin antibody, but this gave us too much background. We will now try to use primers corresponding to the region recognized by the pan-cadherin antibody and oligo dt to amplify the N-terminal region. We will then use this as a probe to screen a library.

2. Retinoic acid and β-catenin/LEF signalling (see results in appendix 5) As we demonstrated previously, retinoid treatment of SKBR3 cells results in a remarkable differentiation of the cells accompanied by a dramatic increase in the level of β-catenin and decreased cell proliferation (39). In contrast, other studies have shown that elevated β-catenin, through its interaction with the transcription factor LEF can act as an oncogene (36-38). In order to reconcile these apparently contradictory findings we carried out the following experiments.

The activity of LEF can be monitored in cells following transfection of a reporter plasmid containing LEF binding elements and luciferase. We transfected cells with this plasmid and measured the activity of the LEF reporter following retinoic acid treatment. Appendix 5 shows that even though retinoid treatment markedly increases the level of β-catenin in the cells it does not result in increased LEF reporter activity. We then repeated this experiment, this time following transfection of β-catenin. As expected transfecting β-catenin into the cells markedly increased reporter activity. However, this increase in β-catenin/LEF signalling was almost completely inhibited by retinoid treatment (appendix 5). This remarkable result prompted us to look at the distribution of β-catenin in the cells. The signalling activity of β-catenin is thought to be exerted by a cytoplasmic pool whereas its function in adhesion is exerted at the membrane. Appendix 5 shows that although retinoid treatment results in an increase in triton-soluble and insoluble membrane pools of β-catenin it does not increase the cytoplasmic pool. Presumably this explains the failure of retinoid treatment to stimulate LEF-reporter activity. Following transfection of β-catenin there was a marked increase in the levels of β-catenin in the cytoplasm, presumably accounting for the increased LEF-reporter activity. Simultaneous treatment with retinoic acid significantly reduced the levels of cytoplasmic β-catenin perhaps accounting for the decrease in LEF-reporter activity. Similar results were obtained with two other retinoid-sensitive breast cancer cells. In general terms these results showed us that treatment of cells with retinoic acid can both increase the adhesive function of β-catenin as well as decrease its signalling activity. Clearly, we will be looking into the mechanism of action in the following year.

3. A role for AP-1 in the action of retinoic acid? Some of the antiproliferative effects of retinoic acid are mediated through direct inhibition of the AP-1 transcriptional activation complex. We tested the hypothesis that the differentiation and cadherin/catenin responses we have reported involve this pathway. A number of experiments using AP-1 reporters and dominant negatives definitively showed that this was not the case (not shown). Considering that AP-1 activation by jun/fos heterodimers is involved in many different pathways our demonstration that it is not involved in the differentiation effects of retinoic acid is quite interesting.

4. β-catenin and the cell cycle (not shown) In the last report we presented preliminary results indicating that cytoplasmic β-catenin levels varied during the cell cycle. We have now confirmed these results and show that cytoplasmic β-catenin levels are highest at G1/S. Cytoplasmic pools of β-catenin in cells that are blocked in G2/M by nocodazol are undetectable indicating that, like cyclin B, β-catenin is degraded at this stage of the cycle and further points to a role for β-catenin the control of the cell cycle.

Conclusions and implications of the completed research

The major findings of the third year of work are:

1. Our demonstration that a mesenchymal cadherin, cadherin 11, is expressed in invasive breast cancer cells represents a paradigm shift for those of us that work in the cadherin and cancer field. The general model that loss of E-cadherin expression or function leads to the invasive, metastatic phenotype may not be the whole picture. Although many breast cancer cells have lost E-cadherin, there are several examples of cells without E-cadherin which are not invasive. Perhaps increased expression of a mesenchymal cadherin is required in order for

the cells to acquire a migratory invasive phenotype. Cadherin 11 may also promote the metastasis of cancer cells to bone where cadherin 11-expressing osteoblasts are present.

2. The newly described role of β-catenin in a growth factor signaling pathway and as a dominant oncogene in several cancers has prompted a flurry of research activity. Our results show that the signaling pool of β-catenin in the cytoplasm is regulated by ubiquitination and proteosomal degradation and that mutation of a particular serine (S37) inhibits this process.

3. Our results show that in addition to its epithelial-differentiation properties, retinoic acid can inhibit the signaling activity of cytoplasmic β-catenin/LEF. This single result has very important implications in the area of cancer therapeutics. If the anti-cancer effects of retinoic acid are mediated in part by inhibition of β-catenin/LEF signaling this could lead to the development of agents which specifically inhibit this pathway in cancers which are resistant to the effects of retinoids.

Recommended changes

In order to complete the additional work outlined above I would like to request an extension of the award period for an additional 12 months. This will enable us to complete the experiments outlined in the original application and those we have added during the course of the grant.

Bibliography

1. Loewnstein, W.R. Junctional intercellular communication and the control of cell growth. Biochim. Biophys. Acta, *560*: 1-65, 1979.
2. Shiozaki, H., Tahara, H., Oka, H., Miyata, M., Kobayashi, K., Tamura, S., Iihara, K., Doki, Y., Hirano, S., Takeichi, M., and et Expression of immunoreactive E-cadherin adhesion molecules in human cancers. Am. J. Pathol. *139*: 17-23, 1991.
3. Shimoyama, Y., Hirohashi, S., Hirano, S., Noguchi, M., Shimosato, Y., Takeichi, M., and Abe, O. Cadherin cell-adhesion molecules in human epithelial tissues and carcinomas. Cancer. Res. *49*: 2128-2133, 1989.
4. Schipper, J.H., Frixen, U.H., Behrens, J., Unger, A., Jahnke, K., and Birchmeier, W. E-cadherin expression in squamous cell carcinomas of head and neck: inverse correlation with tumor dedifferentiation and lymph node metastasis. Cancer. Res. *51*: 6328-6337, 1991.
5. Mareel, M.M., Behrens, J., Birchmeier, W., De Bruyne, G.K., Vleminckx, K., Hoogewijs, A., Fiers, W.C., and Van Roy, F.M. Down-regulation of E-cadherin expression in Madin Darby canine kidney (MDCK) cells inside tumors of nude mice. Int. J. Cancer. *47*: 922-928, 1991.
6. Frixen, U.H., Behrens, J., Sachs, M., Eberle, G., Voss, B., Warda, A., Lochner, D., and Birchmeier, W. E-cadherin-mediated cell-cell adhesion prevents invasiveness of human carcinoma cells. J. Cell Biol. *113*: 173-185, 1991.
7. Mahoney, P.A., Weber, U., Onefrechuk, P., Blessman, H., Bryant, P., and Goodman, C.S. The fat tumor suppressor gene in drosophila encodes a novel member of the cadherin gene superfamily. Cell, *67*: 853-868, 1991.
8. Sommers, C.L., Gelmann, E.P., and Byers, S.W. Characterization of transfected E-cadherin in human breast cancer cell lines. Mol. Cell Biol. *3*: 12431992.(Abstract)
9. Fearon, E.R. and Vogelstein, B. A genetic model for colorectal tumorigenesis. Cell, *61*: 759-767, 1990.

10. Takeichi, M. Cadherins: a molecular family important in selective cell-cell adhesion. Annu. Rev. Biochem. *59*: 237-252, 1990.
11. Takeichi, M. Cadherin cell adhesion receptors as a morphogenetic regulator. Science, *251*: 1451-1455, 1991.
12. Hirai, Y., Nose, A., Kobayashi, S., and Takeichi, M. Expression and role of E- and P-cadherin adhesion molecules in embryonic histogenesis. Development, *105*: 271-277, 1989.
13. Gallin, W.J., Chuong, C.M., Finkel, L.H., and Edelman, G.M. Antibodies to liver cell adhesion molecule perturb inductive interactions and alter feather pattern and structure. Proc. Natl. Acad. Sci. U. S. A. *83*: 8235-8239, 1986.
14. Herrenknecht, K., Ozawa, M., Eckerskorn, C., Lottspeich, F., Lenter, M., and Kemler, R. The uvomorulin-anchorage protein alpha catenin is a vinculin homologue. Proc. Natl. Acad. Sci. U. S. A. *88*: 9156-9160, 1991.
15. Nagafuchi, A., Takeichi, M., and Tsukita, S. The 102 kd cadherin-associated protein: similarity to vinculin and posttranscriptional regulation of expression. Cell, *65*: 849-857, 1991.
16. Hirano, S., Kimoto, N., Shimoyama, Y., Hirohashi, S., and Takeichi, M. Identification of a neural alpha-catenin as a key regulator of cadherin function and multicellular organization. Cell, *70*: 293-301, 1992.
17. Matsuyoshi, N., Hamaguchi, M., Taniguchi, S., Nagafuchi, A., Tsukita, S., and Takeichi, M. Cadherin-mediated cell-cell adhesion is perturbed by v-src tyrosine phosphorylation in metastatic fibroblasts. J Cell Biol. *118*: 703-714, 1992.
18. Lee, S.W., Tomasetto, C., Paul, D., Keyomarsi, K., and Sager, R. Transcriptional downregulation of gap junction proteins blocks junctional communication in human mammary tumor cell lines. J. Cell Biol. *118*: 1213-1221, 1992.
19. Jongen, W.M., Fitzgerald, D.J., Asamoto, M., Piccoli, C., Slaga, T.J., Gros, D., Takeichi, M., and Yamasaki, H. Regulation of connexin 43-mediated gap junctional intercellular communication by Ca2[in mouse epidermal cells is controlled by E-cadherin. J. Cell Biol. *114*: 545-555, 1991.
20. Yeatman, T. and Bland, K. Staging of breast cancer. In: K.I. Bland and E.M. Copeland (eds.), The breast: Comprehensive management of benign and malignant diseases, pp. 313-330, W.B. Saunders and Co. 1991.
21. Gamallo, C., Palacios, J., Suarez, A., Pizarro, A., Navarro, P., Quintanilla, M., and Cano, A. Correlation of E-cadherin expression with differentiation grade and histological type in breast carcinoma. Am. J Pathol. *142*: 987-993, 1993.
22. Oka, H., Shiozaki, H., Kobayashi, K., Inoue, M., Tahara, H., Kobayashi, T., Takatsuka, Y., Matsuyoshi, N., Hirano, S., Takeichi, M., and et Expression of E-cadherin cell adhesion molecules in human breast cancer tissues and its relationship to metastasis. Cancer Res. *53*: 1696-1701, 1993.
23. Rasbridge, S.A., Gillett, C.E., Sampson, S.A., Walsh, F.S., and Millis, R.R. Epithelial (E-) and placental (P-) cadherin cell adhesion molecule expression in breast carcinoma. J Pathol. *169*: 245-250, 1993.
24. Eidelman, S., Damsky, C.H., Wheelock, M.J., and Damjanov, I. Expression of the cell-cell adhesion glycoprotein cell-CAM 120/80 in normal human tissues and tumors. Am. J. Pathol. *135*: 101-110, 1989.
25. Lindblom, A., Rotstein, S., Skoog, L., Nordenskjold, M., and Larsson, C. Deletions on chromosome 16 in primary familial breast carcinomas are associated with development of distant metastases. Cancer Res. *53*: 3707-3711, 1993.

26. Nishida, N., Fukuda, Y., Kokuryu, H., Sadamoto, T., Isowa, G., Honda, K., Yamaoka, Y., Ikenaga, M., Imura, H., and Ishizaki, K. Accumulation of allelic loss on arms of chromosomes 13q, 16q and 17p in the advanced stages of human hepatocellular carcinoma. Int. J Cancer, *51*: 862-868, 1992.
27. Carter, B.S., Ewing, C.M., Ward, W.S., Treiger, B.F., Aalders, T.W., Schalken, J.A., Epstein, J.I., and Isaacs, W.B. Allelic loss of chromosomes 16q and 10q in human prostate cancer. Proc. Natl. Acad. Sci. U. S. A. *87*: 8751-8755, 1990.
28. Byers, S.W., Sommers, C.L., Hoxter, E., Mercurio, A.M., and Tozeren, A. The role of E-cadherin in the response of tumor cell aggregates to lymphatic, venous and arterial flow: Measurement of cell-cell adhesion strength. J. Cell Sci. *108*: 2053-2064, 1995.
29. Orford, K., Crockett, C., Jensen, J., Weissman, A., and Byers, S.W. Serine phosphorylation-regulated ubiquitination and degradation of beta catenin. J. Biol. Chem. *272*: 24735-24738
30. Cowin, P. and Burke, B. Cytoskeleton-membrane interactions. Curr. Opin. Cell Biol. *8*: 56-65, 1996.
31. Brown, A.M., Wildin, R.S., Prendergast, T.J., and Varmus, H.E. A retrovirus vector expressing the putative mammary oncogene int-1 causes partial transformation of a mammary epithelial cell line. Cell, *46*: 1001-1009, 1986.
32. Sommers, C., Heckford, S.E., Skerker, J.M., Worland, P., Thompson, E.W., Byers, S.W., and Gelman, E.P. Loss of epithelial markers and acquisition of vimentin expression in adriamycin-and vinbastine resistant breast cancer cell lines. Cancer Res. *52*: 5190-5197, 1992.
33. Sommers, C.L., Byers, S.W., Thompson, E.W., Torri, J.A., and Gelmann, E.P. Differentiation state and invasiveness of human breast cancer cell lines. Breast Cancer Res. Treatment, *31*: 325-335, 1994.
34. Simonneau, L., Kitagawa, M., Suzuki, S., and Thiery, J.P. Cadherin 11 expression marks the mesenchymal phenotype. Towards new functions for cadherins? Cell Adhes. Commun. *3*: 115-130, 1995.
35. Okezaki, M., Takeshita, S., Kawai, S., Kikuno, R., Tsujimura, A., Kudo, A., and Amman, E. Molecular cloning and characterization of OB-cadherin, a new member of cadherin family expressed in osteoblasts. J. Biol. Chem. *269*: 12092-12098, 1994.
36. Korinek, V., Barker, N., Morin, P.J., van Wichen, D., de Weger, R., Kinzler, K.W., Vogelstein, B., and Clevers, H. Constitutive transcriptional activation by a b-catenin-Tcf Complex in $APC^{-/-}$ colon carcinoma. Science, *275*: 1784-1787, 1997.
37. Morin, P.J., Sparks, A.B., Korinek, V., Barker, N., Clevers, H., Vogelstein, B., and Kinzler, K.W. Activation of b-catenin/Tcf signaling in colon cancer by mutations in b-catenin or APC. Science, *275*: 1787-1790, 1997.
38. Rubinfeld, B., Robbins, P., El-Gamil, M., Albert, I., Porfiri, E., and Polakis, P. Stabilization of β-catenin by genetic defects in melanoma cell lines. Science, *275*: 1790-1792, 1997.
39. Byers, S., Pishvaian, M., Crockett, C., Peer, C., Tozeren, A., Sporn, M., Anzano, M. and Lechleider, R. Retinoids increase cell-cell adhesion strength, β-catenin stability and localization to the cell membrane in a breast cancer cell line: A role for serine kinase activity. Endocrinology. *137*: 3265-3273, 1996

APPENDIX 1

Journal of Cell Science 108, 2053-2064 (1995)
Printed in Great Britain © The Company of Biologists Lim.

Role of E-cadherin in the response of tumor cell aggregates to lymphatic, venous and arterial flow: measurement of cell-cell adhesion strength

Stephen W. Byers[1,*], Connie L. Sommers[1], Becky Hoxter[1], Arthur M. Mercurio[2] and Aydin Tozeren[3]

[1]Department of Cell Biology and the Lombardi Cancer Center, Georgetown University Medical Center, Washington DC 20007, USA
[2]Laboratory of Cancer Biology, Deaconess Hospital, Harvard Medical School, Boston MA 02115, USA
[3]Department of Mechanical Engineering, The Catholic University of America, Washington DC 20064, USA

*Author for correspondence

SUMMARY

Defects in the expression or function of the calcium dependent cell-cell adhesion molecule E-cadherin are common in invasive, metastatic carcinomas. In the present study the response of aggregates of breast epithelial cells and breast and colon carcinoma cells to forces imposed by laminar flow in a parallel plate flow channel was examined. Although E-cadherin negative tumor cells formed cell aggregates in the presence of calcium, these were significantly more likely than E-cadherin positive cell aggregates to disaggregate in response to low shear forces, such as those found in a lymphatic vessel or venule (<3.5 dyn/cm^2). E-cadherin positive normal breast epithelial cells and E-cadherin positive breast tumor cell aggregates could not be disaggregated when exposed to shear forces in excess of those found in arteries (>100 dyn/cm^2). E-cadherin negative cancer cells which had been transfected with E-cadherin exhibited large increases in adhesion strength only if the expressed protein was appropriately linked to the cytoskeleton. These results show that E-cadherin negative tumor cells, or cells in which the adhesion molecule is present but is inefficiently linked to the cytoskeleton, are far more likely than E-cadherin positive cells to detach from a tumor mass in response to low shear forces, such as those found in a lymphatic vessel or venule. Since a primary route of dissemination of many carcinoma cells is to the local lymph nodes these results point to a novel mechanism whereby defects in cell-cell adhesion could lead to carcinoma cell dissemination

Key words: cadherin, tumor, adhesion

INTRODUCTION

Alterations in cell-cell and cell-extracellular matrix adhesion properties are consistently associated with the progression of carcinoma from a non-invasive to an invasive, metastatic phenotype (Liotta and Stetler Stevenson, 1991; Liotta, 1992; Takeichi, 1991; Albelda and Buck, 1990; Hynes, 1992). Several families of adhesion molecules have been implicated in these changes including the cadherins and integrins (Schipper et al., 1991; Frixen et al., 1991; Hynes, 1992). The expression of the calcium-dependent cell-cell adhesion molecule E-cadherin is reduced or completely lost in some invasive carcinomas and carcinoma cell lines (Schipper et al., 1991; Shimoyama et al., 1989; Shiozaki et al., 1991). Although these cells are likely to be capable of forming aggregates using alternative adhesion pathways, the loss of E-cadherin expression and/or function is generally thought to aid the local invasion process (Frixen et al., 1991; Behrens et al., 1989). Nevetheless, in other studies we found that most E-cadherin negative breast cancer cell lines were not more invasive than E-cadherin positive cells (Sommers et al., 1991). Instead, the highly invasive phenotype was invariably associated with expression of the mesenchymal intermediate filament protein vimentin. Disruption of E-cadherin function in E-cadherin positive breast cancer cells resulted in the loss of cell-cell contact but did not result in the cells becoming more invasive (Sommers et al., 1991). Similarly, transfection of E-cadherin into invasive vimentin positive cells did not reverse the invasive phenotype even though it allowed the transfected cells to aggregate specifically with E-cadherin transfected fibroblasts (Sommers et al., 1994). Clearly, in this system loss of functional E-cadherin expression does not necessarily lead to an invasive phenotype. Although it is possible, in certain circumstances, that complete cell-cell detachment might be a required step in local invasion, in many developmental and clinical examples and in other instances of tissue remodeling, invasion of a surrounding tissue or matrix is not necessarily accompanied by complete loss of cell-cell contact. Rather, cohorts of cells migrate as cohesive sheets or as linked cells in single file (the so called 'Native American file'). This is certainly the case in malignant neoplasia of the breast (Pierson and Wilkinson, 1990). Why then should so many breast cancer cells and tumors have lost E-cadherin mediated adhesion if it may not be absolutely required for local invasion? Another important step in carcinoma progression is the movement of tumor cells or emboli to local lymph nodes or distant sites via

the lymphatic or venous circulation. In some situations it is possible that, in order to enter the fluid in a lymph vessel or vein, tumor cells must be detached from the primary tumor mass either as individuals or as aggregates by the laminar flow imposed by the circulatory system. In this case, the physical strength of homotypic cell adhesion may be a significant determinant in the ability of a tumor cell to enter the circulation.

In the present study we test the hypothesis that defects in E-cadherin-mediated adhesion result in a reduction in cell-cell adhesion strength which in turn leads to an increased likelihood of cells detaching from a tumor mass when exposed to lymphatic, venous or arterial flow. In order to exert tensile and shear forces on cell-cell contact sites, laminar flow was imposed on cell aggregates which were adherent to a planar substratum. The time course of the deformation and disaggregation response of the aggregates was recorded at a wide range of flow rates. The cells used in these assays included E-cadherin positive epithelial cells, cells with known defects in E-cadherin expression or function as well as cell lines transfected with E-cadherin. The assays showed that defects in the expression or function of E-cadherin or associated molecules significantly reduces the physical strength of homotypic cell-cell adhesion. We measure for the first time the strength of E-cadherin mediated adhesion and, importantly, show that the shear stresses required to disaggregate E-cadherin negative cells correspond closely to those found in a lymphatic vessel or capillary.

MATERIALS AND METHODS

Cells

The cell lines used in the experiments were E-cadherin positive normal human breast epithelial cells (MCF-10A) (Soule et al., 1990), E-cadherin positive weakly invasive human breast carcinoma cells (MCF-7), E-cadherin negative poorly invasive human breast cancer cell line SKBR3, E-cadherin negative highly invasive human breast carcinoma cells (HS578T, BT549; Sommers et al., 1991), E-cadherin and control transfected HS578T, BT549 cells (HS-Ecad, BT-Ecad; Sommers et al., 1994), E-cadherin transfected mouse L-cells (L-Ecad; Sommers et al., 1994), E-cadherin positive, α-catenin negative human colon cancer cell clone A (Breen et al., 1993), E-cadherin negative human colon cancer cell RKO, and E-cadherin and control transfected RKO cells (RKO-Ecad, Breen et al., 1995). Following 3 days in culture confluent cultures of cells were trypsinized with 0.025% trypsin in the presence of 5 mM Ca^{2+}. The resulting suspension of single cells and small aggregates was washed and resuspended in 5 ml of DMEM containing 5% FBS at a concentration of 2×10^6 cells/ml and maintained at 37°C in a humidified CO_2 incubator for 2-4 hours to regenerate cell surface proteins. All experiments were performed at 32°C within 4 hours of trypsinization.

Flow chamber

A parallel flow chamber of uniform width was used in the laminar flow assays (Chien and Sung, 1987). The chamber consists of (a) an upper plate having appropriate openings for the delivery of the fluid into and out of the channel, (b) a gasket with an opening in the form of a channel, (c) a transparent bottom plate (grade no. 1 coverslip) and (d) top and bottom stainless steel cover plates with observation slots. The bottom plate, the gasket, and the base plate are fastened between the cover plates. The entry port of the chamber is connected through a valve and teflon tubing to two syringes, one filled with cell suspension and the other filled with suspending medium. Before use in the flow chamber glass coverslips were coated with laminin (10 μg/cm^2) or collagen type I (10 μg/cm^2) as described earlier (Tozeren et al., 1994).

A syringe pump (Harvard Apparatus) was used to pump medium into the chamber at specified flow rates. The shear stress on the bottom plate of the chamber along the direction of flow, τ (dyn/cm^2), was evaluated using the following equation, assuming Poiseuille flow:

$$\tau = 6\mu Q/h^2 w, \quad (1)$$

where μ (0.01 dyn-s/cm^2) is the viscosity of the medium, Q (cm^3/s) is the flow rate, h is the gap thickness of the channel (0.012 cm) and w (1 cm) is the width of the chamber (Chien and Sung, 1987).

Laminar flow assays

Laminar flow assays were inititated by placing the flow chamber on the stage of an inverted microscope (Diaphot, Nikon Inc., Garden City, NJ) equipped with 10× and 40× Hoffman and brightfield objective lenses. The cell suspension was gently infused into the flow channel and cell aggregates allowed to interact with the matrix protein-coated glass coverslip for 20 minutes under static conditions. Flow was then initiated at $\tau = 1.75$ dyn/cm^2 and the flow rate increased at 30 second or one minute intervals up to a maximum value of $\tau = 100$ dyn/cm^2.

A video camera (DAGE-MTI) was attached to the side port of the microscope to record the deformation/disaggregation response of cell aggregates to imposed laminar flow. The times were displayed on the video monitor with a data mixer (Vista Electronics, La Mesa, CA) and the length and width of the cell aggregates before and during flow were determined using a position analyzer mixer (Vista Electronics, La Mesa, CA) that provided a digital readout proportional to the distance between two sets of vertical and horizontal lines.

Flow-induced disaggregation of both small (2-6) cells and lar[illegible] aggregates were recorded. Large aggregates were defined as the[illegible] whose largest dimension before the imposition of flow was 70-14[illegible] μm. Large carcinoma cell aggregates typically contained multiple layers of cells with many cells adherent to neighboring cells but not to the planar substratum.

A detachment event was said to occur when a single cell or a small cell aggregate detached from the parent aggregate in response to the imposed flow. In each experiment with a large aggregate, the number of detachment events during a one minute interval of infusion at a constant level of shear stress was determined. The total number of disaggregation events performed with each cell type varied between 8 and 14. The mean and standard deviation of the number of detachment events were computed as a function of the fluid shear stress imposed on the laminin or collagen-coated glass coverslip. The mean value was denoted as the frequency of disaggregation.

RESULTS

Flow-induced disaggregation of large cell aggregates

Laminar flow was imposed on large aggregates which were incubated on the bottom plate of the flow channel for 20 minutes under static conditions. The coverslip was coated with either laminin or collagen depending on the cell type. Pilot experiments showed that MCF-10A and clone A cells attached more firmly to laminin and that MCF-7, HS578T and BT549 cells attached better to collagen type 1. Following the attachment period, a few cells at the bottom of the aggregates formed adhesive contacts that were strong enough to resist detachment by flow. However, most of the cells in the aggregates were not in contact with the substratum and it is these cells that could

be detached (or could not be detached) from one another by flow. In this system, laminar flow will impose force on cell-cell contact sites only if some cells in the aggregate are anchored to the substratum. In this case it is clear that strength of cell-substratum adhesion of those cells which are in contact with the substratum must be strong enough to allow disaggregation without the aggregate detaching from the substrate as a whole. The videomicrographs (particularly Figs 1, 2 and 7) clearly show that even the small aggregates reoriented rapidly in response to the imposition of flow showing that cell-substratum attachment is not involved in the stretching response of the cells to shear forces. Generally, aggregates were anchored to the substrate through one or two cells, which remained attached to the substratum even after the rest of the aggregate completely disaggregated in response to flow. Cells that did become detached from one another were instantly swept away by the flow without any interaction with the substratum, indicating that cell-matrix adhesion did not contribute significantly to the observed phenomena.

MCF-7 and MCF10A cells which were pre-treated for several hours with low calcium medium (50 μM) or with antibodies to E-cadherin prior to laminar flow assays did not form aggregates of measurable adhesive strength (not shown). In other studies using some of the same cells we demonstrate that for those cells with functional E-cadherin-mediated adhesion the ability to form aggregates is lost when cells are exposed to low calcium medium or antibodies to E-cadherin (Sommers et al., 1991, 1994). The E-cadherin positive cells used in these experiments do not form strong aggregates under these conditions, consequently cell-cell adhesion strength is very low and cell aggregates disaggregate as they are being infused into the flow chamber. Preformed aggregates exposed to low calcium medium in the flow chamber exhibited much weaker cell-substratum adhesion and many of the aggregates detached from the substratum as a whole at low shear forces. In two other cell types (L-cells and RKO cells) transfection of E-cadherin restored strong cell cell adhesion whereas neo transfectants behaved as controls. These E-cadherin transfected cells also do not form aggregates in low calcium medium or in the presence of antibodies to E-cadherin (see also results in Sommers et al., 1994: Breen et al, 1995).

The fluid shear stress applied to the coverslip ranged from 2.5 dyn/cm^2 to 100 dyn/cm^2. At low flow rates, aggregates of E-cadherin positive MCF-10A or MCF-7 cells rapidly aligned in the direction of flow in order to reduce fluid drag (Fig. 1). At high flow rates, these aggregates deformed extensively, physically straining cell-cell contact sites (Figs 1, 2). However, cells or small aggregates could not be detached from the aggregates of MCF-10A or MCF-7 cells despite the imposition of high flow rates (τ = 100 dyn/cm^2; Table 1). In a few instances aggregates detached as a whole from the coverslip at high flow rates.

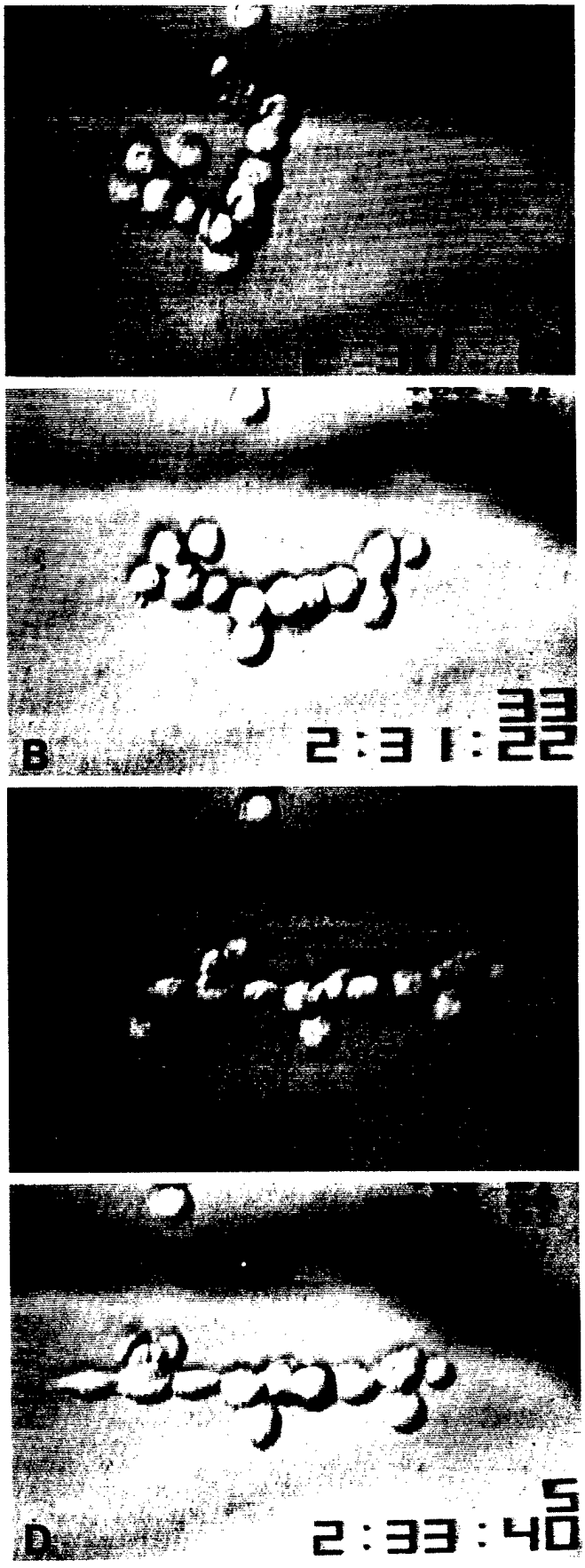

Fig. 1. Sequence of video-micrographs showing the typical deformation response of MCF-10A cells to imposed laminar flow. The numbers at the bottom of the screen represent, hour, minute, second, and tens of milliseconds. Flow was initiated at 2:30:00 at τ – 1.75 dyn/cm^2 and was incrementally increased every 30 seconds such that the shear stress τ took the values 1.75 (A), 3.5, 7.0 (B), 10.5, 14, 21, 35 (C) and 50 dyn/cm^2 (D). The figure shows that the string of MCF-10A cells orient in the direction of flow and deform extensively but do not detach from each other.

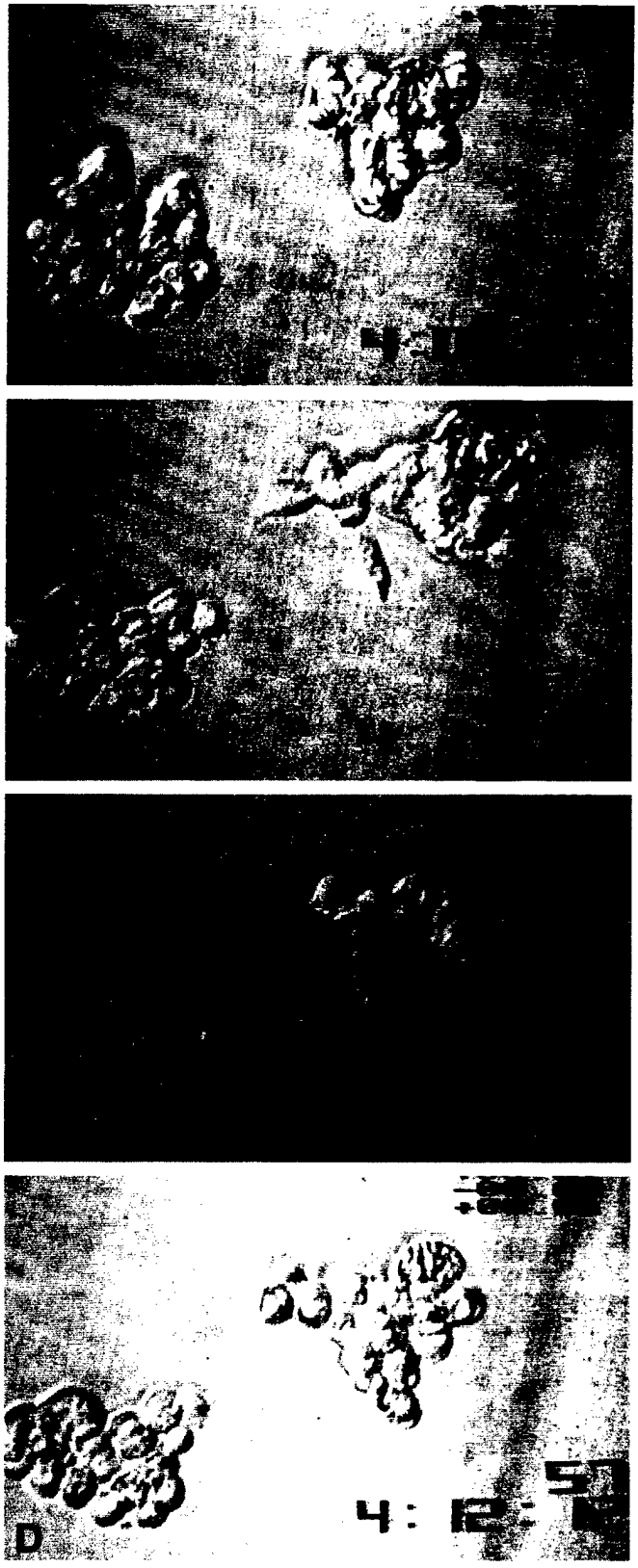

Fig. 2. Sequence of video-micrographs showing the typical deformation response of large aggregates of MCF-7 cells to imposed laminar flow. Flow was initiated at 4:08:00 at $\tau = 1.75$ dyn/cm^2 and was increased every 30 seconds such that the shear stress τ took the values 1.75, 3.5 (A), 7.0, 10.5, 14, 21, 35 dyn/cm^2 (B,C). The flow ceased at 4:12:02 and the aggregate returned to its original configuration in 10 seconds (D).

Table 1. Relationship between E-cadherin protein expression and E-cadherin function

Cell	E-cadherin	E-cad function	τ for disagg.	Invasiveness
MCF-10A	+	+	>100 dyn/cm^2	–
MCF-7	+	+	>100 dyn/cm^2	+
T47D	+	+	>100 dyn/cm^2	+
SKBR3	–	–	<7 dyn/cm^2	+
HS578T	–	–	<7 dyn/cm^2	+++
BT549	–	–	<7 dyn/cm^2	+++
RKO	–	–	<7 dyn/cm^2	+++
L949	–	–	<7 dyn/cm^2	++
HS578T-Ecad	+	–	<7 dyn/cm^2	+++
BT549-Ecad	+	–	<7 dyn/cm^2	+++
L949-Ecad	+	+	7-100 dyn/cm^2	+
RKO-Ecad	+	+	>100 dyn/cm^2	+
Clone A	+	–	>7 dyn/cm^2	++

The relationship was assessed by the presence or absence of Triton-insoluble E-cadherin at points of cell-cell contact and/or the ability of transfected E-cadherin to mediate a morphological change (Sommers et al., 1991, 1994; Breen et al., 1993, 1995), shear stress forces for disaggregation, and invasiveness. The invasive characteristics of these cells have been described previously (Sommers et al., 1991, 1994; Breen et al., 1993, 1995).

In contrast, cells from large aggregates of E-cadherin negative HS578T and BT549 breast carcinoma cells disaggregated in response to the imposed laminar flow at low to moderate flow rates (2.5 dyn/cm^2 ≤ τ ≤ 15 dyn/cm^2). Fig. 3 shows that individual cells and small BT549 cell aggregates detached from the parent aggregate at low levels of fluid shear stress ($\tau = 2.5$ dyn/cm^2).

The flow-induced detachment of cells and cell aggregates from the parent aggregate is a stochastic process that not only depends on the applied fluid shear stress, the geometry of the cell aggregate and its orientation with respect to flow, but also on the number density and the physical strength of the bonds which act to keep the cells together. For these reasons a large number of disaggregation experiments were performed on cell aggregates of comparable size (70-140 μm) for each cell type. The frequency of detachment events from parent aggregates as a function of applied fluid shear stress (τ) for HS-578T and BT-549 cells is presented in Fig. 4. Both these cell types began to disaggregate at fluid shear stress levels found in lymphatics and in the circulation (2.5-15 dyn/cm^2). The frequency of detachment events decreased with increasing shear stress because the number of cells available for detachment was reduced during the course of the experiments. Thus, although the E-cadherin negative highly invasive breast carcinoma cells used in the present study form large aggregates in the presence of calcium the shear forces required to disaggregate these cell aggregates are quite low.

In similar experiments we found that all cells which were E-cadherin negative exhibited a similar detachment response to flow (Table 1). However, the inability of cell aggregates to remain intact in laminar flow was not restricted to aggregates of E-cadherin negative carcinoma cells. Table 1 shows that the E-cadherin positive colon carcinoma cell line clone A also disaggregated in response to low shear stresses. This cell is known not to express the E-cadherin-associated molecule α-catenin, a

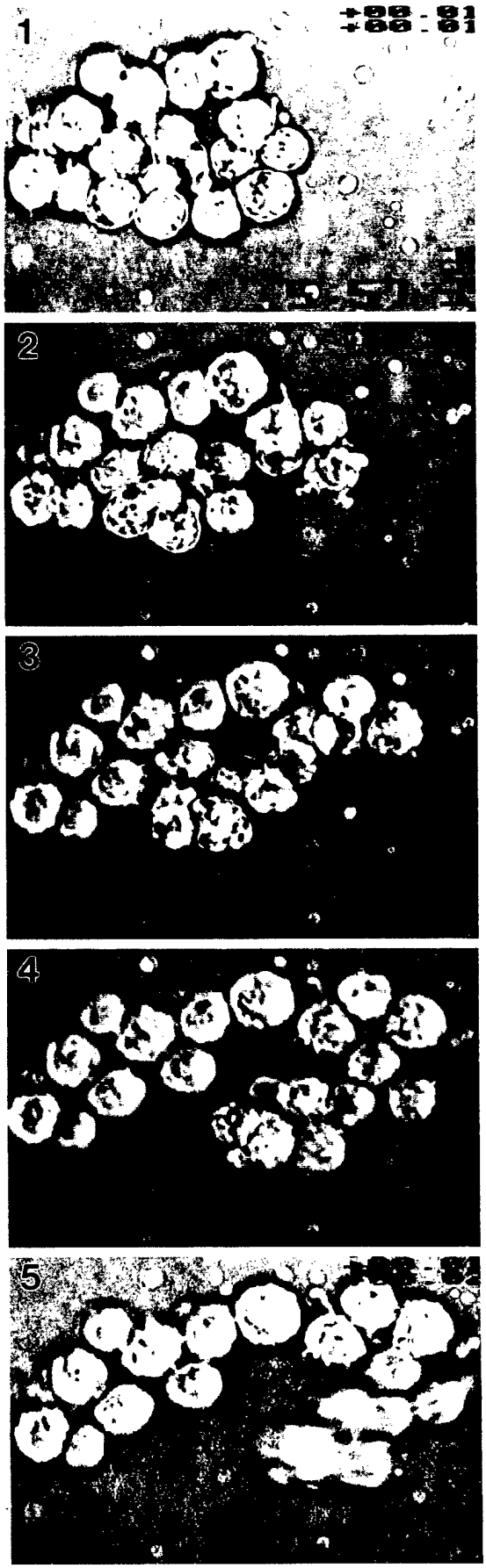

Fig. 3. Sequence of video-micrographs showing the flow-induced disaggregation of a large aggregate of E-cadherin-negative BT-549 cells. Flow was initiated at 5:57:00 at $\tau = 1.75$ dyn/cm^2 and was increased every 60 seconds such that the shear stress τ took the values 2.5 dyn/cm^2 (1, 2), and 5.0 dyn/cm^2 (3, 4, 5).

defect that is likely responsible for the failure of aggregates of these cells to resist low shear stresses (Breen et al., 1993).

E-cadherin transfection prevents flow induced-disaggregation only when it is restricted to cell-cell contact sites

Transfection of BT-549 and HS-578T cells with E-cadherin cDNA did not change their flow-induced aggregation properties (Fig. 4) even though we had demonstrated previously that it could mediate specific aggregation with E-cadherin transfected fibroblasts (Sommers et al., 1994). Expression levels of E-cadherin protein in the transfected cells was similar to those of MCF-7 cells as judged by immunocytochemistry, western analysis and immunoprecipitation (Sommers et al., 1994). In contrast, aggregates of E-cadherin transfected RKO cells remained intact when exposed to high shear stresses (Fig. 5). Similarly, E-cadherin transfected L-cells acquired calcium-dependent cell-cell adhesion properties and their frequency of detachment was much lower at all shear stress levels than E-cadherin negative breast tumor cells (Fig. 5). As shown on several occasions by others, untransfected L-cells did not form aggregates in the presence or absence of calcium (Sommers et al., 1991, 1992, 1994). Similarly, E-cadherin transfected RKO cells do not form aggregates in low calcium medium or in the presence of E-cadherin antibodies (Breen et al., 1995). These results indicate that whereas E-cadherin expression is required for cell aggregates to resist high shear stress forces other factors also contribute to the ability of E-cadherin to mediate strong cell-cell adhesion. It is well known that E-cadherin is linked to the cell cytoskeleton through other molecules, β-catenin, α-catenin, γ-catenin and/or plakoglobin (see for review, Kemler, 1993). Alterations in the expression or phosphorylation state of these E-cadherin-associated molecules have previously been demonstrated to modulate E-cadherin mediated adhesion (Shimoyama et al., 1992; Hirano et al., 1992; Matsuyoshi et al., 1992). The two E-cadherin transfected invasive breast cancer cell lines used in the present study have elevated levels of tyrosine phosphorylated β-catenin and reduced plakoglobin levels (Sommers et al., 1994). In these cells the transfected E-cadherin is not restricted to cell-cell contact sites and is largely Triton soluble. In contrast, exogenous E-cadherin expressed in MCF-7 cells and in L-cells becomes restricted to cell-cell contact sites and is Triton insoluble in these areas (Sommers et al., 1994). Similarly, Triton insoluble E-cadherin is expressed at cell-cell contact sites in the E-cadherin transfected colon carcinoma cell line RKO (Fig. 6). Therefore the ability of cell aggregates to remain intact in laminar flow not only depends upon E-cadherin expression but also on the presence of a Triton-insoluble form of E-cadherin at cell-cell contact sites.

The role of E-cadherin expression in the physical strength of cell-cell contact sites

The capacity of cell-cell contact sites to resist external tensile forces was investigated by determining the deformation response of string-shaped aggregates to imposed laminar flow. Laminar flow imposed on MCF-10A chains led to extensive

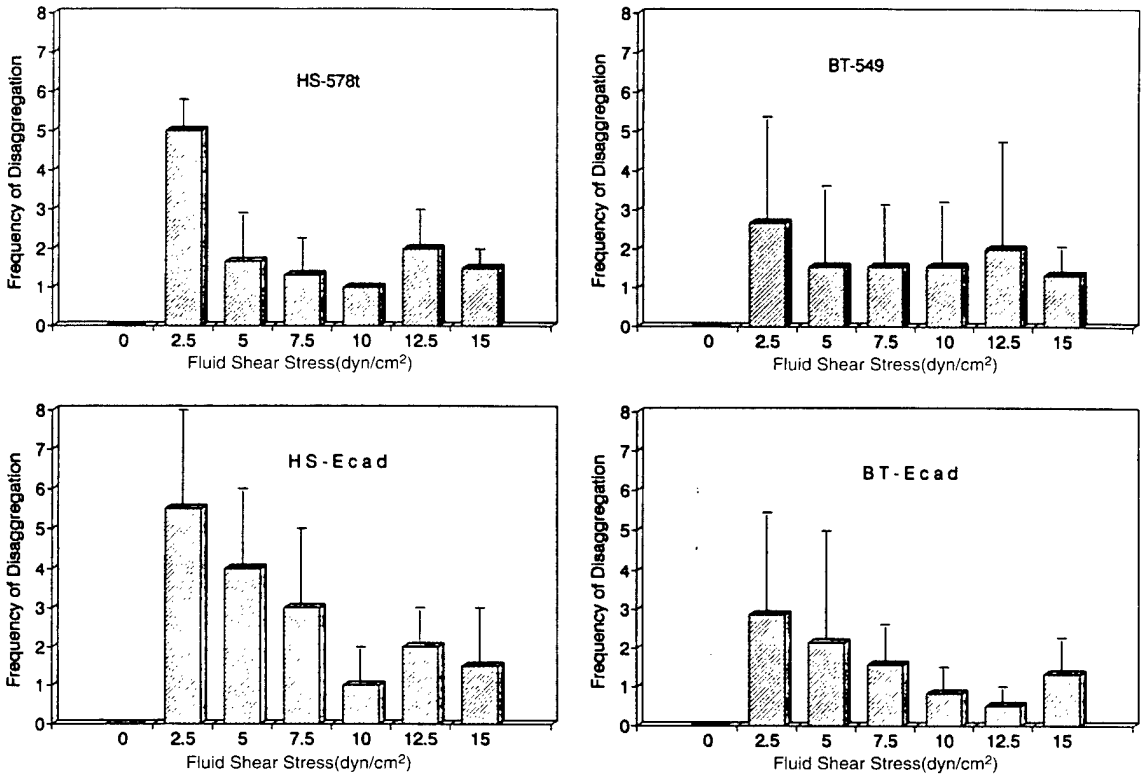

Fig. 4. Frequency of disaggregation of BT-549, BT-Ecad, HS-578T and HS-Ecad cell aggregates in response to applied fluid shear stress. The bars and vertical lines indicate the mean values and the standard deviation of the number of detachment events observed during 60 seconds of flow at a specified shear stress. The total number of experiments was 12. The disaggregation response of aggregates of control (BT-hyg and HS-hyg) cells was similar to that of untransfected cells (not shown).

cell elongation in the direction of flow (Figs 1, 7). As shown in the free body diagram (see Fig. 10) these cells were approximately under uniaxial tension loading. The cell aggregates remained attached to the substratum through a single cell at a few focal contacts and the adhesion contacts between cells could not be broken at levels of fluid shear stress greater than those found in arteries (τ = 100 dyn/cm^2). Flow-induced cell elongation became more pronounced with increasing shear stress and with relative position within the string of cells.

A measure for the extent of cell deformation in the direction of flow is the ratio of instantaneous cell length in the direction of flow (L) to the corresponding length before the imposition of flow (L_0). The deformation index (L/L_0) for three individual cells in different MCF-10A strings was plotted in Fig. 8 as a function of the tensile force exerted on each cell (F_{jm}, see the free body diagram in Appendix). This tensile force was estimated by using the known mathematical solutions of flow past strings of spheres or spheroids (Gluckman et al., 1971) as described in Appendix 1. Fig. 8 shows that MCF-10A cells elongated in the direction of flow as much as 60% under the

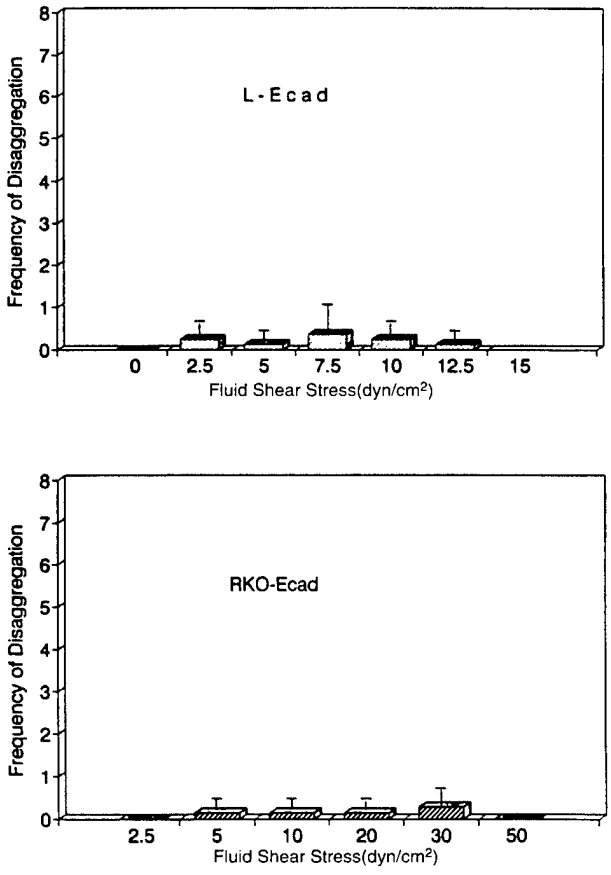

Fig. 5. Frequency of disaggregation of RKO-Ecad and L-Ecad cell aggregates in response to applied fluid shear stress. The bars and vertical lines indicate the mean values and the standard deviation of the number of detachment events observed during 60 seconds of flow at a specified shear stress. The total number of experiments in each case was seven. Aggregates of non-transfected and control RKO transfectants (RKO-neo) disaggregated as they were infused into the flow channel. Untransfected and control (L-neo) L-cells did not form aggregates under the conditions used in the experiments.

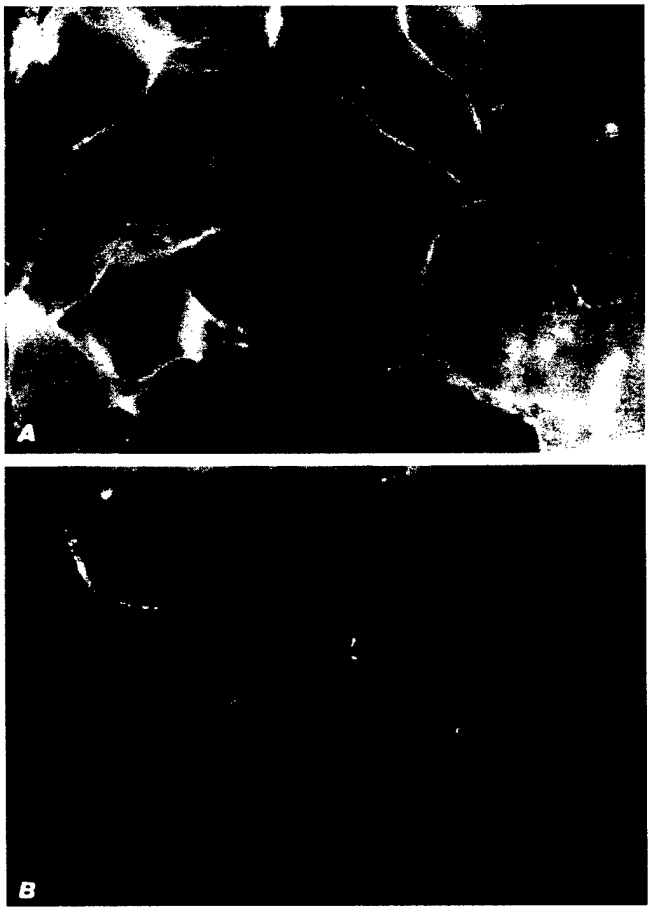

Fig. 6. Triton insoluble E-cadherin is present at cell-cell contact sites in E-cadherin-transfected RKO cells. RKO cells transfected with E-cadherin were immunostained for E-cadherin before (A), or after (B) extraction with Triton X-100 as described previously (Sommers et al., 1994).

action of tensile forces in the order of 10^{-3} dyn. The deformation response of these cells is elastic, as the string of cells returned to their undeformed configuration within a few seconds following the cessation of flow (Fig. 7). The force-deformation response of MCF-7 breast carcinoma cells was similar to that of MCF-10A cells (Table 2).

Fig. 9 shows the deformation and disaggregation response of a typical HS-578T doublet exposed to laminar flow. The cells started to detach from each other at $\tau = 7$ dyn/cm^2. The tensile force that caused detachment in this case (F_{22}) was estimated, using equations (2) to (5) in Appendix, as 10^{-5} dyn, a value that is two orders of magnitude smaller than the external force resisted by MCF-10A cell-cell contact sites. BT549 cells also exhibited a weak adhesive contact (Table 2). Fig. 9 also shows that the HS-578T cell disaggregation was preceded by the formation of a tether between the two cells, a phenomenon that was also frequently observed during the flow-induced detachment of clone A and BT-549 cells.

DISCUSSION

In this study laminar flow assays were used to investigate the forces involved in homotypic cell-cell adhesion. Laminar flow

Table 2. Biophysical parameters of homotypic cell-cell adhesion

Cell type	Flow (dyn/cm^2)*	Tensile contact force (dyn)†	Longitudinal stretching‡
MCF-10A	>100	$>5\times10^{-3}$	>60%
MCF-7	>70	$>2\times10^{-3}$	>60%
HS-578T	>2.5	$\cong10^{-5}$	Tethered
BT-549	>2.5	$\cong10^{-5}$	Tethered

*Fluid shear stress that leads to disaggregation.
†Tensile force resisted by contact sites.
‡Longitudinal stretching before cell detachment.

was imposed on aggregates of cells that were adherent to a laminin or collagen-coated coverslip. The shear flow past aggregates exerted large forces on some of the cell-cell contact sites in the aggregate. The results indicated that cell-cell adhesion strength is severely compromised in E-cadherin negative carcinoma cells and that E-cadherin expression is a necessary but not sufficient condition for firm cell-cell adhesion. Cells which expressed E-cadherin in a Triton-insoluble form at cell-cell contact sites resisted disaggregation when exposed to shear stress forces in excess of 100 dyn/cm^2. In contrast, E-cadherin negative cells or cells in which E-cadherin was present as a diffusely distributed Triton-soluble form detached from one another at values of fluid shear stress comparable to those found in lymphatic and post-capillary blood venules. Consistent with these experimental observations the external forces resisted by adhesive contacts between E-cadherin positive MCF-10A cells were at least two orders of magnitude larger than those between E-cadherin negative breast carcinoma cells.

Transfection of E-cadherin into HS-578T and BT-549 cells does not alter their morphology or invasive properties (Sommers et al., 1994) and we show in this study that it has no effect on the disaggregation response of these cells to flow. However, the absence of a Triton-insoluble pool of E-cadherin in the transfected carcinoma cells points to a defect in E-cadherin interaction with the cytoskeleton (Sommers et al., 1994; Ozawa et al., 1990; Nelson et al., 1990). It is known that these particular invasive breast carcinoma cells have a defect in the expression or function of the cadherin associated molecules β-catenin and plakoglobin (Hirano et al., 1992; Matsuyoshi et al., 1992; Shimoyama et al., 1992; Sommers et al., 1994). The inability of these cells to link transfected E-cadherin to the cytoskeleton probably explains the failure of E-cadherin transfection to alter the disaggregation response of these cells in the present study. In order to rigorously test the contribution of E-cadherin-mediated adhesion to the resistance to disaggregation forces we transfected the mouse fibroblast cell line L-949 with E-cadherin. This line has previously been demonstrated to express several cadherin-associated molecules and to link the transfected cadherin to the cytoskeleton (Ozawa et al., 1990; McNeill et al., 1990). E-cadherin transfected L-cells acquired calcium-dependent cell-cell adhesion and had disaggregation properties in response to shear, similar to those of E-cadherin positive normal breast and non-invasive breast tumor cells (Fig. 4). Although a small number of E-cadherin transfected L-cells could be detached by shear forces the frequency of detachment was 20 fold less than E-cadherin negative tumor cells. As shown on several occasions by others,

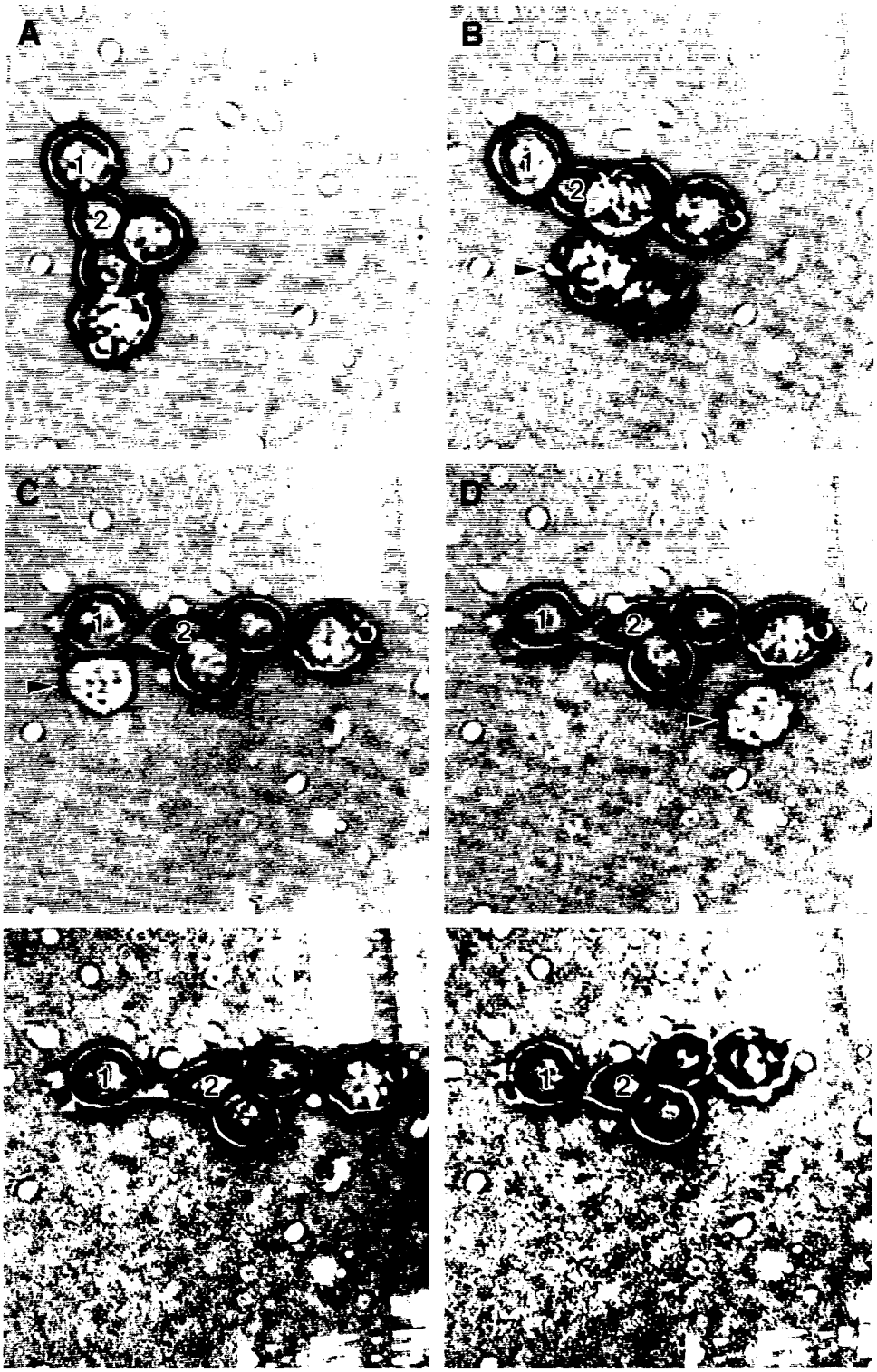

Fig. 7. The effect of shear stress on the orientation and deformation of a small aggregate of E-cadherin positive MCF-10A cells. The fluid shear stress on the laminin-coated coverslip corresponding to micrographs A-F was 0, 7, 35, 70, 100 and 0 dyn/cm^2, respectively. Note the longitudinal stretching between cells 1 and 2. The arrowhead indicates a cell transiently interacting with the substratum.

untransfected L-cells did not aggregate significantly in the presence or absence of calcium (McNeill et al., 1990; Ozawa et al., 1990; not shown). Immunocytochemistry revealed a Triton-insoluble pool of E-cadherin at points of cell-cell contact in aggregates of non-invasive breast tumor cells and E-cadherin transfected L-cells indicating that a strong linkage had been established with the cytoskeleton (Sommers et al., 1994; Ozawa et al., 1990; Nelson et al., 1990). Another E-cadherin negative carcinoma cell line that responds to E-cadherin transfection by a marked change in morphology and motility properties was also used to investigate the role of E-cadherin in adhesion strength (RKO-Ecad; Breen et al., 1995). These cells form few aggregates of low adhesive strength before E-cadherin transfection (Table 1). Following transfection of E-cadherin into these cells they acquired disaggregation properties similar to those of E-cadherin positive epithelial cells such

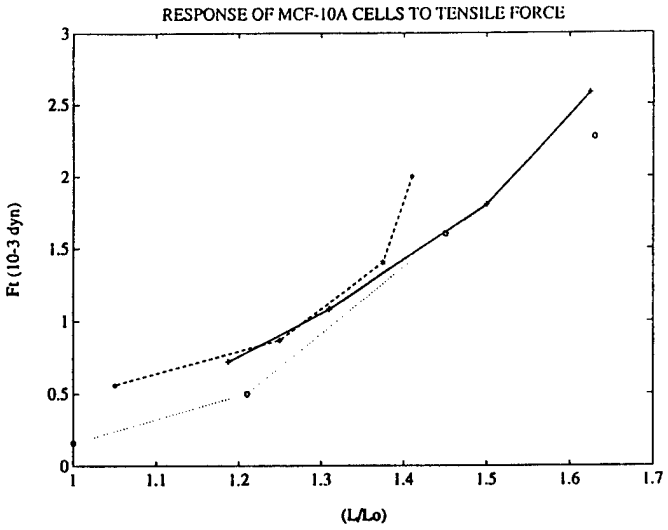

Fig. 8. The deformation response of three typical MCF-10A cells to tensile force. The data shown were obtained in laminar flow assays on MCF-10 cell aggregates in the form of strings of cells. The tensile fluid force (Ft) acting on a cell was computed as described in the appendix. The deformation index (L/L0) denotes the ratio of the cell length at a specified shear stress and time to that before the imposition of flow. The parameter L was measured 28 seconds after the imposition of flow at a given fluid shear stress.

as MCF-10A (Table 1). These results indicate that E-cadherin-mediated adhesion is largely responsible for the disaggregation properties of cells which express this molecule on the cell surface and which are able to link it appropriately to the cell cytoskeleton. It is possible that further strengthening of adhesion may require the assembly of other epithelial cell-specific junctions such as desmosomes.

The physical strength of adhesion between two cells is likely to be dependent upon a number of factors, including the number of adhesion bonds per contact area, their spatial distribution, and linkage to the cytoskeleton. In epithelial cells E-cadherin is generally restricted to the actin-associated adherens junction which forms a belt within which the E-cadherin is presumably present at a high local density and linked to the underlying actin cytoskeleton. The physical strength of MCF-10A cell-cell adhesion is comparable to that between T-lymphocytes and their specific target cells and between phorbol-12-myristate-13-acetate-stimulated T-lymphocytes and planar membranes containing intercellular adhesion molecule-1 (Tozeren et al., 1992a,b; Sung et al., 1986). In these experi-

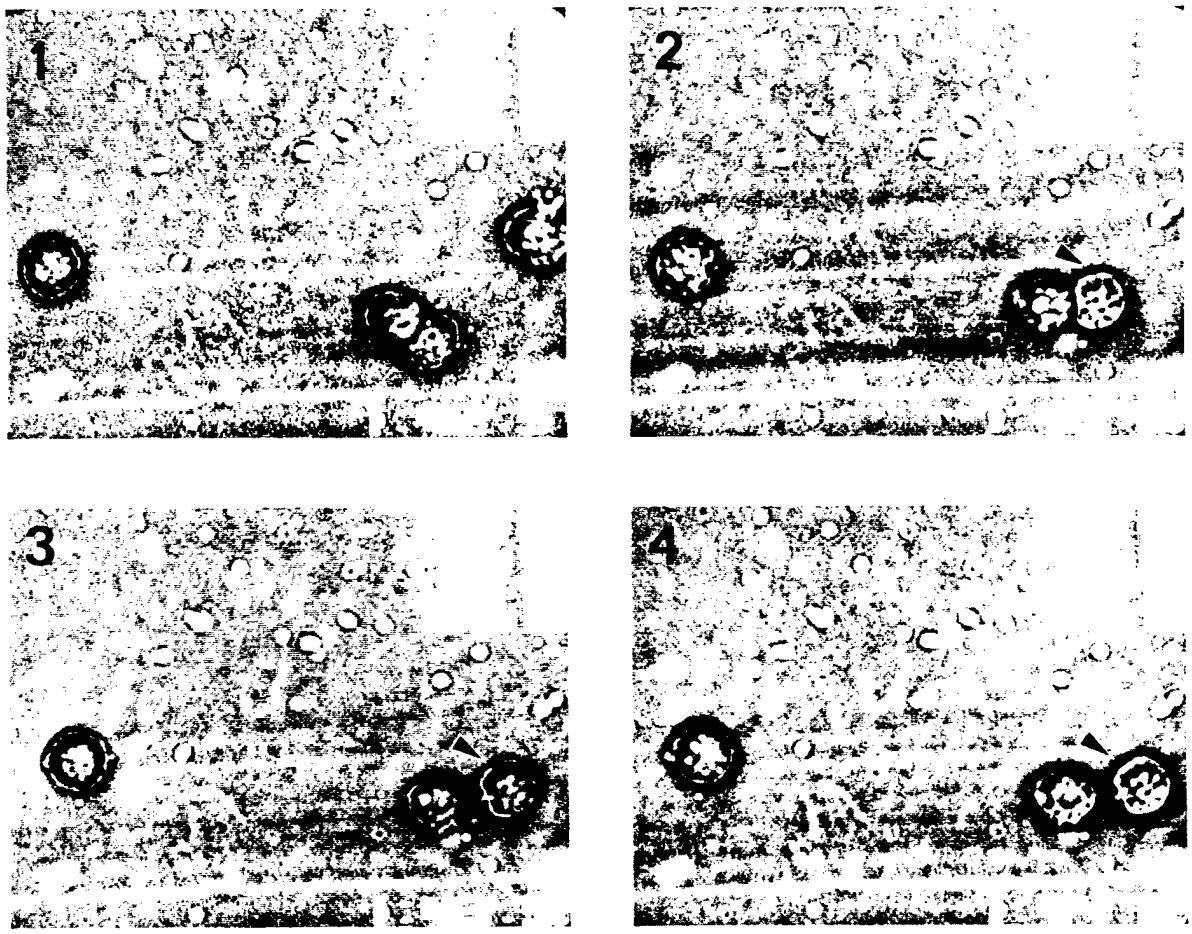

Fig. 9. The effect of fluid shear stress on the deformation and disaggregation of a HS-578T breast carcinoma cell doublet. The flow was imposed on the doublet adherent to a laminin-coated coverslip and was increased incrementally every 30 seconds. In micrographs 1-4 the fluid shear stress on the coverslip was 0, 7, 14 and 21 dyn/cm^2. Note that the cell indicated by the arrowhead detaches from the adjacent cell without appreciable longitudinal stretching.

ments, the tensile forces acting on the adhesion sites were evaluated using a micromanipulation procedure in which cell couples were detached from each other using a micropipette attached to a pressure control system. The extent of MCF-10A elongation in response to tensile force is also comparable to that of T-lymphocytes under similar loading conditions suggesting similar bulk rheological properties (Tozeren et al., 1992a,b; Sung et al., 1986). MCF-10A cells retracted to their undeformed spherical configuration rapidly after the cessation of flow. This elastic behaviour may be due to metabolically regulated tension in the actin-rich submembrane cortical shell (Stossel, 1993). Alternatively, such elastic properties are inherent in the tensegrity model of cytoskeletal organization proposed by Ingber and co-workers (Wang et al., 1993).

The deformation response of E-cadherin-negative breast carcinoma cells to fluid forces is quite different from that observed with MCF-10A cells. At low to moderate flow rates tensile forces acting on contact sites between two cells typically results in the formation of tethers without appreciable change in cell shape. This suggests that although cell-cell adhesion does occur between these cells, the adhesive molecules which mediate it are not linked strongly to the cell cytoskeleton.

To our knowledge the present study is the first to use laminar flow assays to measure epithelial cell-cell adhesion strength. The use of such direct mechanical measurements coupled with the techniques of molecular and cellular biology may lead to a new understanding of the mechanochemical processes which govern many cellular events (Ingber, 1994). In this study such a combination of molecular and cellular manipulations together with biophysical approaches was used to investigate the role of E-cadherin in cell-cell adhesion. The results suggest that E-cadherin negative tumor cells, or cells in which the adhesion molecule is present but is inefficiently linked to the cytoskeleton, are far more likely than E-cadherin positive cells to detach from a tumor mass in response to low shear forces, such as those found in a lymphatic vessel or venule. In these cells the relative strength of cell-substratum (endothelial cells or extracellular matrix) and cell-cell adhesion is likely to determine whether a particular tumor would disaggregate in response to flow. This permits the speculation that once a breast or colon tumor infiltrates a blood or lymphatic vessel, E-cadherin negative cells may be detached by the flow and subsequently be captured by local lymph nodes or become lodged in distant capillary beds. These data, taken together with recent evidence that the E-cadherin-associated molecule β-catenin interacts directly with the tumor suppressor gene APC (Su et al., 1993), strongly suggest that alterations in the cadherin-based adhesion and signalling system not only affect the invasive capacity of tumor cells but may also influence contact-dependent growth control and metastasis.

APPENDIX

Evaluation of external forces acting on cell-cell boundaries

External forces acting on cell-cell contact sites in the direction perpendicular (tensile force) to the contact surface were computed by using data obtained from laminar flow assays on cell aggregates that were composed of a string of cells. Mathematical solution of axisymmetric flow past a finite chain of spheres each having radius R was considered (Fig. 10). Let m denote the number of spheres in the chain and integer j indicate the relative position of spheres along the chain such that $j = 1$ is the free end of the chain and $j = m$ is the end fixed to the substratum (Fig. 10). The drag force fjm exerted by the surrounding fluid on the j sphere in the chain can be computed using the following equation:

$$f_{jm} = 6\pi\mu(U)(R)\lambda_{jm}, \tag{2}$$

where μ is the coefficient of viscosity of the surrounding fluid, U is the velocity of the uniform flow far from the chain of spheres, R is the radius of the identical spheres in the chain and the drag correction factor λjm is a function of the total number of spheres in a chain and the relative position of the sphere

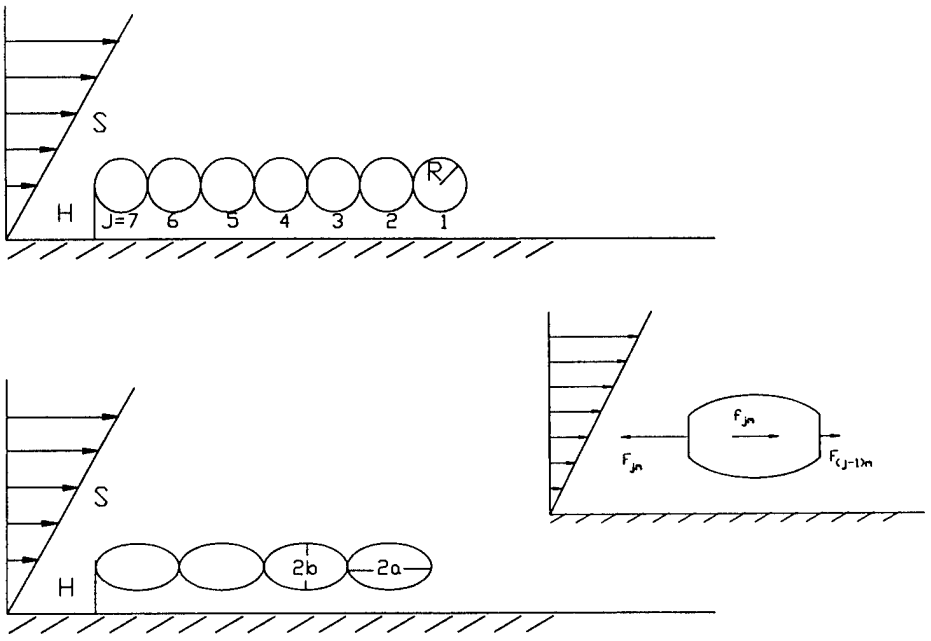

Fig. 10. Schematic diagram showing chains of spheres and spheroids fixed in simple shear flow near a planar boundary. Also shown is a free body diagram of a cell within the chain which indicates the forces exerted on the cell.

within the chain (Gluckman et al., 1971). $\lambda_{jm} = 1$ when $j = m = 1$, and $\lambda_{jm} = 0.65$ for $m = 2$ and $j = 1$ or 2. The solution for five or more chains indicates that the drag on the spheres located in the central portion of the chain changes little as the number of spheres in the chain is increased. As the end of the chain is approached, the drag on the spheres increases rapidly indicating a shielding effect. For example, in a seven sphere chain $\lambda_{17} = \lambda_{77} = 0.56$, $\lambda_{27} = \lambda_{67} = 0.28$, $\lambda_{37} = \lambda_{57} = 0.26$ and $\lambda_{47} = 0.25$ (Gluckman et al., 1971).

Let F_{jm} denote the total external force exterted by the surrounding fluid on the contact area between spheres j and $j + 1$ in a chain composed of m spheres (Fig. 10). The condition of the force balance indicates that:

$$F_{jm} = \sum_1^{j+1} (f_{jm}). \tag{3}$$

This force is tensile in nature, that is, it will tend to stretch the bonds connecting the two cells in the direction perpendicular to the contact surface.

Gluckman et al. (1971) also provided Stokes flow solutions involving chains of prolate spheroids. A prolate spheroid is an axisymmetric body obtained by rotation of an ellipse along its long axis (Fig. 10). In this case of strings of prolate spheroids equation (2) is replaced by the following equation:

$$f_{jm} = 6\pi\mu(U)(b)\lambda_{jm}, \tag{4}$$

where b is the maximal radial distance along the minor axis of the prolate spheroid (Gluckman et al., 1971). In this case, the drag correction factor λ_{jm} depends not only on j and m but also on the ratio of the maximal length of the spheroid ($2a$) to its maximal diameter ($2b$). For two touching spheroids with $a/b = 2$, $\lambda_{12} = \lambda_{22} = 0.85$ the total drag force on a chain of spheroids is approximately equal to that of a chain of spheres having the same length and maximal radial distance (Gluckman et al., 1971).

In the experimental investigation presented here the cell chains were stationary not in uniform flow but in simple shear flow near a planar boundary. In order to use equations (2) and (4) in the actual experimental case, the velocity parameter U appearing in these equations was taken to be equal to the velocity of simple shear flow at the central axis of the string of cells:

$$U = (H)(S) = H\tau/\mu, \tag{5}$$

where H is the distance from the central axis of the cell chain to the planar membrane, S is the shear gradient of the simple shear flow and the wall shear stress τ is equal to the coefficient of friction m times the shear gradient S (Hsu and Ganatos, 1989). In this approximation, the effect of the planar wall on the drag coefficient factor λ_{jm} is not taken into account. The known solution concerning a sphere near a plane wall in simple shear flow indicates that wall effects may result in an increase in the drag force by as much as 60% (Goldman et al., 1967). Thus, the values provided here underestimate the external force resisted by MCF-10A cell-cell contact sites.

In actual computations, the wall shear stress τ was determined from the specified flow rate with the use of equation (1). The geometric parameters a and b were determined from the videotapes of the time course of deformation of the string of cells. The distance from the string center to the glass coverslip (H) was assumed for all cases to be equal to 1.5 times the maximal cell radius (b). The measured distance variations required for the inverted microscope to clearly focus on the strings of cells with a 40× objective indicated that the assumed value of H cannot be different from the actual value by more than 50%. Because the tensile force is proportional to H, the order of magnitude of the estimate for the total drag force must be correct.

The string of cells attached at one end to the laminin-coated glass coverslip also had cells attached to the side of the chain (see Figs 1, 6). In such instances the contact forces between cells positioned upstream of the side-wise attached cell increased by the amount equal to the drag force acting on the side-wise attached cell. This force was computed by using the drag force coefficient factor for two equal spheres whose line of centers is perpendicular to the direction of imposed flow (Ganatos et al., 1978).

The authors are grateful to Drs Richard Skalak and Hynda Kleinman for useful discussions and to Marc Lippmann for his continued support. Supported by a grant from the Department of Defence.

REFERENCES

Albelda, S. M. and Buck, C. A. (1990). Integrins and other cell adhesion molecules. *FASEB J.* **4**, 2868-2880.

Behrens, J., Mareel, M. M., Van Roy, F. M. and Birchmeier, W. (1989). Dissecting tumor cell invasion: epithelial cells acquire invasive properties after the loss of uvomorulin-mediated cell-cell adhesion. *J. Cell Biol.* **108**, 2435-2447.

Breen, E., Clarke, A., Steele, Jr, G. and Mercurio, A. M. (1993). Poorly differentiated colon carcinoma cells deficient in alpha-catenin expression express high levels of surface E-cadherin but lack calcium-dependent cell-cell adhesion. *Cell Adhesion Commun.* **1**, 239-250.

Breen, E., Steele, Jr, G. and Mercurio, A. M. (1995). The cadherin/catenin complex regulates changes in cell-cell and cell-matrix interactions associated with the invasive behavior of colon carcinoma cells. *Arch. Surg. Onc.* (in press)

Chien, S. and Sung, L. A. (1987). Physicochemical basis and clinical implications of red cell aggregation. *Clin. Hemorheol.* **7**, 71-91.

Frixen, U. H., Behrens, J., Sachs, M., Eberle, G., Voss, B., Warda, A., Lochner, D. and Birchmeier, W. (1991). E-cadherin-mediated cell-cell adhesion prevents invasiveness of human carcinoma cells. *J. Cell Biol.* **113**, 173-185.

Ganatos, P., Pfeffer, R. and Weinbaum, S. (1978). A numerical solution technique for three dimensional Stokes flows, with application to the motion of strongly interacting spheres in a plane. *J. Fluid Mech.* **84**, 79-111.

Gluckman, M. J., Pfeffer, R. and Weinbaum, S. (1971). A new technique for treating multiparticle slow viscous flow past spheres and spheroids. *J. Fluid Mech.* **50**, 705-740.

Goldman, A. J., Cox, R. G. and Brenner, H. (1967). Slow viscous motion of a sphere parallel to a plane wall II. Couette flow. *Chem. Eng. Sci.* **22**, 653-660.

Hirano, S., Kimoto, N., Shimoyama, Y., Hirohashi, S. and Takeichi, M. (1992). Identification of a neural alpha-catenin as a key regulator of cadherin function and multicellular organization. *Cell* **70**, 293-301.

Hsu, R. and Ganatos, P. (1989). The motion of a rigid body in viscous fluid bounded by a plane wall. *J. Fluid Mech.* **207**, 29-72.

Hynes, R. O. (1992). Integrins: versatility, modulation, and signaling in cell adhesion. *Cell* **69**, 11-25.

Ingber, D. E. (1994). The riddle of morphogenesis - a question of solution chemistry or molecular cell engineering. *Cell* **75**, 1249-1252.

Kemler, R. (1993). From cadherins to catenins-cytoplasmic protein interactions and regulation of cell adhesion. *Trends Gen.* **9**, 317-321.

Liotta, L. A. and Stetler Stevenson, W. G. (1991). Tumor invasion and metastasis: an imbalance of positive and negative regulation. *Cancer Res.* **51**, 5054s-5059s.

Liotta, L. A. (1992). Cancer cell invasion and metastasis. *Sci. Am.* **266**, 54-9, 62-3.

Matsuyoshi, N., Hamaguchi, M., Taniguchi, S., Nagafuchi, A., Tsukita, S.

and Takeichi, M. (1992). Cadherin-mediated cell-cell adhesion is perturbed by v-src tyrosine phosphorylation in metastatic fibroblasts. *J. Cell Biol.* **118**, 703-714.

McNeill, H., Ozawa, M., Kemler, R. and Nelson, W. J. (1990). Novel function of the cell adhesion molecule uvomorulin as an inducer of cell surface polarity. *Cell* **62**, 309-316.

Nelson, W. J., Shore, E. M., Wang, A. Z. and Hammerton, R. W. (1990). Identification of a membrane-cytoskeletal complex containing the cell adhesion molecule uvomorulin (E-cadherin), ankyrin and fodrin in Madin-Darby canine kidney epithelial cells. *J. Cell Biol.* **110**, 349-357.

Ozawa, M., Ringwald, M. and Kemler, R. (1990). Uvomorulin-catenin complex formation is regulated by a specific domain in the cytoplasmic region of the cell adhesion molecule. *Proc. Nat. Acad. Sci. USA* **87**, 4246-4250.

Pierson, K. K. and Wilkinson, E. J. (1990). Malignant neoplasia of the breast: infiltrating carcinomas. In *The Breast* (ed. K. I. Bland and E. M. Copeland III), pp. 193-209. Philadelphia, PA: W. B. Saunders & Co.

Schipper, J. H., Frixen, U. H., Behrens, J., Unger, A., Jahnke, K. and Birchmeier, W. (1991). E-cadherin expression in squamous cell carcinomas of head and neck: inverse correlation with tumor dedifferentiation and lymph node metastasis. *Cancer. Res.* **51**, 6328-6337.

Shimoyama, Y., Hirohashi, S., Hirano, S., Noguchi, M., Shimosato, Y., Takeichi, M. and Abe, O. (1989). Cadherin cell-adhesion molecules in human epithelial tissues and carcinomas. *Cancer. Res.* **49**, 2128-2133.

Shimoyama, Y., Nagafuchi, A., Fujita, S., Gitch, M., Takeichi, M., Tsukita, S. and Hirohashi, S. (1992). Cadherin dysfunction in a human cancer cell line - possible involvement of loss of alpha-catenin expression in reduced cell - cell adhesiveness. *Cancer Res.* **52**, 5770-5774.

Shiozaki, H., Tahara, H., Oka, H., Miyata, M., Kobayashi, K., Tamura, S., Iihara, K., Doki, Y., Hirano, S., Takeichi, M. et al. (1991). Expression of immunoreactive E-cadherin adhesion molecules in human cancers. *Am. J. Pathol.* **139**, 17-23.

Sommers, C. L., Thompson, E. W., Torri, J. A., Kemler, R., Gelmann, E. P. and Byers, S. W. (1991). Cell adhesion molecule uvomorulin expression in human breast cancer cell lines: Relationship to morphology and invasive capacities. *Cell Growth Differ.* **2**, 365-372.

Sommers, C., Heckford, S. E., Skerker, J. M., Worland, P., Thompson, E. W., Byers, S. W. and Gelman, E. P. (1992). Loss of epithelial markers and acquisition of vimentin expression in adriamycin-and vinbastine resistant breast cancer cell lines. *Cancer Res.* **52**, 5190-5197.

Sommers, C. L., Gelmann, E. P., Kemler, R., Cowin, P. and Byers, S. W. (1994). Alterations in plakoglobin expression and beta-catenin phosphorylation in human breast cancer cell lines. *Cancer Res.* **54**, 3544-3552.

Soule, H. D., Maloney, T. M., Wolman, S. R., Peterson, Jr, W. J., Brenz, R., McGrath, C. M., Russo, J., Pauley, R. J., Jones, R. F. and Brooks, S. C. (1990). Isolation and characterization of a spontaneously immortalized human breast epithelial cell line, MCF-10. *Cancer Res.* **50**, 6075-6086.

Stossel, T. P. (1993). On the crawling of animal cells. *Science* **260**, 1086-1094.

Su, L.-K., Vogelstein, B. and Kinzler, K. W. (1993). Association of the APC tumor suppressor protein with catenins. *Science* **262**, 1734-1737.

Sung, K. L. P., Sung, L. A., Crimmins, M., Burakof, S. J. and Chien, S. (1986). Determination of junction avidity of cyotoxic T-cell and target cell. *Science* **234**, 1605-1608.

Takeichi, M. (1991). Cadherin cell adhesion receptors as a morphogenetic regulator. *Science* **251**, 1451-1455.

Tozeren, A., Mackie, L. H., Lawrence, M. B., Chan, P.-Y., Dustin, M. L. and Springer, T. A. (1992a). Micromanipulation of adhesion of PMA-stimulated T-lymphocytes to planar membranes containing intercellular adhesion molecule-1. *Biophys. J.* **63**, 247-258.

Tozeren, A., Sung, P., Sung, L. A., Dustin, M. L., Chan, P.-Y., Springer, T. A. and Chien, S. (1992b). Micromanipulation of adhesion of a jurkat cell to a planar bilayer membrane containing lymphocyte function-associated antigen 3 molecules. *J. Cell Biol.* **116**, 997-1006.

Tozeren, A., Wu, S., Kleinman, H. K., Mercurio, A. M. and Byers, S. W. (1994). Alpha-6 beta-4 integrin mediates dynamic interactions of breast and colon carcinoma cells on laminin. *J. Cell Sci.* **107**, 3153-3163

Wang, N., Butler, J. P. and Ingber, D. E. (1993). Mechanotransduction across the cell surface through the cytoskeleton. *Science* **260**, 1124-1127.

(Received 30 September 1994 - Accepted 23 January 1995)

Cell Adhesion and Communication
IN PRESS

VINCULIN AND CELL-CELL ADHESION

Aydin Tozeren[1], Stephen Wu[1], Becky Hoxter[2], Weiming Xu[3], Eileen D. Adamson[3] and Stephen W. Byers[2]

[1]Biomedical Engineering Program, The Catholic University of America
620 Michigan Avenue NE, Washington DC 20064

[2]Department of Cell Biology and the Lombardi Cancer Research Center
Georgetown University Medical Center, Washington DC 20007

[3]The Burnham Institute, 10901 North Torrey Pines Road, La Jolla, CA 92037

Running Title: Vinculin and Cell-Cell Adhesion
Key words: Vinculin, Actin, Adhesion, E-cadherin

Corresponding Author: Aydin Tozeren
Phone: 202-319-5671
Fax: 202-319-4499

ABSTRACT

Vinculin, a 117-kDa protein, is a constituent of adhesion plaques and adherence junctions in non-muscle cells. We investigated the role of vinculin on the physical strength of cell-cell adhesion by conducting disaggregation assays on aggregates of parental wild-type F9 mouse embryonal carcinoma cells (clone BIM), two vinculin-depleted F9 cell lines, γ227 and γ229, and a reconstituted γ229 cell line (R3) that re-express vinculin. Immunoblotting demonstrated that the four cell lines used in the study had similar expressions of the cell-cell adhesion molecule E-cadherin and associated membrane proteins α- and β-catenin. Double immunofluorescence analysis showed that, in contrast to the vinculin-null cell lines, BIM and R3 cells expressed abundant vinculin at the cell margins in adhesion plaques and in cell-cell margins that also contained actin. Laminar flow assays showed that both the vinculin-positive and vinculin-negative cell aggregates that were formed in culture in the course of 24 to 48 hours largely remained intact despite the imposition of shear flow at high shear rates. Since laminar flow imposed on cell aggregates act to separate cells from each other, our data indicate that F9 cells that were adherent to a substrate formed strong cell-cell adhesion bonds independent of vinculin expression. On the other hand, aggregates of vinculin-depleted γ229 and γ227 cells that were formed in suspension during a two-hour static incubation at 37°C were desegregated more easily with the imposition of shear flow than the BIM and R3 cell aggregates formed under identical conditions. Loss of vinculin was associated with a reduction in cell-cell adhesion strength only among those cells lacking contact to a substrate. Overall, the results indicate that vinculin is not needed for forming strong cell-cell adhesion bonds between neighboring carcinoma cells which are adherent to the basal lamina.

INTRODUCTION

Vinculin is a cytoskeletal protein molecule closely associated with cell matrix and cell-cell junctions. Vinculin binds strongly to actin-binding proteins such as α-actinin and talin and its affinity to actin depends strongly on its conformational state (Johnson and Craig, 1995), suggesting that it serves as a dynamic link between the cell cytoskeleton and cell surface adhesion molecules such as integrins and E-cadherins (Jockusch and Rudiger, 1996).

Vinculin expression is dramatically downgraded in many highly-malignant and metastatic tumor cells and the tumorigenity of these cells could be suppressed by transfecting them with vinculin cDNA (Rodriguez Fernandez et al., 1992). 3T3 clones displaying decreased vinculin expression showed a round phenotype with a few vinculin-positive plaques localized mostly at the periphery of the cell-substrate contact. These cells displayed an increased motility compared to controls (Rodriquez Fernandez et al., 1993), and produced large colonies in soft agar than the parental counterparts, suggesting that vinculin expression is a determinant of malignant phenotype.

Similarly, a role for vinculin in development is suggested by studies that showed regulation of vinculin expression during embryonic morphogenesis (Lehtonen and Reima, 1986) and during cell migration in vivo (Zieske et al., 1989). Culturing of cells on highly adhesive matrices induce vinculin gene expression, indicating a functional role for vinculin in cell-substrate adhesion (Coll et al., 1995).

To elucidate the exact role of vinculin in cell adhesion and motility, Coll et al (1995) generated stable clones with vinculin-null mutations by disrupting the vinculin gene in F9 embryonal carcinoma and embryonal stem cell clones using homologous recombination. When compared with wild-type cells, vinculin-mutant cells displayed a rounder morphology and a reduced ability to adhere to plastic and fibronectin after one-hour of static incubation. The loss

of vinculin expression resulted in a significant increase in cell motility.

The physical strength of cell-cell adhesion is known to be dependent on the linkage of E-cadherin to the actin-cytoskeleton (McNeill et al., 1993; Byers et al., 1995; Agnes et al. 1996) and vinculin is present in cell-cell junctions. Whether this cytoplasmic molecule has a role in cell-cell adhesion is yet to be determined. In this study, using a laminar flow assay procedure introduced by Byers et al. (1995), we investigated the role of vinculin on cell-cell adhesion, as measured by the capacity of cell aggregates to resist shearing forces. Our study showed that F9 carcinoma cells that were adherent to a substrate formed strong bonds with each other independent of the presence of vinculin in cell-cell junctions. The data also suggest that vinculin might contribute to the stability of colonies formed by carcinoma cells at the initial stages of colony formation.

METHODS

A. Cells

F9 mouse embryonal carcinoma cells (Clone BIM, Grover et al., 1983) were used as the parental wild-type (BIM). Two vinculin null F9 cell lines, γ227 and γ229 (Coll et al., 1995), were compared with BIM and with R3, the reconstituted γ229 cells that re-express vinculin (83% of wt levels). To achieve this, the γ229 cells were transfected with an expression vector in which the β-actin promoter drives the expression of full-length vinculin cDNA. The vector and the resulting cell lines will be described in another paper (W.Xu and E.D. Adamson, in preparation).

B. Indirect Immunofluorescence

Trypsinized washed cells were seeded onto fibronectin (5μg/ml) and polysine-coated

coverslips (5μg/cm^2) as described (Coll et al., 1995) and allowed to grow 1 to 2 days. In this time individual colonies containing from 20 to 40 cells were obtained, with the aim of observing both cell-matrix and cell-cell interfaces within the colonies. The cells were fixed 8 min in 4% paraformaldehyde and permeabilized for 2 min in 0.1% Triton in phosphate-buffered saline. The procedure for double fluorescence staining of vinculin and F-actin was as described previously (Coll et al., 1995). Briefly, rhodamine-phalloidin was used to mark actin and fluorescein-labeled secondary antibodies detected vinculin (rabbit anti-human vinculin, Sigma Chemical Co, St. Louis, Mo) in cells. The cells were viewed in a Zeiss LSM 410 laser scanning confocal microscope. Images were printed in a Sony UP/D7000 digital printer.

C. Immunoblotting

Cells in monolayers at 70% confluence in 100 mm dishes were washed and scraped up with a rubber policeman and lysed in Laemmli sample buffer without 2-mercaptoethenol and bromophenol Blue (BPB). Lysates containing 5 μg/ml leupeptin, 5 μg/ml aprotinin and 1 mm PMSF protease inhibitors were placed in boiling water for 10 min, an aliquot was removed for measurement of the O.D. and equal amounts of protein were analyzed at three different concentrations (the two lowest levels are shown in Fig. 2). The samples were further heated after they were adjusted to contain 2-mercaptoethanol and BPB, and loaded into individual lanes for 7.5% SDS-PAGE (Laemmli, 1970). After electrotransfer to PVDF (Immobilon, Milipore Corp., Bedford, MA) membranes, the blots were processed to reveal E-cadherin, using a rabbit anti-mouse gp84 (Vestweber and Kemler, 1983) at 10 μg/ml together with a mouse monoclonal antibody to β-actin (clone AC-15, Sigma Chemical). Suitable peroxidase secondary antibodies were used to reveal the cellular protein on the membrane. The enhanced chemical luminescence procedure (ECL, Amersham, Little Chalfont, UK) was used to detect the antigen

to which the primary and secondary antibodies had adsorbed. The resulting protein signal on film was analyzed by NIH-Image to estimate the relative levels of each protein band. After removing this first signal from the membrane as described (Krajewski et al., 1995), antibodies to α-catenin (C2081, Sigma) and β-catenin (C2206, Sigma) were used in a second cycle on the same membrane. The level of actin was used to normalize the levels of the other cytoskeletal proteins in each of the four cell lines.

D. Formation of Cell Aggregates

In order to obtain pre-formed cell aggregates, cells were harvested from subconfluent flasks of cells by extensive pipetting. They were then kept at room temperature (24^{o}C) up to an hour before use in laminar flow assays. This method provided large aggregates for cell cultures whose duration ranged between 24 to 48 hours. At shorter incubation times, mechanical disturbance of the cultured cells yielded a combination of single cells and small aggregates, indicating that strong cell-cell adhesion bonds between cultured cells had not yet developed.

In another set of experiments disaggregation assays were performed on aggregates that were formed from single cells in suspension during a two-hour incubation period. Cells were trypsinized for twenty minutes and the resulting single cells were resuspended in DMEM supplemented by 10 percent fetal calf serum at a concentration of 1x10^{6} cells/ml (Hyclone Lab., Inc., Logan, UT). Light microscopy on a sample taken from the cell suspension confirmed the absence of cell doublets or larger aggregates in the suspension. The resulting cell suspension was maintained 2 hrs at 37^{o}C in a 5% CO^{2} incubator to regenerate cell surface proteins and to form cell-cell contacts. Then the disaggregation experiments were performed at 24^{o}C in the next hour. To assure that the differences in the capacity of various cell lines to resist flow-

induced disaggregation did not depend on the small differences in the incubation time, order in which various cell types were used in laminar flow assays were systematically altered.

E. Flow Chamber and Laminar Flow Assays

A parallel plate flow chamber of uniform width was used in the laminar flow assays. The chamber consisted of: (1) a transparent top plate having appropriate openings for the delivery of the fluid into and out of the channel; (2) a 0.15 mm thick thin plastic gasket; (3) a grade no. 1 glass coverslip serving as the bottom plate of the channel (Fisher Scientific, Pittsburgh, PA); and (4) top and bottom stainless steel cover plates with observation slots (Tozeren et al., 1994).

The glass coverslips used as bottom plates were coated with fibronectin (Becton Dickinson Labware, Bedford, MA). Briefly, proteins were diluted in serum-free culture medium (DMEM) from a stock-solution to reach a final concentration of 50 μg/ml and placed on the centers of coverslips in the form of 50 μl drops. Such drops eventually coat an approximately circular region of 0.5 cm^2 in area, yielding a surface concentration of 5 $\mu g/cm^2$ (Tozeren et al., 1994). The coverslips were then incubated at 24°C for two hours and were rinsed in distilled water three times before use in the experiments.

The bottom plate, the gasket and the top plate were fastened between the cover plates. The entry port of the chamber was connected through a valve and teflon tubing to a syringe filled with suspending medium. The cell suspension was infused directly into a chamber from a small opening through the top plate.

The shear stress on the bottom plate of the chamber in the direction of flow, τ_b (dyn/cm^2), was evaluated using the following equation, assuming Poiseuille flow:

$$\tau_b = 6\mu Q/(h^2 w) \qquad (1)$$

where μ (~0.01 dyn-s/cm^2) is the viscosity of the cell medium, Q (cm^3/s) is the flow rate, h (0.012 cm) is the gap thickness of the channel and w (1 cm) is the width of the channel (Tozeren et al., 1994).

Flow-induced disaggregation of large aggregates were performed as described in Byers et al. (1995). Experiments were initiated by placing the flow chamber on the stage of an inverted microscope (Diaphot, Nikon Inc., Garden City, NJ). The cell suspension (containing cell aggregates as well as single cells) were infused into the chamber and allowed to interact with the fibronectin-coated glass coverslip under static conditions for 15 minutes. A syringe pump (Harvard Apparatus, South Natick, MA) was then used to pump the cell medium into the chamber at specified flow rates. A 40x phase contrast objective and a videocamera system (DAGE-MTI) attached to the side port of the microscope were used to record the disaggregation events.

Aggregates whose largest dimension before the imposition of flow was 70 to 140 μm were classified as large aggregates. These aggregates typically contained multiple layers of cells, with many cells adherent to neighboring cells but not to the planar substratum. A detachment event was said to occur when a cell or a cluster of cells detached from the remaining stationary aggregate in response to the imposed flow. The average number of detachments per cell aggregate and its standard deviation were determined by quantifying the number of detachment events per aggregate for at least 12 large cell aggregates of a given cell type (Byers et al., 1995).

RESULTS

Location of Vinculin at Cell Margins

We used double immunofluorescence analysis to confirm the lack of vinculin and the

presence of F-actin in γ227 and γ229 cells (Fig. 1). The actin filaments were, on average, slightly shorter due to the smaller diameter of these rounded cells, but this was not obvious in Fig. 1. The result of a similar analysis of the cell line R3 is shown in Fig. 1b. This cell line was produced from the transfection of full-length mouse vinculin cDNA in an expression vector into γ229 cells as described in the Methods section. R3 is one clone from the seven or so that were derived as "rescued" from the null phenotype (W. Xu and E.D. Adamson, in preparation). Rescued cells have similar properties to the wild type in that adhesion, cell shape and motility are within the normal range for F9 cells, in contrast to the γ227 and γ229 vinculin null cell lines (Coll et al., 1995). R3 cells show abundant vinculin (Fig. 1b, green) at the cell margins in adhesion plaques and in cell-cell margins that also contain actin (red, and where coincident, yellow). The outlines of cells within the colony where actin and vinculin occur together, are occasionally visible (yellow dashes). The appearance of R3 cells was very similar to wt F9 cells (BIM), illustrating the rescue of the phenotype by exogenous vinculin and the correct location of the vinculin in adhesion plaques.

Expression of E-cadherin, α- and β-catenin

Our previous study showed that the capacity epithelial cell aggregates would disaggregate only infrequently in response to shear forces imposed on them if cell-cell adhesion bonds were firmly linked to the cell cytoskeleton (Byers et al., 1995). Moreover, flow-induced disaggregation of cell aggregates was not very sensitive to perturbations in the amount of E-cadherin on the cell surface. In order to insure that the differences in the adhesive properties of the four cell lines considered in this study was due to vinculin and not to clonal differences in adhesive protein levels between the cell lines, we used immunoblotting to estimate the levels of E-cadherin, α-catenin, β-catenin and β-actin expressed in BIM, R3, γ227 and γ229 cells.

Figure 2 shows that the levels of these proteins were very similar. NIH Image analysis of the immunoblasts indicated that E-cadherin expression in the four different cell lines used in the study differed by at most 6% from the average of this protein in the four cell lines. The highest deviation, 10.8%, was observed in the expression of β-catenin. These perturbations in the expressions of E-cadherin, α-catenin and β-catenin are rather small in comparision to the differences in vinculin expression between vinculin-null γ-227 and γ-229 F9 cell lines and the wild-type and rescued F9 cell lines. Therefore, it is reasonable to conclude that any differences in the adhesive properties of these cell lines can largely be attributed to presence or absence of vinculin in these cell lines.

Vinculin and Cell-Cell Adhesion

The method we used to elucidate the difference in cell-cell adhesion strength between vinculin-null and vinculin-expressing cells is based on the fluid mechanics principle that laminar flow imposed on a cell aggregate that is adherent to the bottom plate of a flow channel exerts peeling forces on the cell-cell adhesion bonds (Byers et al., 1995). In general, cells in the top layer of an aggregate attached to the bottom plate of a flow channel are exposed to greater levels of shear stress than the lower layers (Brooks and Tozeren, 1996). A cell or a cell aggregate will detach from the parent aggregate when the external fluid force acting on it is large enough to overcome adhesion to neighboring cells. Although the fluid forces acting on cells in an aggregate depend on the geometry of the aggregate, our previous study showed that crosslinking of adhesion bonds to the cell cytoskeleton is the most important determinant of the capacity for disaggregation in response to shear force.

In laminar flow assays, cell suspension was introduced into a flow channel and cell aggregates were allowed to settle on the fibronectin-coated bottom plate of the flow channel for

15 minutes before the imposition of flow. Flow rate was increased at 20 second intervals so that the wall shear stress acting on the bottom plate of the chamber took the values 0, 7, 21, 35, 49, 63, 77, 91, and 105 dyn/cm^2.

First, we present the data corresponding to aggregates formed by incubating single-cell suspensions in test tubes for two hours at 37^{o}C under static conditions. Fig. 3 shows micrographs depicting the response of a large R3 cell aggregate to the imposed shear flow. With an increase in flow rate, R3 cell aggregate shown in the figure unfolded in the direction of flow but did not disaggregate at the highest level of fluid shear stress used in the experiments (91 dyn/cm^2). In contrast, γ227 cell aggregate shown in Fig. 4 unfolded and aligned in the direction of flow at low levels of flow (<21 dyn/cm^2). Further increases in flow rate caused extension of cells in the aggregate in the direction of flow and failure of some cell-cell adhesion bonds, resulting in the disaggregation of the γ227 cell aggregate.

Overall, we conducted 12 such disaggregation experiments with each of the γ227, γ229, BIM, and R3 cell lines. The results, the average number of detachment events per aggregate per cell type and its standard deviation, are presented in Fig. 5. The data shown in the figure indicate that both the vinculin-positive and vinculin-negative cells formed cell-cell adhesion bonds during two hours of incubation, but vinculin-negative γ227 and γ229 cell aggregates disaggregated in response to shear flow more frequently than the BIM and R3 cell aggregates. These results indicate that loss of vinculin was associated with a significant reduction in the cell-cell adhesion strength under the conditions of this experiment.

Next we conducted disaggregation assays on aggregates that were formed in culture during the course of 24 to 48 hours. These pre-formed aggregates were subjected to the same flow conditions as aggregates that were formed during 2 hours of incubation. Micrographs selected from these experiments are shown in Figs. 6 and 7. Overall, there was little

difference between the four cell lines in their capacity to resist disaggregation when aggregates were formed in culture dishes (Fig.5). These results indicate that with time and assembly of mature junctional complexes, vinculin-depleted γ227 and γ229 cells are able to form cell-cell adhesion bonds comparable in strength to the vinculin-positive BIM and R3 cells.

DISCUSSION

In this study we investigated the role of vinculin in the physical strength of cell-adhesion in F9 mouse carcinoma cell lines. Previous studies have shown that the crosslinking of cell-cell adhesion bonds to the cell cytoskeleton is a strong determinant of cell-cell adhesion strength (Byers et al., 1995; Agnes et al., 1996). Since vinculin is present in cell-cell junctions and can bind to actin and other actin-binding molecules, it may serve as a link between E-cadherins and the actin cortex underlying the cell membrane (Lodish et al., 1996).

The vinculin-null F9 cells were obtained by disrupting the vinculin gene in wild-type F9 cells using homologous recombination (Coll et al., 1995). The "rescued" R3 cells were derived from γ229 cells by transfecting them with full-length cDNA (W. Xu and E.D. Adamson, in preparation). R3 cells expressed vinculin at 83 percent of wild-type levels. The expression of E-cadherin and associated proteins (α- and β-catenin) were similar in the cell lines used so that large changes in the expression of vinculin accounted for most of the differences in the adhesive properties of these cell lines. Furthermore, both in parental wild type (BIM) and R3 cells, vinculin was colocalized with actin in cell-cell margins.

Since a number of crosslinking molecules coexist at cell-cell contact sites, role of vinculin on homotypic cell adhesion is likely to be uncovered with an assay that can quantify the level of resistance forces associated with a certain adhesion pathway. In the present study, we adopted a laminar flow assay (disaggregation assay) to examine the role of the intracellular

linking protein vinculin on cell-cell adhesion strength. When disaggregation experiments are performed on cell aggregates of comparable size, the average number of disaggregation events per cell type is quite sensitive to the physical strength of cell-cell adhesion (Byers et al., 1995).

Our experiments showed that aggregates of vinculin-negative γ227 and γ229 cells, formed by incubating single-cell suspensions in test tubes for two hours, desegregated in response to the imposed shear flow more frequently than the aggregates of vinculin-positive BIM and R3 cells, obtained under identical conditions. The data indicate that cell-cell adhesion strength is partially compromised in vinculin-deficient cells during early stages of colony formation in cell suspension. In contrast, when aggregates that were detached from a confluent cell culture (pre-formed aggregates) were used in adhesion assays, differences in cell-cell adhesion strength between vinculin-positive and vinculin-negative cells were not significant. Thus, given the opportunity to adhere to a substrate, F9 mouse carcinoma cells can form strong cell-cell adhesion bonds independent of vinculin.

The results presented here exhibit parallels with the data presented by Coll et al.(1995) on the role of vinculin on cell-matrix adhesion. These authors showed that vinculin-depletion was associated with decreased binding to fibronectin-coated surfaces at early stages of adhesion, however, given time, vinculin-null cells formed focal adhesions that were similar to those formed by vinculin-positive cells. Quantitative digitized microscopy indicated that α-actinin, talin and paxillin were found in focal adhesions at higher concentrations in cells lacking vinculin (Volberg et al., 1995), indicating the existence of molecular mechanisms for formation of focal contacts in the absence of vinculin.

These observations, taken together with our data, indicate that vinculin is not needed for adhesion between neighboring carcinoma cells that are adherent to a substrate.

Although our results indicate that vinculin might enhance stability of carcinoma cell colonies at early stages, contribution of vinculin to cell-cell adhesion need not be through the E-cadherin adhesion pathway. Vinculin might contribute to the stability of carcinoma cell colonies by crosslinking the cytoskeleton of cells to the β1 integrins that are attached to the extracellular matrix proteins (fibronectin) surrounding each cell in the colony.

FIGURE CAPTIONS

Fig. 1. Double immunofluorescence staining of actin and vinculin in a)γ229 vinculin null F9-derived cells, and b) in the same cells that had been transfected with an expression vector for full-length vinculin cDNA (see Methods). F-actin is visible (red) because of the specific binding of rhodamine-labeled phalloidin. Vinculin is present in the "rescued" cell line. Clone R3, shown in b) and stained using monoclonal antibodies to human vinculin followed by secondary fluorescein-labeled goat antimouse Ig. The bar denotes 25 μm.

Fig. 2. Immunoblot analysis of four components found in cell-cell adhesive plaques. E-cadherin (E-cad), α-catenin (α-cat), β-catenin (β-cat), and β-actin (β-act) was analyzed in lysates of the four cell lines used in these studies. There was no significant difference in the levels of these proteins in the cell lines.

Fig. 3. Micrographs showing the physical response of a F9-R3 cell aggregate, formed during two hours of static incubation, to the imposed shear flow. The cell aggregate was allowed to adhere to fibronectin for 15 min under static conditions. Flow was then introduced at 1:40:00 at $\tau = 7$ dyn/cm^2 for 20 s and subsequently increased every 20 s to take on the values: 7, 21, 35, 49, 63, and 77 dyn/cm^2. The cell aggregate remained intact during the course of the experiment. The micrographs A and B show the aggregate before the initiation of flow and in the presence of flow at 77 dyn/cm^2, respectively

Fig. 4. Micrographs showing the physical response of a γ227 cell aggregate, formed during two hours of static incubation, to the imposed shear flow. The cell aggregate was allowed to adhere to fibronectin for 15 min under static conditions. Flow was then introduced at 2:32:00 at $\tau = 7$ dyn/cm^2 for 20 s and subsequently increased every 20 s to take on the values: 7, 21, 35, 49, 63, and 77 dyn/cm^2. The cell aggregate desegregated

during the course of the experiment. The micrographs A, B, and C show the shape of the aggregate before the initiation of flow (A), in the presence of flow at 35 dyn/cm^2 (B), and 35, 49, 63, and 77 dyn/cm^2 (C), respectively.

Fig. 5. Average number of detachment events per cell aggregate per cell type. The figures at the top and bottom, show, respectively, the results for aggregates formed from a single-cell suspension during a two-hour incubation and aggregates formed in culture (pre-formed aggregates). Disaggregation properties of fourteen large cell aggregates (containing at least ten cells) were studied for each case. The bars in the figure indicate standard deviations.

Fig. 6. Micrographs showing the physical response of a pre-formed F9-BIM cell aggregates to the imposed shear flow. The numbers shown on the screen indicate the time of the experiment in hours, minutes, seconds, and microseconds, respectively. In the experiment, the cell aggregate was incubated on fibronectin for 15 min under static conditions. Flow was initiated at 3:33:13 at $\tau = 7$ dyn/cm^2 for 20 s and subsequently increased every 20 s to take on the values: 7, 21, 35, 49, 63, 77, 91, and 105 dyn/cm^2. Micrographs A and B show, respectively, the shape of the aggregate before the initiation of flow (A) and in the presence of flow at105 dyn/cm^2 (B). Although the cell aggregate elongated extensively in the direction of flow, it remained intact during the course of the experiment.

Fig. 7. Micrographs showing the physical response of a pre-formed γ229 cell aggregate to the imposed shear flow. The numbers shown on the screen indicate the time of the experiment in hours, minutes, seconds, and microseconds, respectively. The cell aggregate was incubated on fibronectin for 15 min under static conditions (A). Flow was initiated at 5:43:00 at $\tau = 7$ dyn/cm^2 for 20 s and subsequently increased every 20 s to

take on the values: 7, 21, 35, 49, 63, 77, and 91 dyn/cm^2. Note that the cell aggregate first aligned itself to the direction of flow and then desegregated at $\tau = 35$ dyn/cm^2 (B).

REFERENCES

Angres, B., Barth, A., and W.J. Nelson. (1996). Mechanism for transition from initial to stable adhesion: Kinetic analysis of E-Cadherin-mediated adhesion using a quantitative adhesion assay. J. Cell Biol. 134: 549-557.

Brooks, S. and A. Tozeren (1966). Laminar Flow Past an Array of Cells That are Adherent to the Bottom Plate of a Flow Channel. Computers and Fluids 25: 741-757.

Byers, S.W., Sommers, C.L., Hoxter, B., Mercurio, A.M., and A. Tozeren. (1995). Role of E-cadherin in the response of tumor cell aggregates to lymphatic, venous and arterial flow: measurement of cell-cell adhesion strength. J. Cell Science 108: 2053-2064.

Coll, L., Ben-Ze'ev, A., Ezzell, R.M., Fernandez, J.L.R., Baribault, H., Oshima, R.G., and D.E. Adamson. (1995). Targeted disruption of vinculin genes in F9 and and embryonic stem cells changes cell morphology, adhesion, and locomotion. Proc. Natl. Acad. Sci. USA 92: 9161-9165.

Grover, A., Oshima, R.G., and E.D. Adamson. (1983). Epithelial layer formation in differentiating aggregates of F9 embryonal carcinoma cells. J. Cell Biol. 96: 1690-1696.

Jockusch, B.M., and Rudiger, M. (1996). Crosstalk between cell adhesion:vinculin as a paradigm for regulation by conformation. Trends Cell Biol. 6: 311-315.

Johnson, R.P. and Craig, S.W. (1995). F-actin binding site masked by intramolecular association of vinculin head and tail domains. Nature 373, 261-264.

Krajewski, S., Zapata, J.M., and Reed, J.C. (1996). Detection of multiple antigens on Western blots. Annal. Biochem. 221-228.

Laemlli, U. K. 1970. Cleavage of structural proteins during assembly of the head of bacteriophage T4. *Nature* 227:680-685.

Lee, S-W. and J.J. Otto. (1997). Vinculin and Talin: Kinetics of Entry and Exit from the

Cytoskeletal Pool. Cell Motility and the Cytoskeleton 36: 101-111.

Lehtonen, E. and Reima, R. (1986). Changes in the distribution of vinculin during preimplantation mouse development. Differentiation, 32: 125-134.

Lodish, H., Baltimore, D., Berk, A., Zipurski, S. L., Matsudaira, P., and J. Darnell. (1995). Molecular Cell Biology. Scientific American Books, New York, NY, 1344 pp.

Rodriguez Fernandez, J.L., Geiger, B., Salomon, D., Sabanay, I., Zoller, M., and Ben-Ze'ev, A. (1992). Supression of Tumorigenity in Transformed Cells after Transfection with Vinculin cDNA. J. Cell Biol. 119: 427-438.

Rodriguez Fernandez, J.L., Geiger, G., Salomon, D. and Ben-Ze'ev, A. (1993). Suppression of Vinculin Expression by Antisense Transfection Confers Changes in Cell Morphology, Motility, and Anchorage-Dependent growth of 3T3 Cells. J. Cell Biol. 122: 1285-1294.

Tozeren, A., S. Wu, H. K. Kleinman, A. M. Mercurio, and S. W. Byers. 1994. Alpha-6 beta-4 integrin mediates dynamic interactions of breast and colon carcinoma cells on laminin. *J. Cell Sci.* 107:3153-3163.

Vestweber, D. And R. Kemler. (1984). Rabbit antiserum against a purified surface glycoprotein decompacts mouse preimplantation embryos and reacts with specific adult tissues. Exp. Cell Res. 152: 169-178.

Volberg, T., Geiger, B., Kam, Z., Pankov, R., Simcha, I., Sabanay, H. Coll, J-L., Adamson, E., and Ben-Ze'ev, A. (1995). Focal adhesion formation by F9 embryonal carcinoma cells after vinculin gene disruption. J. Cell Science, 108: 2253-2260.

Zieske, J.D., Bukusoglu, G., and Gibson, I.K. (1989). Enhancement of Vinculin Synthesis by Migrating Stratified Epithelium. J. Cell Biol. 109: 571-576.

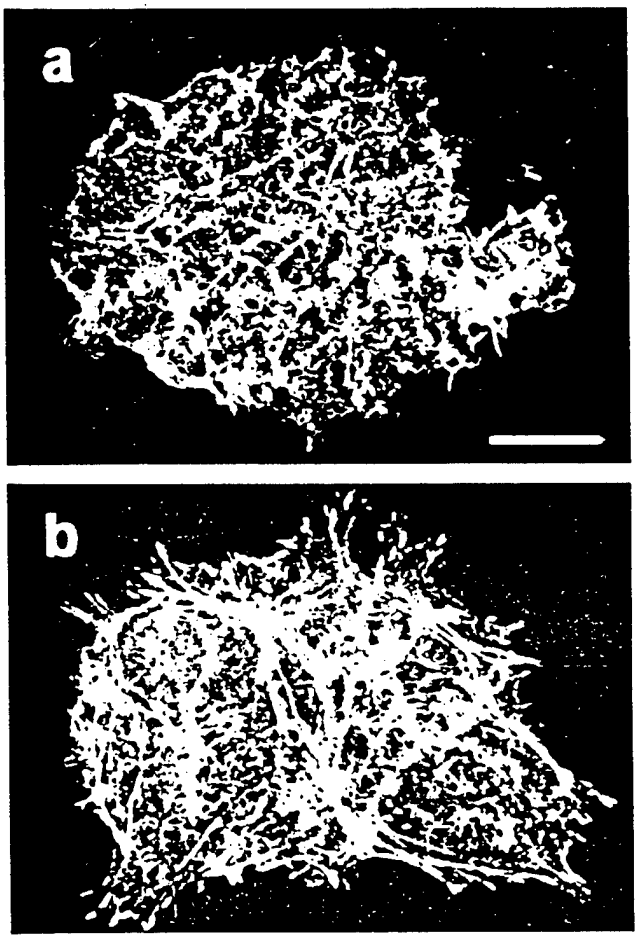

Figure 1

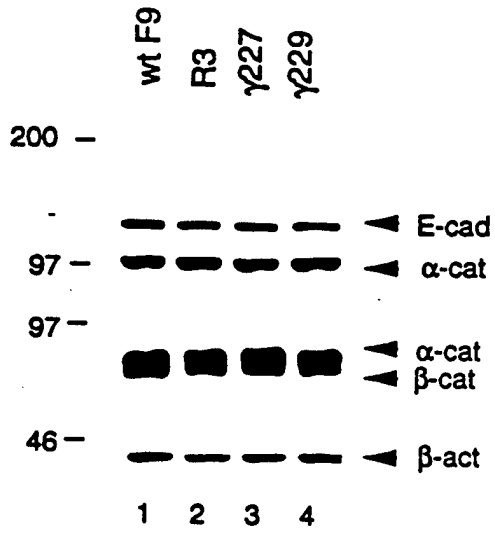

Figure 2

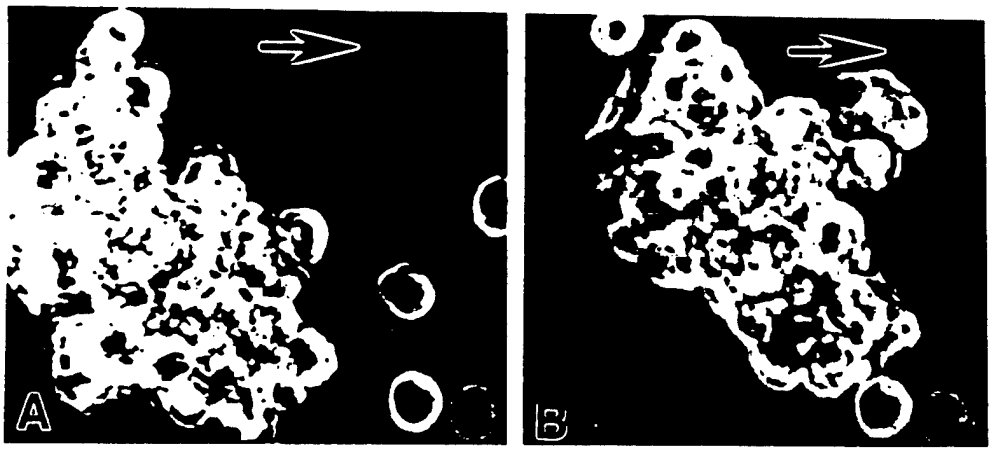

Figure 3

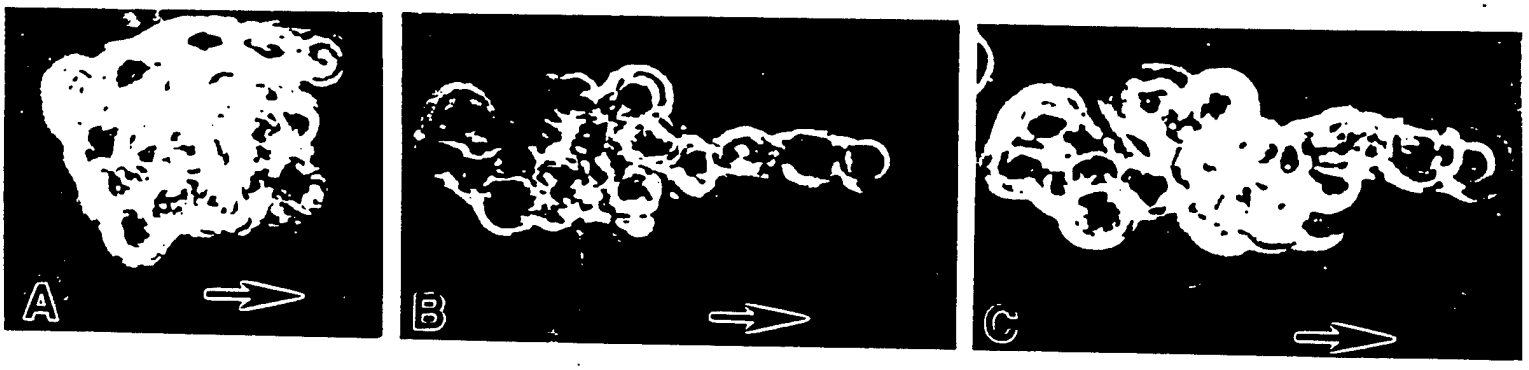

Figure 4

Disaggregation Assay

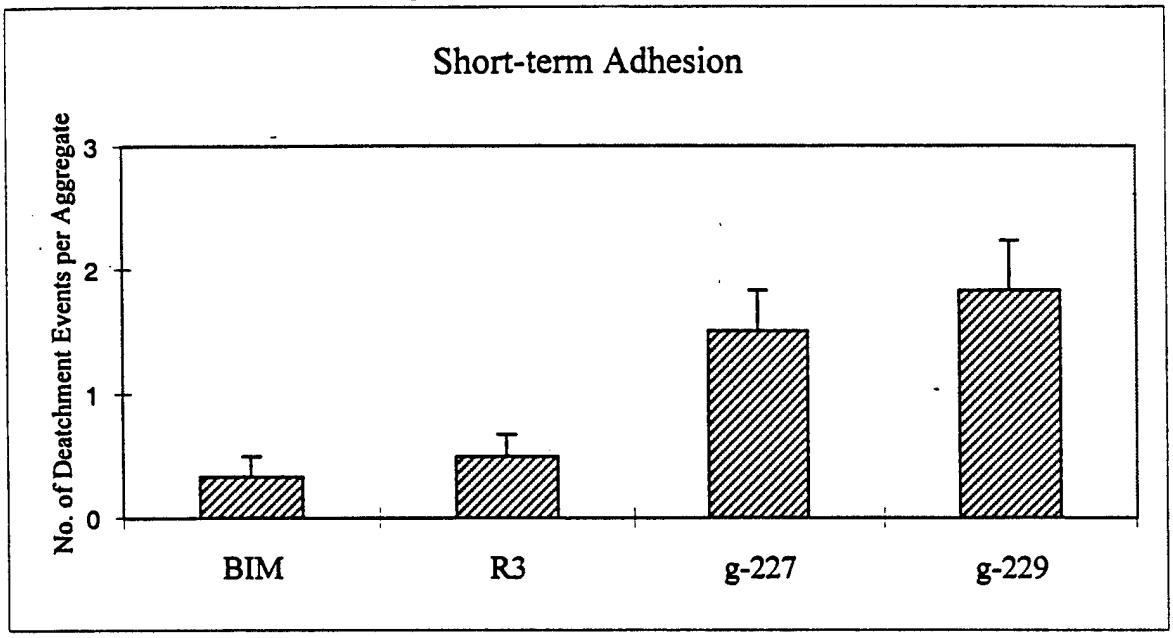

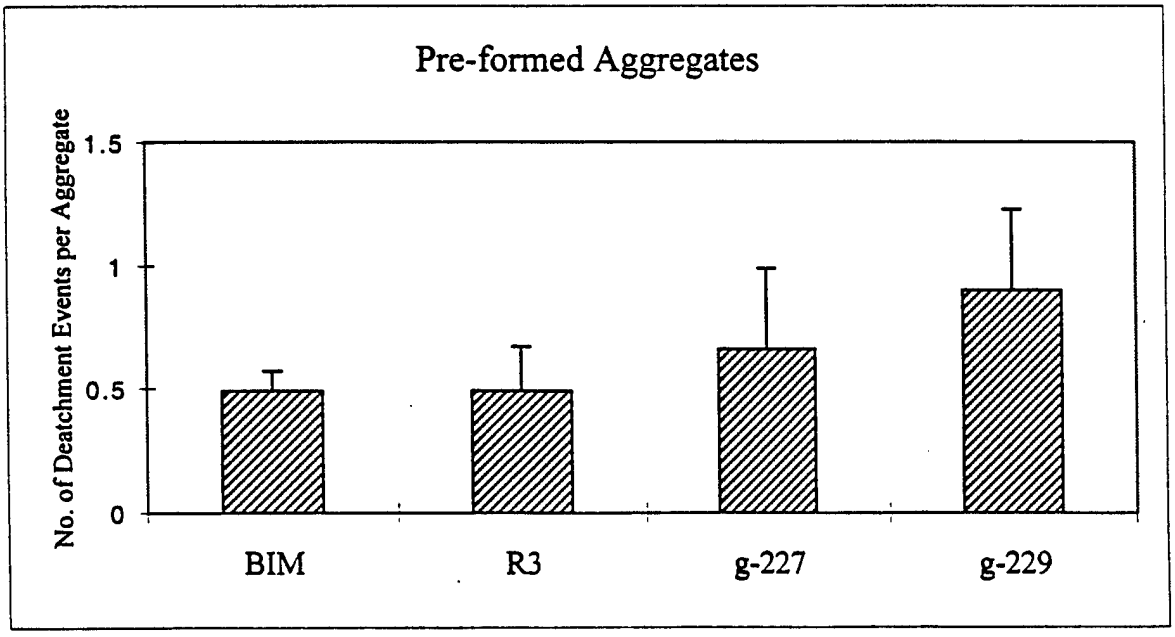

Figure 5

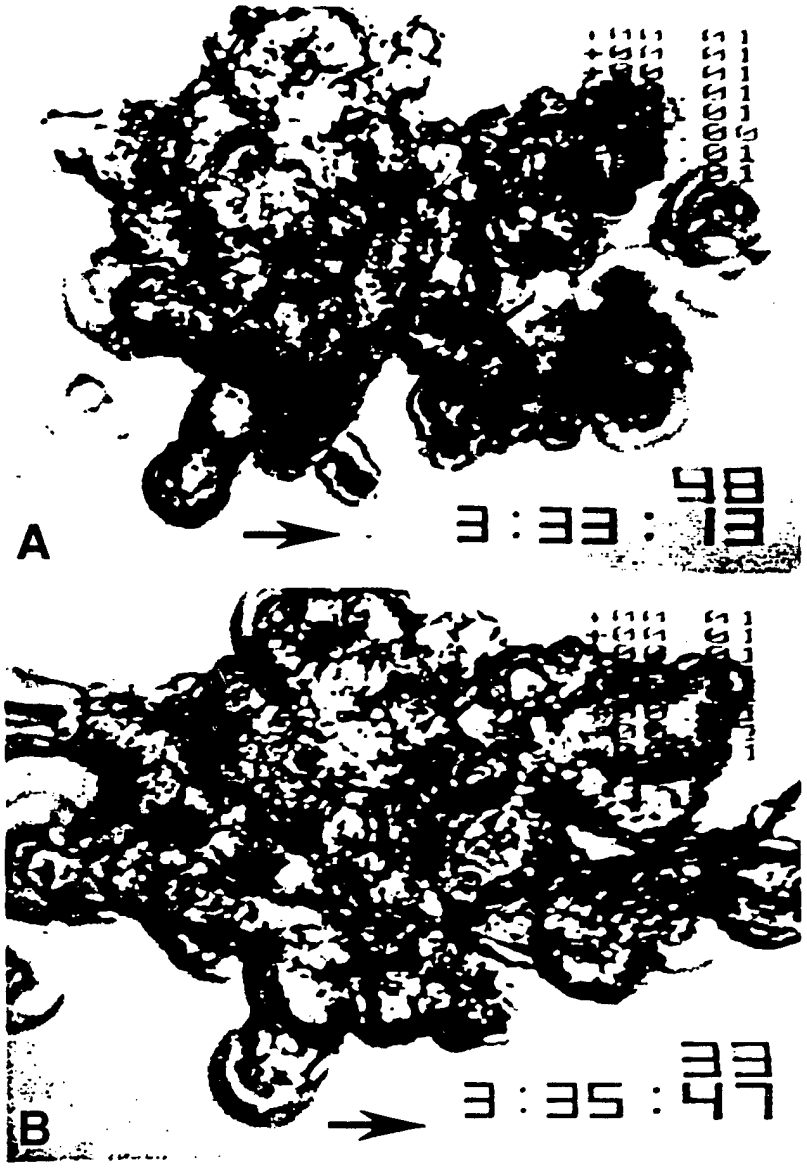

Figure 6

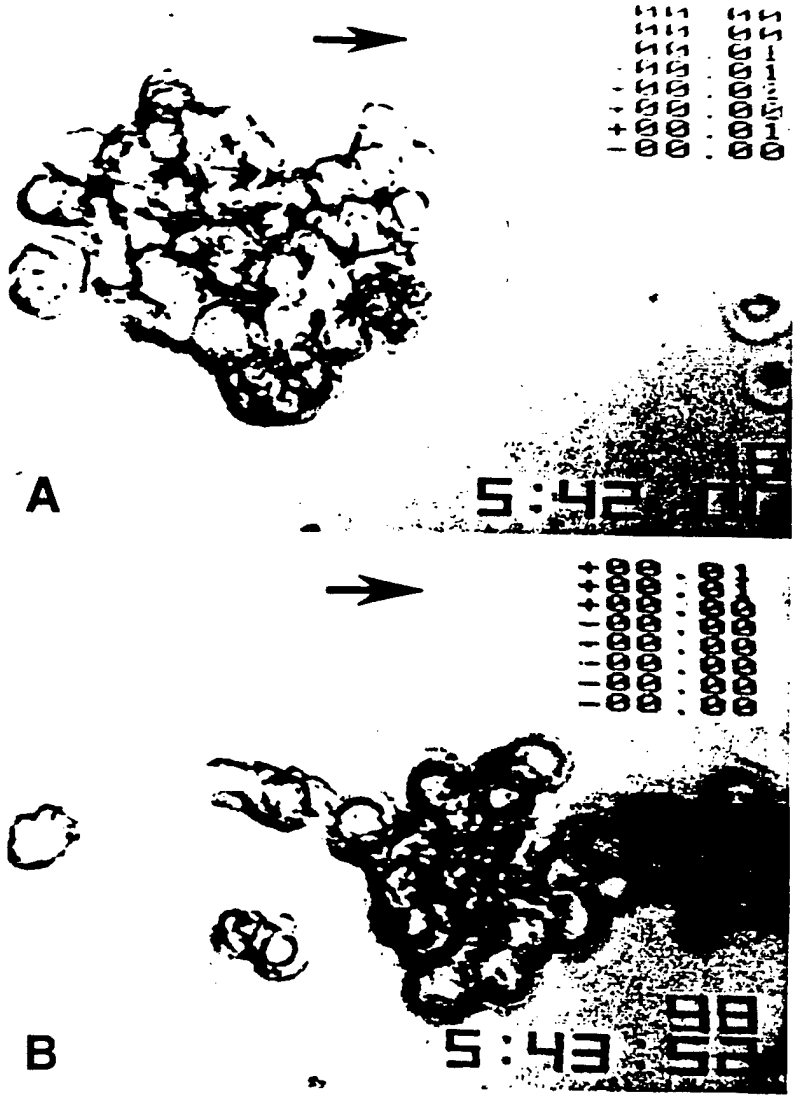

Figure 7

APPENDIX 2

Communication

THE JOURNAL OF BIOLOGICAL CHEMISTRY
Vol. 272, No. 40, Issue of October 3, pp. 24735–24738, 1997
Printed in U.S.A.

Serine Phosphorylation-regulated Ubiquitination and Degradation of β-Catenin*

(Received for publication, June 23, 1997)

Keith Orford‡, Caroline Crockett‡, Jane P. Jensen§, Allan M. Weissman§, and Stephen W. Byers‡¶

From the ‡Lombardi Cancer Center, Georgetown University Medical Center, Washington, D. C. 20007 and the §NCI, DCBD, National Institutes of Health, Bethesda, Maryland 20892

Several lines of evidence suggest that accumulation of cytoplasmic β-catenin transduces an oncogenic signal. We show that β-catenin is ubiquitinated and degraded by the proteosome and that β-catenin stability is regulated by a diacylglycerol-independent protein kinase C-like kinase activity, which is required for β-catenin ubiquitination. We also define a six-amino acid sequence found in both β-catenin and the NF-κB regulatory protein IκBα, which, upon phosphorylation, targets both proteins for ubiquitination. Mutation of a single serine within the ubiquitination targeting sequence prevents ubiquitination of β-catenin. Mutations within the ubiquitination targeting sequence of β-catenin may be oncogenic.

β-Catenin plays an important role in both cell-cell adhesion and growth factor signal transduction (1, 2). Consistent with these two functions within the cell, the protein is localized primarily in two intracellular pools; a membrane pool involved in cadherin-mediated cell-cell adhesion and a cytoplasmic pool important for signaling (1, 2). The role of β-catenin in cell-cell adhesion has been well studied. It links cadherins to α-catenin and the actin cytoskeleton, which results in the formation of the adherens junction (1, 2). Tyrosine phosphorylation of β-catenin can regulate cell-cell adhesion by disrupting particular protein-protein interactions (3, 4).

The *Drosophila* and *Xenopus* homologs of β-catenin are also known to be involved in signaling pathways that regulate embryonic patterning. The *Drosophila* homolog Armadillo (Arm)[1] lies downstream of the Wingless (Wg) receptor and the serine kinase Zeste-White 3 (ZW3) in the Wingless pathway that regulates segmental pattern formation. The *Xenopus* pathway is comprised of the vertebrate homologs of the *Drosophila* proteins Wg and Zw3 (Wnt-1 and glycogen synthase kinase 3β (GSK3β), respectively) and regulates dorsal axis formation (2). More recently, the interaction of β-catenin with members of the LEF/TCF family of transcription factors was shown to be important in Wnt signaling and in colon cancer (5–8).

β-Catenin signaling in embryogenesis and oncogenesis appears to be regulated by controlling the accumulation of cytoplasmic β-catenin. Activation of the Wnt (Wg) pathway results in the inhibition of GSK3β (ZW3) activity, which, in turn, results in stabilization of cytoplasmic β-catenin (Arm) (1, 9, 10). The tumor suppressor protein APC appears to be required for the normal degradation of β-catenin as mutated forms of APC result in high levels of free (*i.e.* cytoplasmic) β-catenin with a longer half-life (11). The mechanism by which GSK3β and APC regulate β-catenin stability is unknown. Although GSK3β can directly phosphorylate APC and β-catenin *in vitro*, it is not clear how these interactions regulate β-catenin stability *in vivo* (12, 13).

In this report we show that β-catenin is normally degraded by the ubiquitin/proteosome pathway. We also show that certain protein kinase C (PKC) inhibitors cause a dramatic accumulation of cytoplasmic β-catenin by inhibiting its ubiquitination. In addition, we define a six-amino acid motif that is involved in targeting both β-catenin and the inhibitor of NF-κB, IκBα, for ubiquitination. A serine to alanine mutation within this ubiquitination targeting sequence (UTS) stabilizes the protein by inhibiting its ubiquitination.

EXPERIMENTAL PROCEDURES

Reagents, Antibodies, and Cells- ALLN (calpain inhibitor I), ALLM (calpain inhibitor II), GF-109203X (bisindoylmaleimide), and TPA were purchased from Boehringer Mannheim. Lactacystin and calphostin C were purchased from Calbiochem. Ro31-8220 was a gift from Dr. Robert Glazer. The monoclonal anti-β-catenin was purchased from Transduction Laboratories. The anti-ubiquitin polyclonal was raised by Dr. Weissman (23). The anti-HA antibody (monoclonal clone HA-11) was purchased from Babco. SKBR3 and HBL100 cell lines were acquired from the ATCC and maintained in Dulbecco's modified Eagle's medium with 10% fetal bovine serum and 1% penicillin/streptomycin.

Cellular Fractionation—Nonidet P-40 extractions were performed as described previously (14) except that 10 mM *N*-ethylmaleimide (NEM) was added to the lysis buffer. Cytoplasmic fractionation was performed by washing cells twice in phosphate-buffered saline and removing all remnants of the final wash. The cells were incubated in ice-cold hypotonic lysis buffer (10 mM Tris, pH 7.4, 0.2 mM $MgCl_2$, 5 mM NEM, and 10 mM ALLN) for 5 min on ice. The cells were scraped and mechanically disrupted by 30 strokes in a Dounce homogenizer. Greater than 95% of the cells were lysed as judged by light microscopy. The lysates were transferred to an ultracentrifuge tube containing a 5 × inhibitor solution (250 mM NaF, 5 mM sodium vanadate, 25 mM NEM, aprotinin, leupeptin, pepstatin A, and 4-(2-aminoethyl)benzenesulfonyl fluoride). The insoluble components of the lysates were pelleted at 100,000 × *g* for 1 h. The supernatant was designated the S100 or cytoplasmic fraction, and the pellet was the P100 fraction. In some experiments the P100 fraction was extracted with Nonidet P-40 buffer. Lysates were boiled in 2 × Laemlli sample buffer with 10% β-mercaptoethanol and separated on 8% or 4–12% polyacrylamide gels (Novex).

Immunoprecipitations—Immunoprecipitations were performed on equal amounts of Nonidet P-40 lysates. The lysates were precleared once with 10 μg non-immune mouse IgG and 100 μl of protein G-Sepharose (Life Technologies, Inc.) and once with 100 μl of protein G-Sepharose, both for 1.5 h in the cold. The lysates were incubated in the cold for 1.5 h with 6 μg of non-immune mouse IgG or monoclonal anti-β-catenin. Protein G-Sepharose was added for 45 min. The protein G-antibody-antigen complexes were pelleted in a cold microcentrifuge and washed six times in cold Nonidet P-40 buffer without inhibitors.

* This work was supported by Grant DAMD17-95-1-5012 from the Department of Defense. The costs of publication of this article were defrayed in part by the payment of page charges. This article must therefore be hereby marked "*advertisement*" in accordance with 18 U.S.C. Section 1734 solely to indicate this fact.

¶ To whom correspondence should be addressed. Tel.: 202-687-1891; Fax: 202-687-7505; E-mail: byerss@gunet.georgetown.edu.

[1] The abbreviations used are: Arm, Armadillo; Wg, Wingless; ZW3, Zeste-White 3; GSK3β, glycogen synthase kinase-3β; PKC, protein kinase C; UTS, ubiquitination targeting sequence; ALLN, *N*-acetyl-Leu-Leu-norleucinal; ALLM, *N*-Acetyl-Leu-Leu-methional; TPA, 12-*O*-tetradecanoylphorbol 13-acetate; NEM, *N*-ethylmaleimide; HMW, high molecular weight; aPKC, atypical protein kinase C; PAGE, polyacrylamide gel electrophoresis; HA, hemagglutinin; EGF, epidermal growth factor; IGF, insulin-like growth factor; DAG, diacylglycerol.

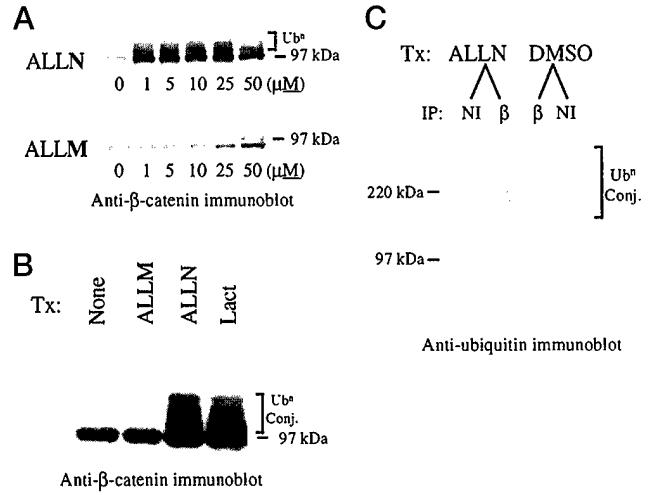

FIG. 1. **β-Catenin is ubiquitinated and degraded by the proteosome.** Immunoblots and immunoprecipitations were performed with equal amounts of Nonidet P-40 lysates. *A*, SKBR3 cells were treated for 4 h with increasing amounts of either the peptide aldehyde proteosomal inhibitor ALLN or the related peptide aldehyde calpain protease inhibitor ALLM. Cells were lysed in Nonidet P-40, separated by SDS-PAGE, and immunoblotted with an anti-β-catenin monoclonal antibody. *B*, SKBR3 cells were treated (*Tx*) overnight with the proteosomal inhibitors ALLN (10 μM) and lactacystin (*Lact.*) (100 μM) and with ALLM (10 μM) and the lactacystin vehicle ethanol (20 μl). The cells were lysed and analyzed as in *A*. *C*, HBL100 cells were treated overnight with either 10 μM ALLN or vehicle (Me_2SO (*DMSO*)) overnight. The cells were lysed in Nonidet P-40 and immunoprecipitated (*IP*) with 6 μg of either anti-β-catenin monoclonal antibody (*β*) or non-immune mouse IgG (*NI*). The precipitated proteins were separated by SDS-PAGE and transferred to polyvinylidene difluoride. The membrane was treated as in Ref. 15 and probed with an anti-ubiquitin antibody.

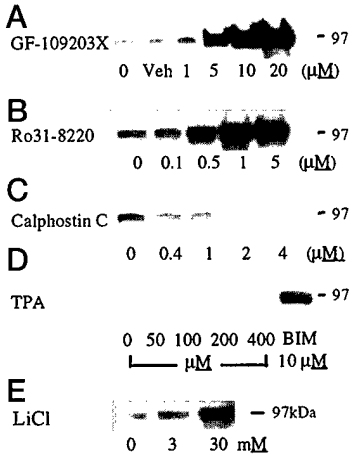

FIG. 2. **Cytoplasmic β-catenin accumulates in response to bisindoylmaleimide PKC inhibitors and lithium.** Confluent plates of HBL100 s (*A*, *B*, *C*, and *E*) were treated overnight with the PKC inhibitors GF-109203X (*A*), Ro31-8220 (*B*), and calphostin C (*C*), and the pluripotent inhibitor lithium chloride (*E*) at increasing doses. SKBR3 (*D*) cells were treated with increasing doses of PMA for 3 days. Cytoplasmic extracts were made from all of these cells and the proteins separated by SDS-PAGE and immunoblotted with anti-β-catenin monoclonal antibody. Equal amounts of cytoplasmic extracts were loaded per well for immunoblotting. Calphostin C was toxic to the cells at 4 μM.

The immunoprecipitated proteins were boiled for 5 min and separated by SDS-PAGE. The proteins were transferred to polyvinylidene difluoride (Millipore) and treated as described in Ref. 15.

β-Catenin Construct and Mutagenesis—The nine-amino acid HA-tag was added to the C terminus of β-catenin using polymerase chain reaction. The β-catenin/HA construct was cloned into the *Bam*HI site of the pcDNA3 vector (Invitrogen). Mutagenesis of serine 37 was performed using the Quick-Change site-directed mutagenesis kit (Stratagene).

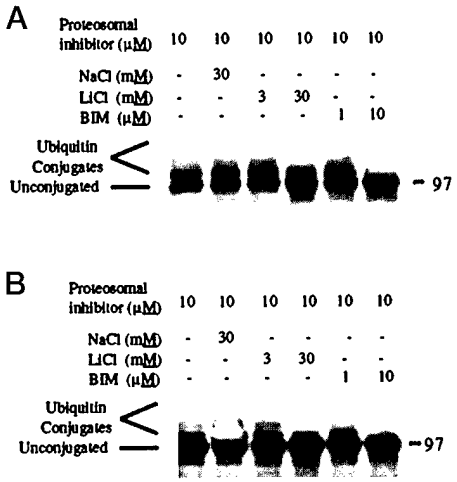

FIG. 3. **GF-109203X and lithium inhibit β-catenin ubiquitination.** Immunoblots were performed with equal amounts of Nonidet P-40 lysates. Confluent plates of SKBR3s (*A*) and HBL100s (*B*) were treated with ALLN (10 μM) overnight. In addition, cells were treated with: control (*lane 1*), 30 mM NaCl, 3 mM LiCl, 30 mM LiCl, 1 μM GF-109203X, or 10 μM GF-109203X. The cells were lysed and fractionated as in Fig. 1*A*. Immunoblotting was performed with monoclonal anti-β-catenin.

Transfections—Transfections were performed by calcium-phosphate precipitation (16). The calcium-phosphate/DNA precipitate was incubated with the cells for 6 h. SKBR3 cells were shocked with 20% glycerol in serum-free medium for 4 min before washing and then the medium was replaced. Assays were performed 24–72 h after transfection.

RESULTS AND DISCUSSION

β-Catenin Is Degraded by the Ubiquitin-Proteosome Pathway—Proteins that are to be degraded by the ubiquitin/proteosome system are first conjugated to multiple copies of the small protein ubiquitin through isopeptide linkages (17). These ubiquitinated proteins are then recognized and degraded by the 26 S proteosome. Inhibition of the proteosome results in the accumulation of the ubiquitinated forms of those proteins normally degraded by the proteosome. To determine whether β-catenin is degraded by this system, human breast epithelial cell lines were treated with the peptide aldehyde proteosomal inhibitor ALLN or a related peptide aldehyde that has 50–100-fold lower potency as a proteosomal inhibitor. Anti-β-catenin immunoblots revealed that the proteosomal inhibitor at a dose as low as 1 μM resulted in the accumulation of β-catenin, including the appearance of high molecular weight (HMW) β-catenin species (Fig. 1*A*). The same result was found using the specific proteosomal inhibitor lactacystin (Fig. 1*B*). These experiments were conducted with both SKBR3 and HBL100 cell lines with similar results.

To show that β-catenin is ubiquitinated before proteosomal degradation, we immunoprecipitated β-catenin from HBL100 cells treated with either ALLN or vehicle (Me_2SO) alone and detected ubiquitinated material by immunoblot. Only when cells were treated with the proteosomal inhibitor did a significant amount of ubiquitin immunoreactivity co-precipitate with β-catenin, indicating that it is conjugated to ubiquitin prior to degradation by the proteosome. These data demonstrate unequivocally that β-catenin is normally degraded by the proteosome following ubiquitination.

An Atypical PKC-like Kinase Regulates Cytoplasmic β-Catenin Accumulation—GSK3β is a member of the Wnt/Wg pathway, and its activity is required to maintain low levels of cytoplasmic β-catenin (9, 12). In addition, GSK3β itself can be regulated by several other serine kinases. *In vitro,* p70 S6 kinase, $p90^{Rsk}$, Akt/protein kinase B (PKB), and certain PKC isoforms phosphorylate and regulate GSK3β activity (18–21).

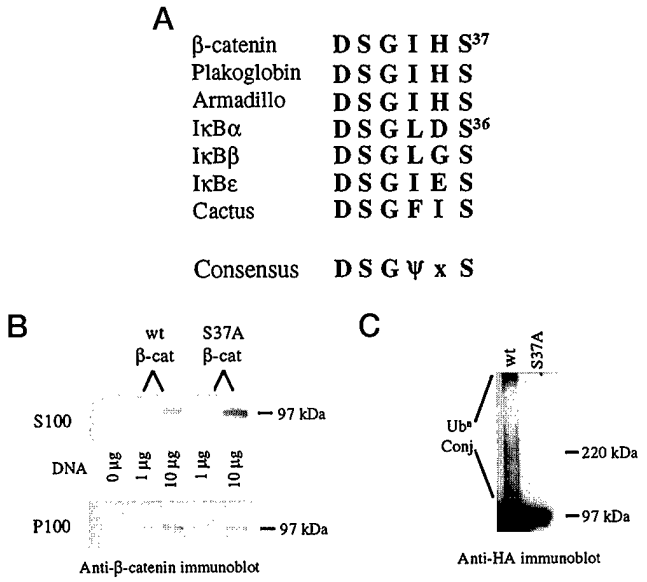

FIG. 4. **β-Catenin contains an IκBα-like six-amino acid sequence, which, when phosphorylated, targets β-catenin for ubiquitination.** *A*, the six-amino acid motif is well conserved in both IκBα and β-catenin family members. *B*, either 0, 1, or 10 μg of wild-type and S37A mutant β-catenin constructs were transfected into SKBR3 cells. 36 h later, the cells were fractionated into S100 (cytoplasmic) and P100 (pellet) pools. The proteins were separated by SDS-PAGE and immunoblotted with monoclonal anti-β-catenin antibody as in Fig. 2. *C*, 10 μg of wild-type β-catenin or S37A mutant β-catenin were transfected into SKBR3 cells. 30 h later, cells were treated with ALLN (5 μM) and clasto-lactacystin (5 μM) overnight. The cells were fractionated into S100 and P100 pools, and the cytoplasmic proteins were separated by SDS-PAGE and immunoblotted with anti-HA antibody. Note the accumulation of HMW HA-tagged wild-type, but not mutant, β-catenin in the cytoplasmic fraction. Cells transfected with vector alone showed no anti-HA immunoreactivity (data not shown).

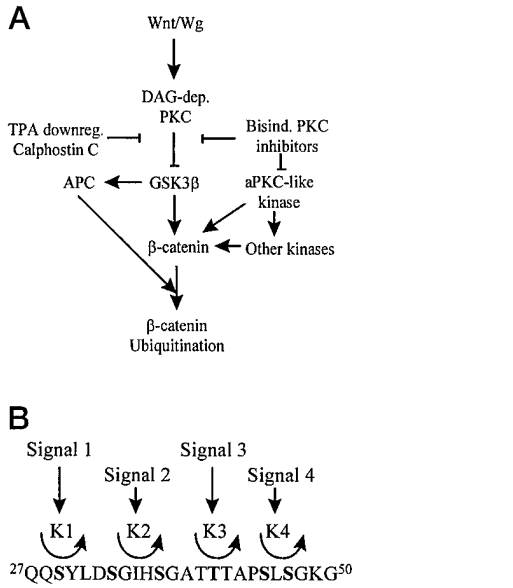

FIG. 5. **A complex array of kinases regulates β-catenin stability.** *A*, inhibitor studies from Cook *et al.* (23) and the present work indicate that several serine kinases are likely to be important in the regulation of β-catenin ubiquitination. A DAG-dependent classical PKC is required to mediate the inhibitory effects of Wnt/Wg on GSK3β activity. It should be noted that other serine kinases can also phosphorylate and inactivate GSK3β. Active GSK3β can phosphorylate APC and β-catenin. The present study implicates an additional DAG-independent PKC-like activity in the modulation of β-catenin ubiquitination and stability. *B*, conserved serine and threonine residues in the ubiquitin-targeting sequence at the N-terminal of β-catenin may also be the target of several kinases. These could act sequentially or in concert to prepare β-catenin for ubiquitination and/or interaction with the ubiquitin-conjugating machinery. Mutation of any one of these serines may be transforming. It is not clear if all of these serines need to be phosphorylated in order for β-catenin to be ubiquitinated, but it is clear that mutation of a single residue (S37A) is sufficient to prevent ubiquitination.

Several other growth factors, including EGF and IGF also result in the inactivation of GSK3β (22). In cultured cells, inhibitor studies showed that the activity of a TPA-sensitive PKC isoform is required to inactivate GSK3β in response to the Wg signal (23). This PKC isoform appeared to be specifically involved in Wg-mediated regulation of GSK3β, as it was not involved in other GSK3β regulating signals (*e.g.* insulin, EGF, IGF-1, and serum) (23). No studies have determined the effect of PKC inhibition on β-catenin accumulation.

Cells were treated with different PKC inhibitors and assayed for β-catenin accumulation. In the HBL100 cell line, which has high levels of membrane-associated and low levels of cytoplasmic β-catenin, two bisindoylmaleimide-type PKC inhibitors (GF-109203X and Ro31-8220) caused a dramatic increase in the cytoplasmic pool but not the membrane pool (Fig. 2*B*). The same result was seen in Madin-Darby canine kidney cells (data not shown). In SKBR3 cells, which have very low levels of β-catenin protein in both pools, there was a large increase in both cytoplasmic and membrane (Nonidet P-40-soluble) pools (data not shown). PKC activity is required for Wnt-1 signaling to inhibit GSK3β activity (23). Although this study did not investigate the effect of PKC inhibitors on β-catenin stability, one would anticipate that inhibition of PKC would have resulted in decreased β-catenin stability. TPA-induced down-regulation of DAG-dependent PKCs also prevented Wnt from inhibiting GSK3β (23). In contrast, neither the PKC inhibitor calphostin C nor TPA-induced down-regulation of PKCs had a significant effect on the accumulation of cytoplasmic β-catenin in the present study (Fig. 2, *C* and *D*). In this experiment, TPA treatment completely down-regulated PKCα, the major PKC isoform expressed in these cells (data not shown). Our interpretation of these results is based on the different mechanisms of the inhibitors. The bisindoylmaleimides inhibit both DAG-dependent and -independent PKC isoforms by competing with ATP for binding to the kinase, whereas calphostin C and long term phorbol ester treatment inhibit only DAG-dependent PKC activities. It should be noted that the bisindoylmaleimide Ro31-8220 has no direct effect on GSK3β activity and actually acts to prevent the decrease in activity normally induced by Wg (23). The inhibitor profile of the PKC isoform involved in β-catenin accumulation indicates that it may be a member of the DAG-independent class of PKCs known as atypical PKCs (aPKC). These results distinguish it from the DAG-dependent PKC isoform that is responsible for Wnt-dependent GSK3β regulation (23).

In addition to inhibitors of PKC, lithium chloride, which is an inhibitor of GSK3β (as well as other enzymes), was used to investigate its effects on β-catenin accumulation (24, 25). Treatment of *Xenopus* embryos with lithium chloride results in the formation of a secondary dorsal axis in the embryo, phenotypes that are also characteristic of ectopic Wnt or β-catenin overexpression (2, 26). Treatment with 30 mM results in the accumulation of cytoplasmic β-catenin within HBL100 and SKBR3 cells (Fig. 2*E*). This suggests that the effects of lithium that are seen in *Xenopus* embryos are a result of increased cytoplasmic β-catenin.

GF-109203X and Lithium Inhibit Ubiquitination of β-Catenin—The bisindoylmaleimide PKC inhibitors and lithium may increase cytoplasmic β-catenin by inhibiting its ubiquitination and, therefore, its degradation. To investigate this possibility, SKBR3 and HBL100 cells were treated overnight with the

proteosomal inhibitor ALLN to generate the HMW ubiquitin-conjugated forms of β-catenin. In addition to the proteosomal inhibitor, we treated some cells with inhibitory or non-inhibitory doses of the PKC inhibitor GF-109203X and LiCl. The reduction or complete abrogation of β-catenin ubiquitination by these inhibitors demonstrates that the aPKC-like activity and GSK3β, respectively, are required for ubiquitination of β-catenin (Fig. 3). This parallels other work regarding the role of GSK3β in regulating β-catenin degradation and introduces the possibility that an atypical PKC-like enzyme may also play a role in this important process.

A Conserved Six-amino Acid Sequence Targets β-Catenin and IκBα for Ubiquitination—Since N-terminal truncated forms of β-catenin and Arm accumulate in the cytoplasm, we analyzed the N terminus of β-catenin for serine residues that might be involved in regulating β-catenin ubiquitination (27). Five N-terminal serines that are well conserved between β-catenin, *Armadillo,* and plakoglobin are present between β-catenin amino acids 29 and 47. Mutation of three of these serines as well as a conserved threonine results in β-catenin accumulation and axis duplication in *Xenopus* (12). Interestingly, two of these serines lie within a six-amino acid region that is almost identical to a motif in the protein IκBα, which, upon serine phosphorylation, targets it for ubiquitination (see Fig. 4*A*) (28). Mutations of one or both of the serines in this motif stabilize IκBα by inhibiting its ubiquitination (28). Mutations of β-catenin serine 37 were recently reported to occur in several melanoma cell lines (29). To determine the role that phosphorylation of this motif within β-catenin might play in its ubiquitination and degradation, a serine to alanine mutation was made at residue 37 of β-catenin.

The wild-type and mutant β-catenin constructs were transfected into SKBR3 cells. The cytoplasmic proteins (S100) were isolated from the other cellular proteins (P100), and both fractions separated by SDS-PAGE and immunoblotted for β-catenin. The S37A mutant β-catenin accumulated to approximately 3-fold the levels of the wild-type 36 h after transfection (Fig. 4*B*). This differential accumulation was only detected in the cytoplasmic pool of β-catenin as the P100 fraction shows approximately equal accumulation of the two forms of β-catenin.

To determine whether this increased accumulation was due to reduced ubiquitination of the mutant, SKBR3 cells were transfected with wild-type, the S37A mutant, or vector alone. The transfectants were lysed and assayed for the accumulation of HMW ubiquitinated β-catenin by immunoblotting with an anti-HA antibody (Fig. 4*C*). The wild-type β-catenin was ubiquitinated efficiently, while the mutant form was not ubiquitinated. Interestingly, ubiquitinated β-catenin only accumulated in the S100 fraction of the SKBR3 cell line (data not shown). This result strongly suggests that, like IκBα, a specific serine (residue 37, in β-catenin) must be phosphorylated prior to ubiquitination of β-catenin. Phosphorylation of this serine is probably an important mechanism by which the amount of β-catenin within the cell is regulated. Indeed, mutations of this serine and serine 33, which is also located within the UTS, occur in several melanoma and colon cancer cell lines (8, 29). In these cases, the mutant forms of β-catenin were presumed to be transforming.

These data show that β-catenin is normally degraded by the ubiquitin/proteosome system and that at least two serine/threonine kinases regulate this process, GSK3β and an aPKC-like enzyme. We also identify a common motif within β-catenin and IκBα, which, upon being phosphorylated, regulates the stability of these proteins by targeting them for ubiquitination. The identity of the kinase(s) that phosphorylates the IκBα UTS is unknown. The aPKC-like kinase activity that regulates β-catenin ubiquitination may directly phosphorylate the UTS, or it may be involved in the regulation of the kinase that does. Regardless of the specific interactions, it is likely that signaling through β-catenin is regulated by a complex network of kinases that regulate its ubiquitination (Fig. 5*A*).

The regulation of β-catenin signaling *per se* may well be an important mechanism by which multiple intracellular signals are integrated. We propose that several signaling pathways, such as signaling through growth factors (*e.g.* the Wnts, EGF, IGF, insulin), APC, and retinoic acid-induced adhesion, may converge by regulating the accumulation of cytoplasmic β-catenin (Fig. 5*B*) (10, 14). Several conserved serines and threonines within a small region of the N terminus of β-catenin are targets for mutation in colon cancers and melanomas. It is likely that many, if not all, of these residues must be phosphorylated to target β-catenin for degradation (8, 29). We propose that as the cellular context changes, β-catenin phosphorylation will be altered, and these alterations will determine whether or not it is ubiquitinated and degraded.

The definition of a specific region that targets an oncogenic protein for degradation may prove to be useful in the design of modalities for cancer therapy. We hypothesize that the UTS will be recognized by β-catenin-directed ubiquitin-conjugating enzymes, which may themselves constitute therapeutic targets.

Acknowledgments—We thank Robert Glazer for supplying the Ro31-8220 and Robert Lechleider for his critical review of the manuscript.

REFERENCES

1. Peifer, M. (1995) *Trends Cell Biol.* **5,** 224–229
2. Gumbiner, B. (1997) *Curr. Opin. Cell Biol.* **7,** 634–640
3. Behrens, J., Vakaet, L., Friis, R., Winterhager, E., Van Roy, F., Mareel, M. M., and Birchmeier, W. (1993) *JCB* **120,** 757–766
4. Sommers, C. L., Gelmann, E. P., Kemler, R., Cowin, P., and Byers, S. W. (1994) *Cancer Res.* **54,** 3544–3552
5. Behrens, J., von Kries, J. P., Kuhl, M., Bruhn, L., Wedlich, D., Grosschedl, R., and Birchmeier, W. (1996) *Nature* **382,** 638–642
6. Molenaar, M., van de Wetering, M., Oosterwegel, M., Peterson-Maduro, J., Godsave, S., Korinek, V., Roose, J., Destree, O., and Clevers, H. (1996) *Cell* **86,** 391–399
7. Korinek, V., Barker, N., Morin, P. J., van Wichen, D., de Weger, R., Kinzler, K. W., Vogelstein, B., and Clevers, H. (1997) *Science* **275,** 1784–1787
8. Morin, P. J., Sparks, A. B., Korinek, V., Barker, N., Clevers, H., Vogelstein, B., and Kinzler, K. W. (1997) *Science* **275,** 1787–1790
9. Peifer, M., Sweeton, D., Casey, M., and Wieschaus, E. (1994) *Development (Camb.)* **120,** 369–380
10. Papkoff, J., Rubinfeld, B., Schryver, B., and Polakis, P. (1996) *Mol. Cell. Biol.* **16,** 2128–2134
11. Munemitsu, S., Albert, I., Souza, B., Rubinfeld, B., and Polakis, P. (1995) *Proc. Natl. Acad. Sci. U. S. A.* **92,** 3046–3050
12. Yost, C., Torres, M., Miller, J. R., Huang, E., Kimelman, D., and Moon, R. T. (1996) *Genes Dev.* **10,** 1443–1454
13. Rubinfeld, B., Albert, I., Porfiri, E., Fiol, C., Munemitsu, S., and Polakis, P. (1996) *Science* **272,** 1023–1026
14. Byers, S., Pishvaian, M., Crockett, C., Peer, C., Tozeren, A., Sporn, M., Anzano, M., and Lechleider, R. (1996) *Endocrinology* **137,** 3265–3273
15. Hou, D., Cenciarelli, C., Jensen, J. P., Nguygen, H. B., and Weissman, A. M. (1995) *J. Biol. Chem.* **269,** 14244–14247
16. Chen, C., and Okayama, H. (1987) *Mol. Cell. Biol.* **7,** 2745–2752
17. Ciechanover, A. (1994) *Cell* **79,** 13–21
18. Goode, N., Hughes, K., Woodgett, J. R., and Parker, P. J. (1992) *J. Biol. Chem.* **267,** 16878–16882
19. Sutherland, C., Leighton, I. A., and Cohen, P. (1993) *Biochem. J.* **296,** 15–19
20. Sutherland, C., and Cohen, P. (1994) *FEBS Lett.* **338,** 37–42
21. Cross, D. A. E., Alessi, D. R., Cohen, P., Andjelkovich, M., and Hemmings, B. A. (1995) *Nature* **378,** 785–789
22. Woodgett, J. R., Plyte, S. E., Pulverer, B. J., Mitchell, J. A., and Hughes, K. (1993) *Biochem. Soc. Trans.* **21,** 905–907
23. Cook, D., Fry, M. J., Hughes, K., Sumathipala, R., Woodgett, J. R., and Dale, T. C. (1996) *EMBO J.* **15,** 4526–4536
24. Manji, H. K., Potter, W. Z., and Lenox, R. H. (1995) *Arch. Gen. Psychiatry* **52,** 531–543
25. Klein, P. S., and Melton, D. A. (1996) *Proc. Natl. Acad. Sci. U. S. A.* **93,** 8455–8459
26. Funayama, N., Fagotto, F., McCrea, P., and Gumbiner, B. M. (1995) *J. Cell Biol.* **128,** 959–968
27. Munemitsu, S., Albert, I., Rubinfeld, B., and Polakis, P. (1996) *Mol. Cell. Biol.* **16,** 4088–4094
28. Chen, Z., Hagler, J., Palombella, V. J., Melandri, F., Scherer, D., Ballard, D., and Maniatis, T. (1995) *Genes Dev.* **9,** 1586–1597
29. Rubinfeld, B., Robbins, P., El-Gamil, M., Albert, I., Porfiri, E., and Polakis, P. (1997) *Science* **275,** 1790–1792

APPENDIX 3

Figure 1

The tumor suppressor APC regulates β-catenin/LEF signalling via the ubiquitin- proteosome pathway. SW480 cells with an APC truncating mutation express high levels of β–catenin and have high constitutive LEF promoter activity. Cells were transfected with APC 3, the inactive C-terminal of APC, APC 25, the β-catenin binding active region of APC, or full length APC (wt). All cells were co-transfected with an LEF-promoter-luciferase reporter construct. Results are expressed as relative light units from the luciferase reporter. Note that APC 3 does not decrease the high endogenous level of reporter activity but that both APC 25 and full length APC do. The proteosomal inhibitor ALLN completely reverses the effects of APC 25 and partially reverses the effects of full length APC. This indicates that the ability of APC to inhibit the transcription of β-catenin/LEF-regulated genes depends upon an active proteosome.

The tumor suppressor APC regulates β–catenin - LEF signaling via the ubiquitin-proteasome pathway

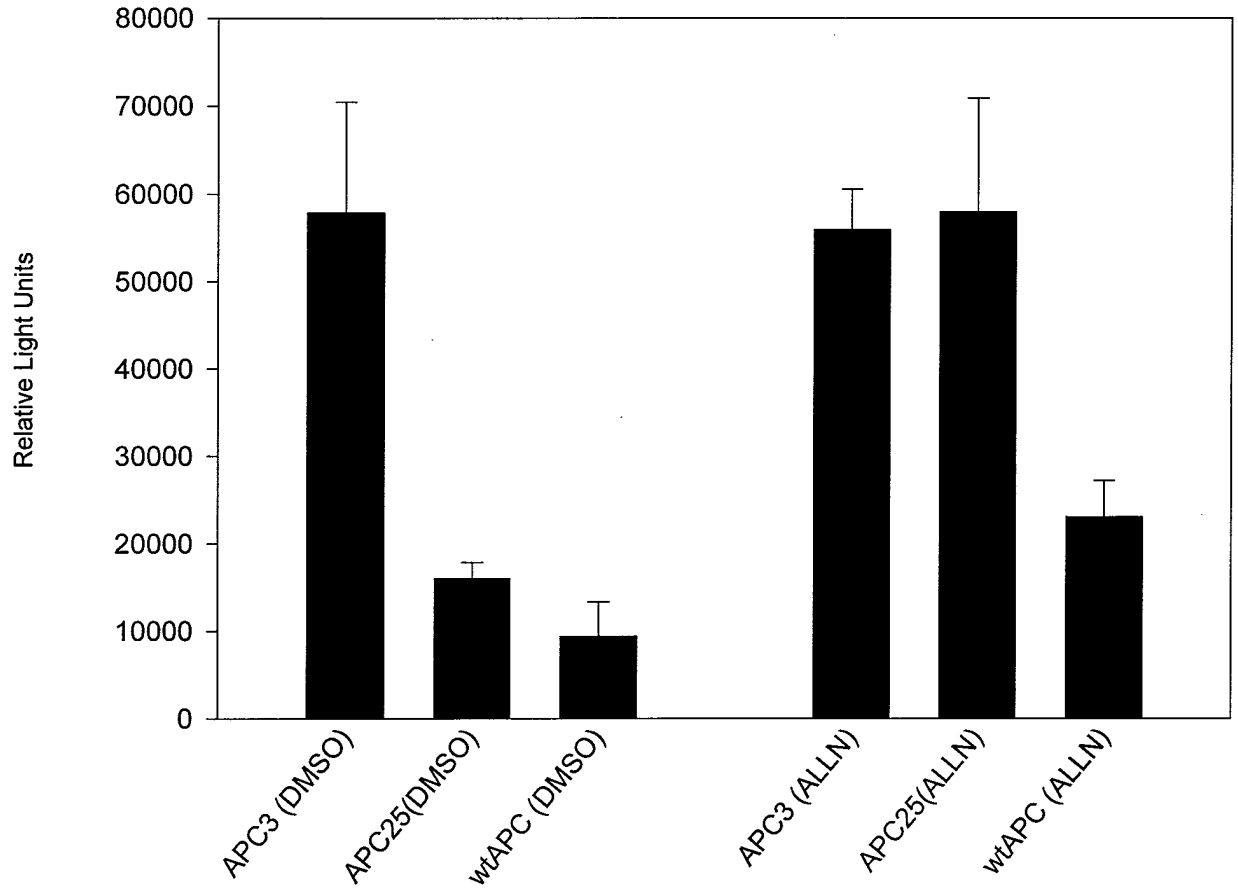

Figure 1

APPENDIX 4

Figure 1

Invasive breast cancer cells express the mesenchymal cadherin, cadherin 11. RT-PCR analysis of mRNA from a panel of breast cancer cells arranged from left to right in order of increasing invasiveness. MRC-5 cells (embryonic lung fibroblasts) are a positive control.

Figure 2

Cadherin 11 Northern blot from the same cells indicated in figure 1.

Figure 3

Cadherin 11 associates with β-catenin in invasive breast cancer cells. β-catenin immunoprecipitates were probed with cadherin 11 (upper panel), a pan-cadherin antibody (middle panel) or β-catenin (lower panel). Note that in all cells which contain cadherin 11 it co-precipitates with β-catenin. The middle panel shows that another cadherin recognized by a pan-cadherin antibody is present. Other results not shown but summarized in table 1 demonstrate that this is N-cadherin.

Table 1

Summary of the cadherin status of a panel of breast cancer cell lines and relationship to morphology in Matrigel.

Figure 1

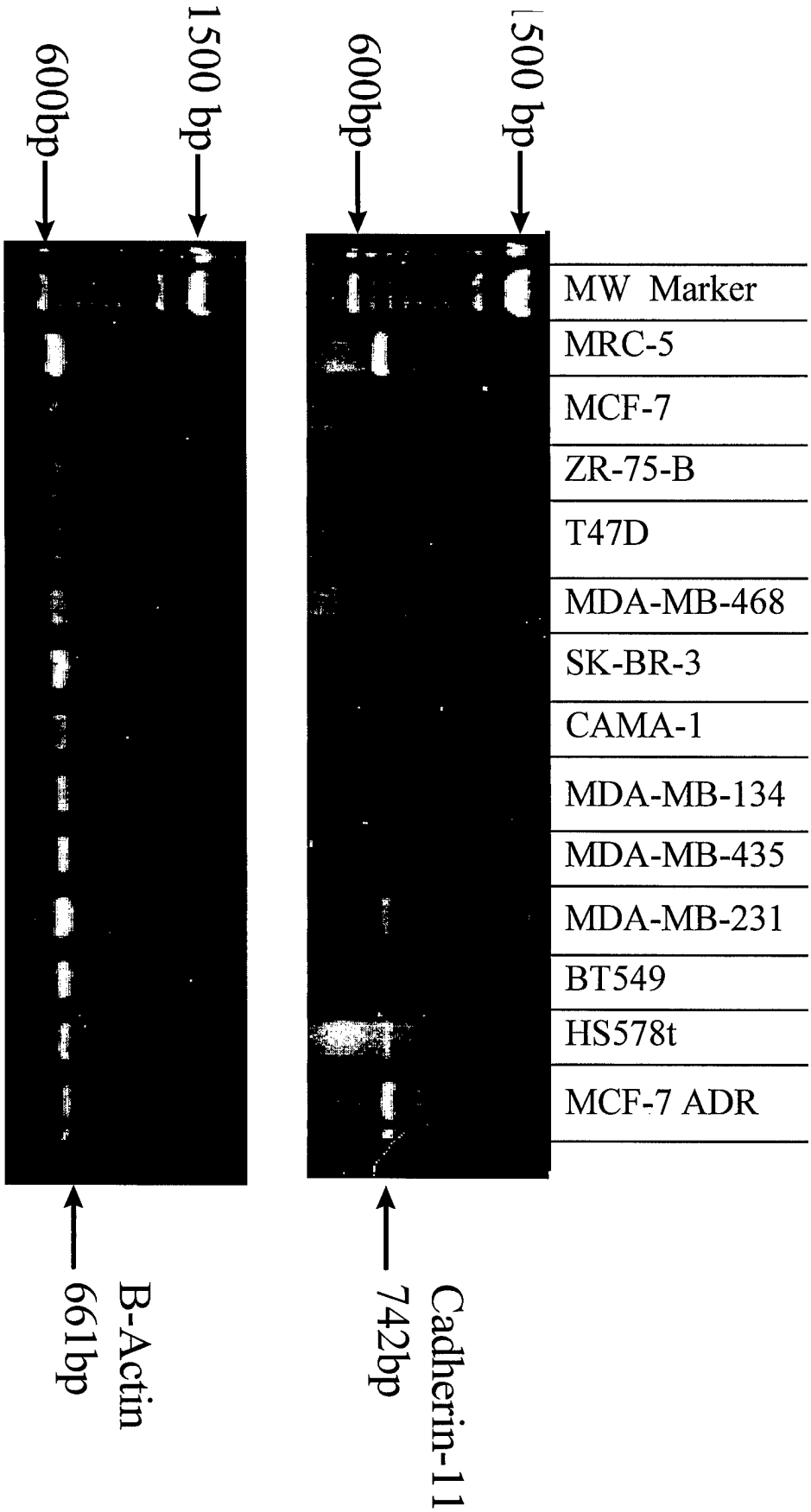
1500 bp
600bp
1500 bp
600bp
MW Marker
MRC-5
MCF-7
ZR-75-B
T47D
MDA-MB-468
SK-BR-3
CAMA-1
MDA-MB-134
MDA-MB-435
MDA-MB-231
BT549
HS578t
MCF-7 ADR
B-Actin
661bp
Cadherin-11
742bp

Figure 2

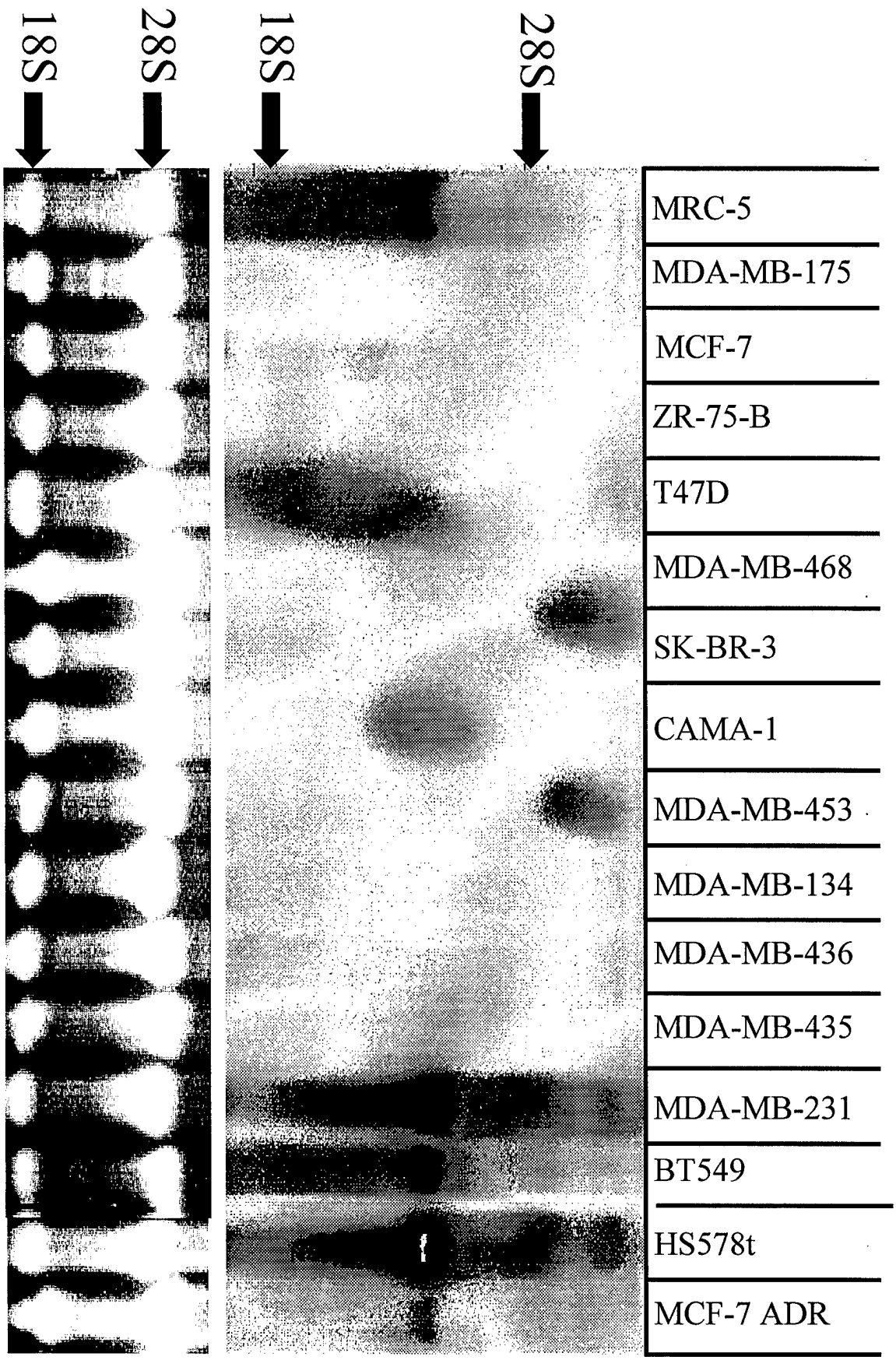
18S
28S
18S
28S
MRC-5
MDA-MB-175
MCF-7
ZR-75-B
T47D
MDA-MB-468
SK-BR-3
CAMA-1
MDA-MB-453
MDA-MB-134
MDA-MB-436
MDA-MB-435
MDA-MB-231
BT549
HS578t
MCF-7 ADR

Figure 3

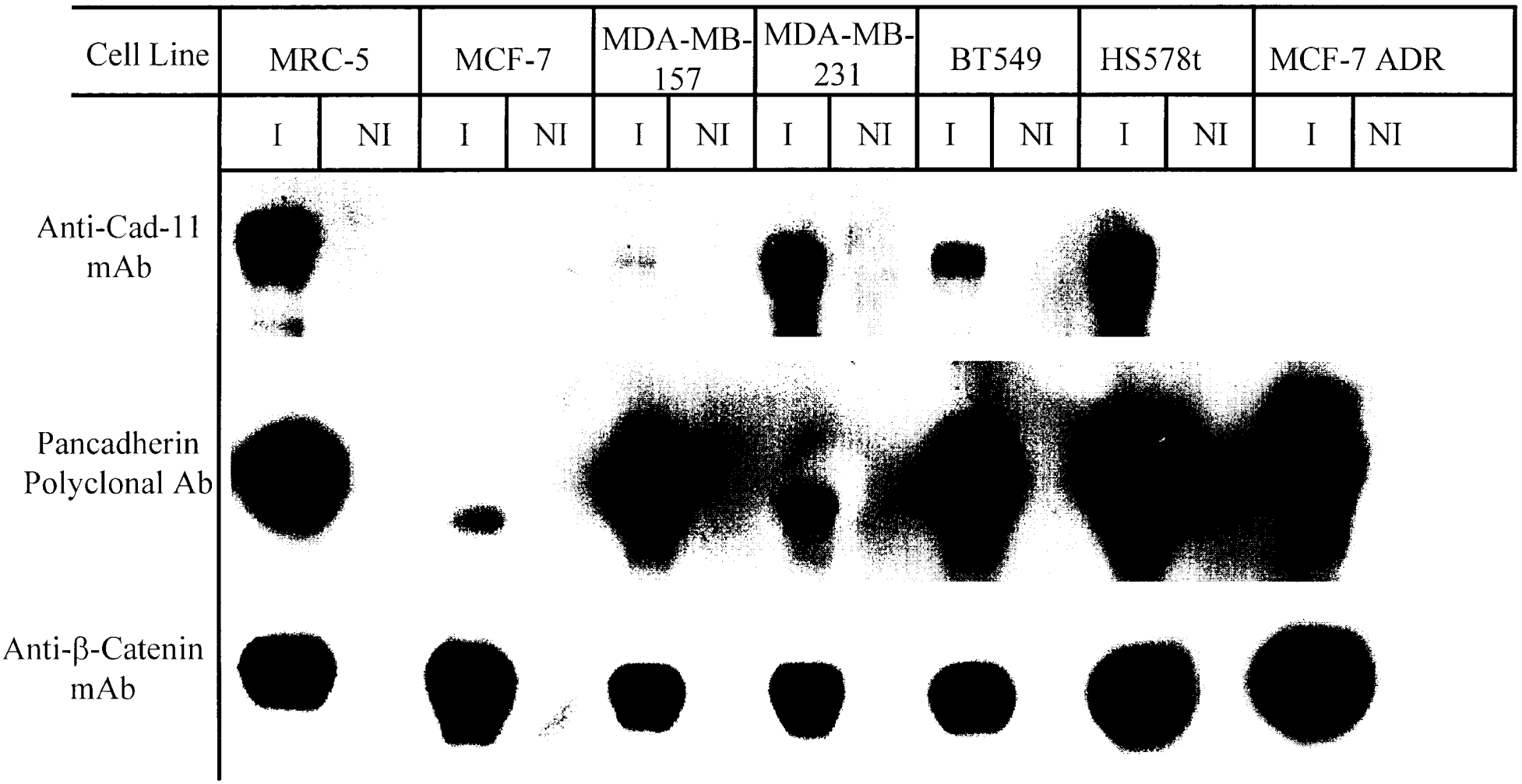
Cell Line
MRC-5
MCF-7
MDA-MB-157
MDA-MB-231
BT549
HS578t
MCF-7 ADR
I
NI
Anti-Cad-11 mAb
Pancadherin Polyclonal Ab
Anti-β-Catenin mAb

Cell Line	Matrigel	Invasion	E-cad-mRNA	N-cad-mRNA	N-cad-protein	Cad-11-mRNA	Cad11var-mRNA
A1N4		0	2	3		0	0
MCF-10A		0	2	3			
SKBR3 + RA	Fused	0	0	0		0	1
MDA-MB-175-7	Fused	2	2	1		0	0
MCF-7	Fused	2	2	0	0	1	0
ZR-75-B	Fused	2	2	1		0	0
T47D	Fused	2	2	1		0	0
BT474	Fused	2	2	2		1	0
MDA-MB-468	Fused	2	0	2		0	0
ZR-75-30	Spherical		0	0		1	0
CAMA-1	Spherical	2	0	1		0	0
MDA-MB-453	Spherical	2	0	3		0	0
MDA-MB-134	Spherical	2	0	3		0	0
MDA-MB-436	Stellate	3	0	3	2	1	0
MDA-MB-435	Stellate	3	0	3	2	0	0
MDA-MB-231	Stellate	4	0	1	0	2	2
BT549	Stellate	4	0	3	2	3	2
HS578t	Stellate	4	0	3	2	3	2
MCF-7ADR	Stellate	3	0	3		2	2
HBL-100	Stellate		0	3		2	1
MDA-MB-157	Stellate	3	0	3		2	1
A1n4-myc			2	2		0	0
BTP13	Stellate		2	3		3	2
HSP5	Stellate		2	3		2	2
	0=Neg	1=+/-	2=+			3=++	

Table 1 Appendix 4

APPENDIX 5

Figure 1

9-cis retinoic acid down-regulates β-catenin-LEF signalling. SKBR3 cells were transfected with the LEF-promoter-luciferase construct (TOPFlash) or a mutated form (FOPFlash) with reduced (but not absent) activity or vector alone. Note that treatment of control cells with RA does not influence the activity of the cells even though we showed previously that it increases β-catenin levels (39). In cells which are also transfected with β-catenin (to stimulate the activity of the promoter) RA reverses the stimulatory activity of the exogenous β-catenin.

Figure 2

9-cis retinoic acid down-regulates β-catenin-LEF signalling in cells expressing a mutated, stable form of β-catenin. The experiment described in figure 1 was repeated following transfection of a mutated β-catenin (S37A) which is not ubiquitinated and is stable.

Figure 3

9-cis retinoic acid down-regulates endogenous β-catenin signalling in HS578 cells. As figure 2 but HS578T cells which have high levels of endogenous cytoplasmic β-catenin were used.

Figure 4

9-cis retinoic acid decreases cytoplasmic β-catenin in cells expressing wild type or S37A mutated β-catenin. Cells were transfected with FLAG tagged β-catenin and immunoprecipitated with anti FLAG. Blots were then probed with antibodies to β-catenin.

9-cis RA down-regulates β–catenin - LEF signaling

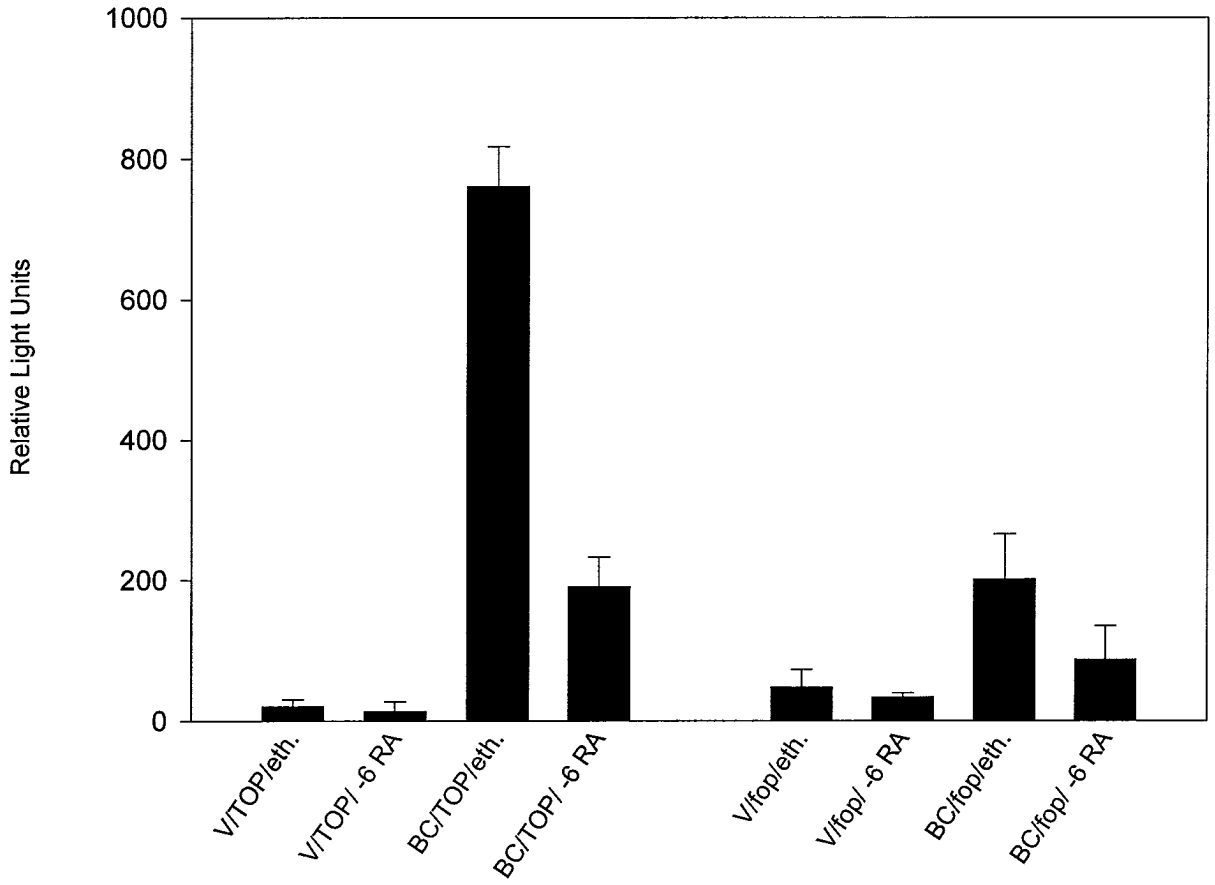

Figure 1

Figure 2

VJ - 1-24-98

SKBR3 + V / Wt / S37 β-cat -/+RA (10^{-6} M, 48 hr)

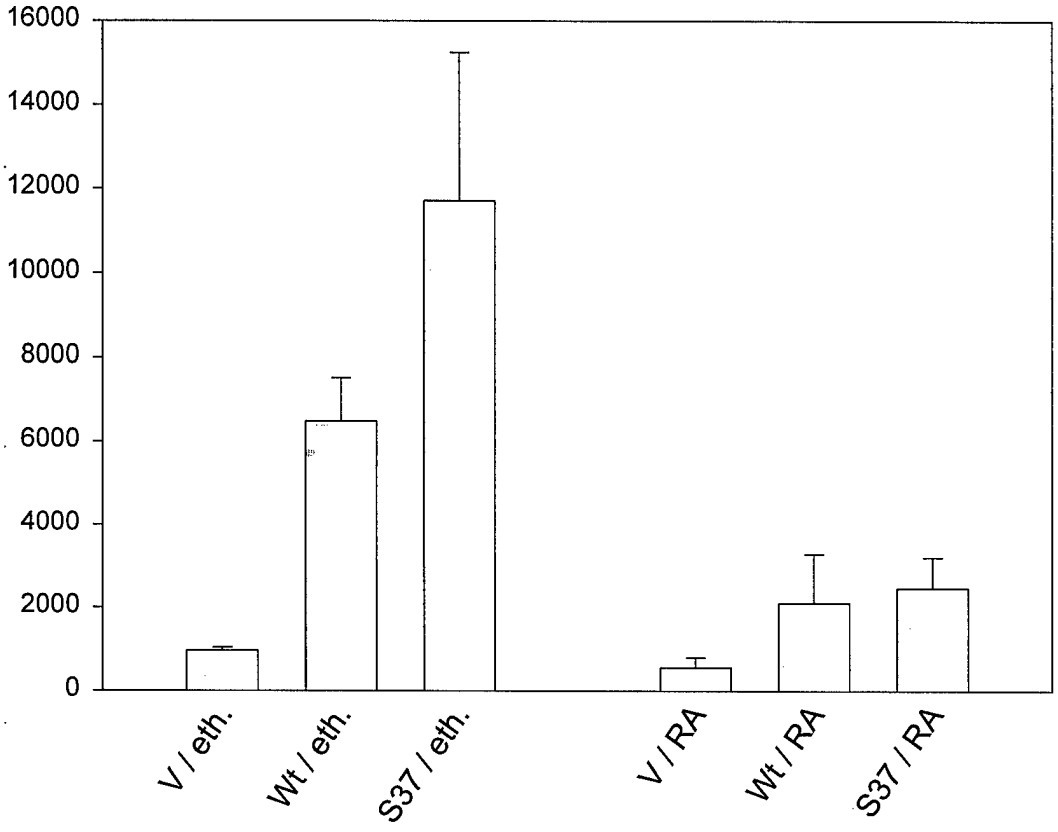

9-cis RA down-regulates endogenous β–catenin - LEF signaling in HS578t cells

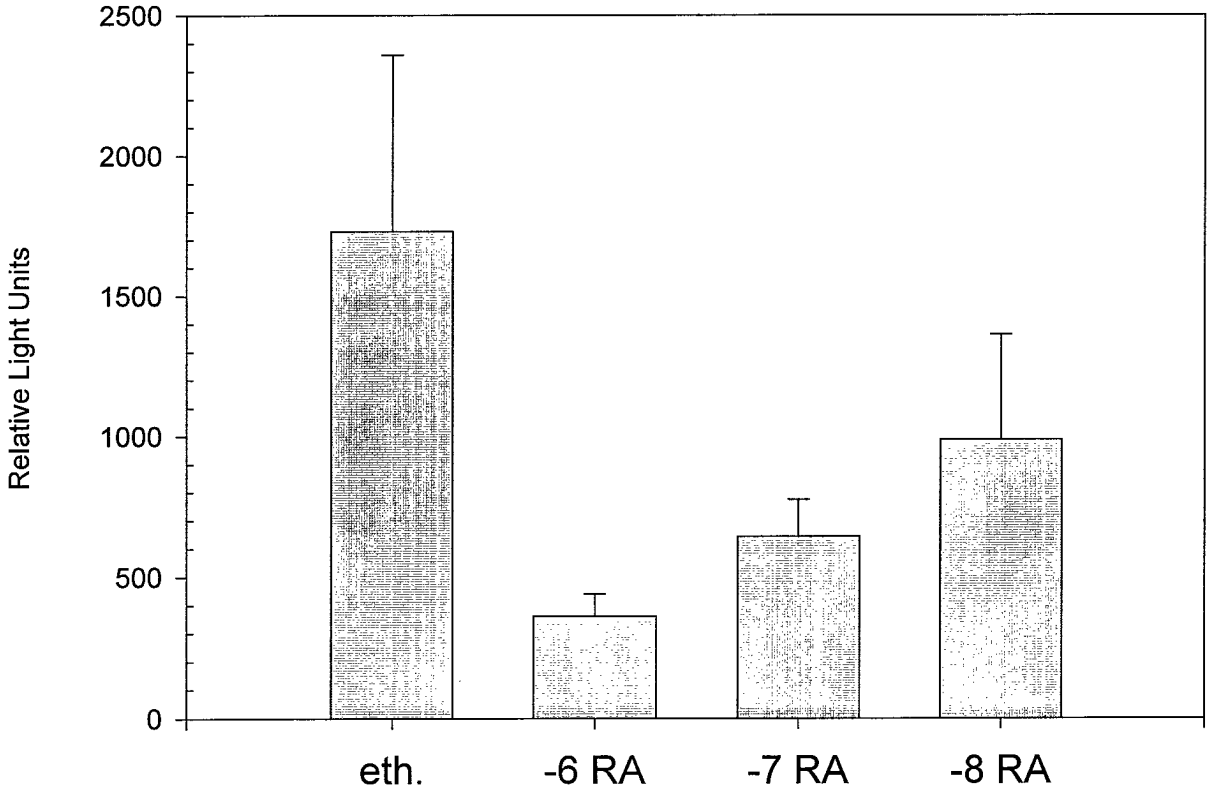

Figure 3

Figure 4

Vector Alone				WT β-Catenin				Ser-37 Mutant			
No Tx		RA		No Tx		RA		No Tx		RA	
I	NI	I	NI	I	NI	I	NI	I	NI	I	NI